Transcriptional Regulation and Functional Analysis of SK3

By

David Jacobson

A DISSERTATION

Presented to the department of Molecular and Medical

Genetics and the Oregon Health & Science University

School of Medicine

in partial fulfillment of

the requirements for the degree of

Doctor of Philosophy

January, 2003

School of Medicine
Oregon Health & Science University

CERTIFICATE OF APPROVAL

This is to certify that the Ph.D. thesis of

David Jacobson

has been approved

Professor in charge of thesis

Member

Member

Member

Member

TABLE OF CONTENTS

SK3 regulation by estrogen

SK3 and muscle physiology

(a) Denervated Skeletal Muscle

(b) Myotonic Dystrophy

Sp factor regulation of SK3 gene expression

Estrogen regulation of SK3 gene expression

LIST OF FIGURES

AT,   anterior tibial

DM, myotonic dystrophy

Dox, doxycycline

e-c,   excitation contraction

E_K,   potassium equilibrium potential

E2, 17βestradiol

EMG, electromyography

ERα, estrogen receptor alpha

FDB, flexor digitorum brevis

MCK, muscle creatine kinase

MCK-SK3 mice, muscle creatine kinase driving SK3 transgenic mice

OVX, ovariectomized

PSD, power spectral density

RMP, resting membrane potential

SK channel, small conductance Ca^{2+}-activated K^+ channel

SK3tTA mice, SK3 tetracycline regulatable transgenic mice

WT, wild type

Acknowledgment

I am very thankful for all of the wonderful interactions I have experienced throughout my doctorate work. As elegantly described by Albert Schweitzer, "At times our own light goes out and is rekindled by a spark from another person. Each of us has cause to think with deep gratitude of those who have lighted the flame within us." This work was made possible by the tremendous encouragement and support of many kind people.

I would like to thank John for constant inspiration through his enthusiastic drive to design an elegant study, give an informative and enjoyable talk, write a powerful passage, and enjoy the challenge. He has helped me learn the marvels of molecular biology, as well as the intricacies of crocket and basketball, and has been an outstanding mentor and friend. I would also like to thank James Maylie for patiently teaching me electrophysiology with a great sense of humor and insightful interpretation; he has also been a great friend and mentor. As well I thank David Pribnow for his relaxed and cheerful approach to teaching and for inspiring me to attempt novel techniques.

The entire Adelman lab has been a great source of knowledge, encouragement, stimulation, and entertainment. In particular I must thank CB for her never ending bag of molecular tricks, which she was always willing to teach me, as well as taking time to listen and provide knowledgeable suggestions with stimulating

discussions. Paco was invaluable in focusing my energy providing outstanding technical support and taking time to enjoy congratulate and celebrate every important step of the process. As for Andre, wow, this guy keeps you entertained with everything from his toys to his stories he makes you smile.

I would also like to thank my family and friends for all the constant love and support they provided. Especially my twin brother Doug whom I share a synergistic bond with, he has been a constant source of energy, encouragement, generosity, and love. I am profoundly grateful for the constant and comforting love my mother Mary Jean provides with an unyielding sense of benevolence. As well I thank my father Kirk and sisters Molly and Katie for believing in me and always providing love and encouragement.

Thanks to my thesis committee: Drs. James Maylie, Marcus Grompe, Matt Thayer, and John Bissonnette for their time, support, and advice.

Abstract

The SK3 gene encodes a small conductance calcium-activated potassium channel that influences many important cellular processes through calcium-dependent potassium flux. Transcription of the SK3 gene is regulated by the muscle-nerve status of skeletal muscle and hormonal control through estrogen. Aberrant expression of SK3 channels in skeletal muscle is associated with the hyperexcitability observed in patients with myotonic dystrophy (DM) or denervated skeletal muscle. The SK3 channels are implicated in the genesis of the symptoms because blocking them with the selective peptide blocker, apamin, blocks the hyperexcitability. In the hypothalamic-pituitary-gonadal axis, estrogen regulation of SK3 gene expression influences the release of gonadotropin releasing hormone (GnRH) from neuroendocrine cells in the preoptic hypothalamus, and affects LH and FSH release from pituitary gonadotropes. The aim of the work presented in this dissertation is to address the physiological role of SK3 in skeletal muscle hyperexcitability, and its transcriptional regulation by estrogen.

Skeletal muscle hyperexcitability

Skeletal muscle hyperexcitability is characteristically associated with both denervation and myotonic conditions. Expression of SK3 in skeletal muscle is induced by denervation and SK3 channels are also expressed in the skeletal

muscle of patients with DM. To investigate the role of SK3 channels in skeletal

muscle hyperexcitability, a transgenic mouse in which the muscle creatine kinase

(MCK) promoter was used to direct SK3 expression to skeletal muscle was

generated. The MCK-SK3 mouse expressed SK3 RNA and protein in skeletal

muscle, however Electromyographic (EMG) recordings from skeletal muscle

showed no difference in excitability compared to wild type animals. To further

investigate the role of SK3 channels in skeletal muscle hyperexcitability,

expression was manipulated using a transgenic mouse that harbors a

tetracycline-regulated SK3 gene. EMG recordings from skeletal muscle showed

equivalent hyperexcitability in denervated muscle from transgenic animals

expressing SK3 or wild-type animals. In contrast, denervated skeletal muscle

from SK3tTA mice lacking SK3 channels showed little or no hyperexcitability,

similar to wild-type innervated skeletal muscle. The results demonstrate that

SK3 channels are necessary but not sufficient for denervation-induced skeletal

muscle hyperexcitability. The mechanisms responsible for the paradoxical

hyperexcitability induced by the SK3 potassium channel were addressed through

electrophysiological measurements made from dissociated fibres from flexor

digitorum brevis muscle. The data suggest that SK3 expression in denervated

muscle causes accumulation of extracellular K^+ in the transverse tubules

resulting in a depolarized, hyperexcitable condition.

Transcriptional regulation:

SK3 is expressed in developing and denervated skeletal muscle as well as in innervated myotonic dystrophic muscle. The SK3 gene is also expressed in GnRH neurons in the preoptic hypothalamus, gland cells, and smooth muscle endothelium. The L6 rat skeletal muscle cell line, which serves as a model for SK3 expression in denervated skeletal muscle, was used to investigate the factors responsible for expression of the rat SK3 gene. The transcriptional start site in the rat SK3 gene was determined and functional analysis of the 5' flanking region identified the basal SK3 promoter. In addition, a 33 bp sequence adjacent to the SK3 basal promoter affected enhanced expression in differentiated L6 myotubes and endowed expression to an otherwise inactive heterologous promoter in L6 myotubes but not Cos7 cells.

Using this information, the mechanisms of SK3 transcriptional regulation by estrogen (E2) were examined. In Cos7 cells, an estrogen sensitive motif was identified, and was the same 33 bp motif that had been identified from the L6 studies. This motif endowed estrogen sensitive expression upon a heterologous promoter in Cos7 cells transfected with ERα. Indeed, expression of ERα in Cos7 cells and E2 treatment was sufficient to induce expression of the endogenous simian SK3 gene. Examination of proteins that bound to the 33 bp motif revealed that only Sp1 and Sp3 were bound to the enhancer from Cos7 and L6 nuclear extracts and that ERα increased Sp1 binding. In an in vivo system, the uterus

showed reduced expression of SK3 in response to estrogen. Interestingly a short form of Sp3, which decreases transcription, was only present in estrogen treated uterine tissue. A model consistent with the data is that immediately following estrogen stimulation ERα increases the binding of Sp1 to the SK3 33 bp enhancer, stimulating transcription, whereas continued E2 stimulation leads to accumulation of the short isoforms of Sp3 which competes with Sp1, reducing SK3 transcription.

This dissertation clearly defines a role for SK3 in denervation-induced skeletal muscle hyperexcitability and identifies important determinants contributing estrogen regulation of the SK3 gene. These data are important contributions to the hyperexcitable condition myotonic dystrophy and to estrogen regulated processes such as parturition. Future studies can use this information to ultimately control SK3 gene expression as a mechanism to control various cellular processes.

CHAPTER 1

Introduction

I. Ion Channel Overview

Cellular autonomy is achieved by a lipid membrane that serves as a physical barrier between the two water-based compartments, the cytoplasm and the extracellular fluid. For virtually all dynamic metabolic processes, there must be molecular mechanisms that preserve the cell's autonomy but permit regulated exchange of materials into and out of the cytoplasm. This is accomplished by integral membrane proteins that interface with the lipid bilayer yet provide an accommodating aqueous pathway for the exchange of soluble metabolites. These membrane-spanning proteins comprise remarkably diverse molecular populations that vary dramatically in their structures and selective functions.

Ion channels are an important class of transmembrane proteins. Many cellular processes rely upon the maintenance of an electrical gradient across the cell membrane, a separation of charge, and regulated changes in the transmembrane potential are used to drive active transport processes, exchanging metabolites across the membrane, and to propagate electrical signaling. The exquisite precision required for integrated regulation of membrane potential has driven the evolution of a vast array of ion channel proteins, integral membrane proteins that provide an aqueous pathway, or pore, for their charged substrates. Although they display radical variations in their structures and functions they share essential core properties. In almost all cases, ion

channels respond to metabolic cues by gating, opening and closing the pore, and in this manner directly couple their activities to the cell's metabolic status. In addition, they display, to varying extents, the property of selectivity, the ability to distinguish between different substrates. At one end of this continuum are gap junction proteins that permit the passage of large or small molecules with relative ease (Rousset, 1996). In contrast, diverse, molecularly distinct channel families have evolved that are highly selective for the four principal biological ions, Na^+, K^+, Ca^{2+}, and Cl^- (Hille, 2001) The degree of selectivity presents almost as much diversity as the array of channels proteins themselves. Some ion channels are limited only to particular monovalent cations, while others pass mono or divalent cations. Similarly, some Cl- channels prefer only Cl- ions others permit a broader spectrum of negatively charged small molecules (Hille, 2001). Some ion channels have low permeability ratios, the relative ease with which two related ions pass through the pore, as with nonselective cation channels that permit Na^+ or K^+ to transit the pore with approximately equal facility. In contrast, K^+ channels, select with remarkable fidelity K^+ ions over chemically similar Na^+ ions, showing several orders of magnitude difference in their permeabilities (Miller, 2000). Not only do K^+ channels show exquisite selectivity, at the same time they pass ions across the membrane at incredible rates, on the order of 10e6-7 ions per second (Miller, 2000). The molecular, indeed atomic, basis underlying this paradox of high selectivity and rapid flux has recently been revealed and will be discussed below.

2

Electrical signaling underlies a host of fundamental biological properties. The central nervous system is an electrically based machine, operated by a cell-type specific symphony of ion channels; the integral blend of the specific types of ion channels expressed in a neuron determines its excitability profile. In gonadotropes, hormone release is acutely regulated by small changes in membrane potential that result in large changes in secretion (Hille, 2001). Skeletal muscle cells perform their central function, excitation-contraction coupling, based upon surface membrane potential as well as potential changes in the specialized transverse tubular network, an intricate lattice of ion channel–filled membrane. Cardiac muscle maintains and varies heartbeat through a complex array of ion channel activities (Pennisi, 2002). Smooth muscle function is regulated by neurotransmitters released from autonomic nerve cells that initiate membrane potential changes, and changes in the membrane potential of the endothelial cells lining smooth muscles results in regulated release of paracrine factors that further tune smooth muscle tone (unpublished). ATP-dependent K^+ channels, monitors of cellular energy levels, regulate insulin secretion from pancreatic beta cells (Ashcroft and Gribble, 1998).

Built around the common features of regulated gating in response to diverse metabolic cues, and defined selectivity for their substrates, each of the major classes of ion channels has undergone evolutionary diversification that accommodates virtually every metabolic situation. For example, small differences in the activation threshold of voltage-dependent K^+ channels have large effects on the rate of action potential

3

repolarization, propagation, and transmitter release (Hille, 2001). Similarly, the rates of Na$^+$ channel recovery from inactivation, differing between members of the Na$^+$ channel family, will determine the rate at which a subsequent action potential may be propagated (Hille, 2001). Different types of voltage-dependent Ca^{2+} channels expressed in skeletal, smooth and cardiac muscles underlie the most fundamental differences in the contractile properties of these tissues. Hundreds of different voltage- and calcium-activated, BK, K$^+$ channels arise from a single gene through alternative splicing, each with distinct biophysical properties, and each endowing a slight but significant difference upon their host cell (Fettiplace and Fuchs, 1999). In addition, the subcellular localization of ion channels within each specialized cell type in which they are expressed, and their relative placement among the various types of ion channels have profound consequences for the integrated electrical activity of the cell. Selective association with beta subunits, proteins that interact with the pore forming subunits and modulate channel activity, endows further variation in function.

In summary, the magnificent variation in the mechanisms that generate diversity among ion channels, the selective blend of channels expressed in each cell coupled with their relative intracellular placement in many ways comprises the identity, the fingerprint, of the cell.

The Action Potential (neurons)

Using a diverse ensemble of ion channels, neurons respond to stimuli through regulated ionotropic changes that lead to the propagation and directed flow an action potential. Neurotransmitters bind to their postsynaptic receptors, many of which are ionotropic, and induce a local depolarization that activates voltage-gated sodium channels (Kandel et al. 2000). The voltage change causes opening of voltage-gated calcium channels that increases intracellular calcium further depolarizing the membrane. A large positive ion influx leads to the initial depolarization and characteristic action potential spike that is shunted by the inactivation of voltage-gated sodium channels and activation of voltage-gated potassium channels (Kandel et al. 2000). Voltage-gated sodium channels are inactivated for a short refractory period by a specialized gate, which leads the depolarizing signal to move from the dendrite to the soma and onward to the axon, activating other voltage-gated sodium channels in their resting state. The initial repolarization is begun through activation of voltage-gated potassium channels, Kv channels, which cause a fast extrusion of potassium and the beginning of the characteristic falling phase of the action potential (Hille, 2001). Voltage and calcium dependent potassium channels are also activated, which lead the membrane to a more hyperpolarized potential than the normal resting potential. The resulting hyperpolarization is another key phase during the action potential that controls the return of the neuron to its resting membrane potential. In many neurons, three kinetic components of the afterhyperpolarization, the AHP, may be distinguished, fast, medium, and slow (Figure 1). In many cases, activation of voltage- and calcium-dependent

5
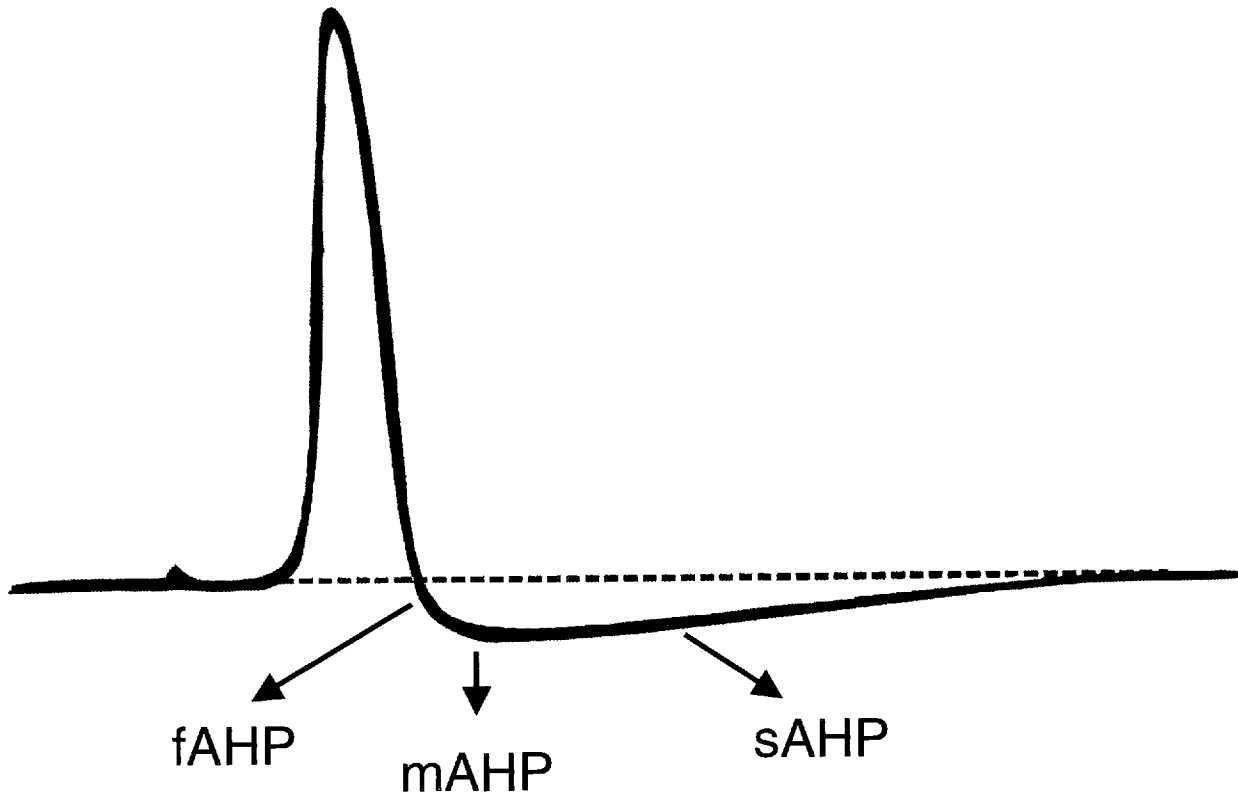
Figure 1

Figure 1. The Action potential recorded intracellularly from a squid giant axon. The lower dashed line indicates the resting potential. From Baker, Hodgkin, and Shaw (1961). The fast component of the afterhyperpolarization (fAHP) the medium component (mAHP) and the slow component (sAHP) are labeled accordingly.

potassium channels underlies the fast afterhyperpolarization (fAHP; Hille, 2001). Small conductance calcium activated (SK) potassium channels, which are activated solely by calcium, underlie the medium component of the AHP and continues the flux of potassium out of the neuron following the deactivation of the fAHP channels (Savic et al. 2001). The slow AHP is the final phase of the action potential, and is shaped by another potassium conductance that is also dependent upon calcium (Sah and Faber, 2002). Following the AHP the resting membrane potential of a neuron is set at about −70 mV by the coordinated effects of many ion channels. "Leak" potassium channels for example, which are not affected by voltage, allow potassium flux or "leak" out of the cell at −70mV, work in concert with Cl- channels to maintain the resting membrane potential at −70 mV (Lesage, 2000).

The action potential is a rapidly propagated electrical waveform, exquisitely shaped by the ion channel composition of neurons. To help propagate and boost the action potential, the axon is insulated with a myelin sheath with small gaps, the nodes of Ranvier, where dense pockets of voltage-gated sodium channels are found. The action potential spreads rapidly over the internode due to the low conductance of the myelin sheath and slows down at each high conductance node thus helping the action potential move quickly down the axon. Once the signal reaches the presynaptic terminal of a synapse, where the concentration of voltage-gated calcium channels is dense, calcium influx leads to neurotransmitter release. Potassium channels are fundamental in

shaping the falling and hyperpolarizing phases of the action potential; they repolarize and thus reset the neuron allowing it to fire again (Sah and Faber, 2002).

Muscle Cells

Action potentials in muscle cells generate contraction and movement. The neuromuscular junction provides an electrical connection between the nerve and the muscle. Following an action potential a motor nerve terminal becomes depolarized and releases acetylcholine that binds to Ach receptors on the muscle membrane that open and allow the passage of sodium into the muscle. Voltage-gated sodium channels are then activated by the local depolarization, initiating the characteristic action potential spike as in neurons. The architecture of skeletal muscle allows for delivery of action potentials to the area near the contractile machinery as quickly and uniformly as possible. Action potentials travel through transverse-tubules (t-tubules), extensions of the muscle fibre membrane (the sarcolemma) that are perpendicular to the plasma membrane (Figure 2). The terminal cisterna, chambers that are located along the t-tubule system containing a large concentration of calcium, are part of the sarcoplasmic reticulum, membrane bound structures within skeletal muscle that regulate calcium ion homeostasis within muscle. Terminal cisternae rest against t-tubules allowing a connection, termed junctional feet structures, between the ryanodine receptor (calcium channel) of the sarcoplasmic reticulum membrane and the dihydropyridine receptor (calcium channel) of the t-tubule membrane. The ryanodine receptor forms a calcium induced calcium release channel as a tetramer with a large cytoplasmic foot structure

Figure 2
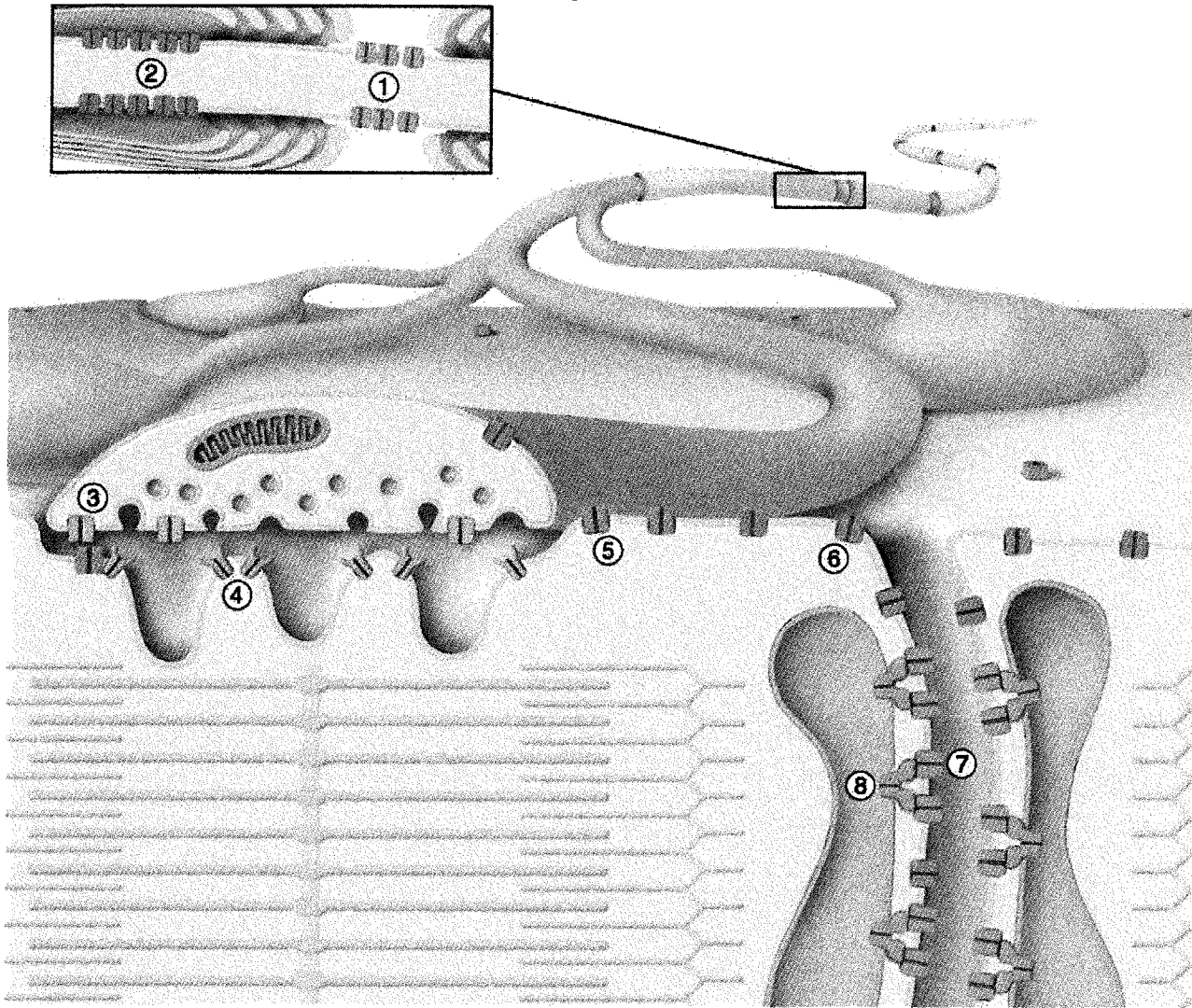
▥	①	Nerve voltage-gated sodium channel	▥	⑤	Skeletal muscle voltage-gated sodium channel
▥	②	KCNA voltage-gated potassium channel	▥	⑥	Skeletal muscle voltage-gated chloride channel
▥	③	Nerve voltage-gated calcium channel	▥	⑦	Transverse tubule voltage-gated calcium channel
Ψ	④	Nicotinic acetylcholine receptor	Ψ	⑧	Sarcoplasmic reticulum calcium release channel

Figure 2. Innervated skeletal muscle. The transverse tubules (containing the number 7) are lined by sarcoplasmic reticulum (one containing the number 8) which contain many important ion channels required for proper muscle contraction.

that interacts with four separate dihydropyridine sensitive voltage-gated calcium channels (Franzini-Armstrong and Protasi, 1997). Calcium release in skeletal muscle is induced through the voltage change during the action potential that travels down the t-tubule activating the dihydropyridine receptor voltage sensor and through a physical interaction with the ryanodine receptor, activates calcium release from the sarcoplasmic reticulum. Muscle contraction occurs when troponin, on the thin filament of the myofibril, binds the calcium and causes tension between actin and myosin. As with neurons, skeletal muscle action potentials also have a falling phase that is controlled by the inactivation of sodium channels and the activation of potassium channels. The depolarization following the initial action potential spike causes activation of voltage-gated (Kv) potassium channels that extrude potassium from the muscle helping to repolarize the muscle membrane (Vullhorst et al. 1998). The importance of potassium channels is also apparent with the resting membrane potential (RMP) of skeletal muscle that is set around −80 mV, close to the potassium equilibrium potential (E_k), by inward rectifier potassium channels (Kir) and chloride channels. Inward rectifier potassium channels influence the RMP, regulating the flow of potassium ions around E_k, passing potassium ions out of the cell when it is slightly depolarized from E_k and passing potassium ions into the cell when it is hyperpolarized from E_k (Hille, 2001). Skeletal muscle relies on ion channels within its functional framework to rapidly orchestrate and regulate muscle contraction. As with neurons, the potassium channel makeup of the skeletal muscle plays an essential role in controlling the muscle contraction through influences on both the falling phase of the action potential and the resting membrane

potential.

Potassium channels also influence smooth muscle contraction. K^+ channels found in the vascular endothelium exert a relaxing influence on the smooth muscle cells located in the arterial wall through an Endothelium-Derived Hyperpolarizing Factor (EDHF; unpublished). SK channels have been implicated in this process because apamin, a specific SK channel blocker, attenuates EDHF-mediated dilations (Murphy and Brayden 1995, Corriu et al. 1996, Doughty et al. 1999, Lagaud et al. 1999). Recent studies on SK3, one of the three cloned SK channels, have demonstrated that it is coupled to EDHF dilation of smooth muscle, detailed below.

Gland cells

Potassium channels also play an important role in regulating hormone release in the constituent cell types of the hypothalamic pituitary-axis. Gonadotropin releasing hormone (GnRH) is released from hypothalamic neurons in the arcuate and preoptic areas of the brain into portal veins where it travels to the pituitary. GnRH binds to cells in the anterior lobe of the pituitary, gonadotropes, causing release of follicle stimulating hormone and luetinizing hormone (gonadotropins). Synchronized bursting patterns allow for an episodic and regulated release of GnRH from the GnRH neurons (Suter et. al. 2000). The bursting pattern of action potential firing leads to an increase in intracellular calcium levels that activates SK channels, which hyperpolarize the membrane and terminate excitability. Pulsatile GnRH release results in the rhythmic

11

release of gonadotropins from anterior pituitary gonadotropes, caused by oscillations in the levels of intracellular calcium. Each rise in calcium initiates a burst of secretory granules containing gonadotropins from the gonadotrope (Tse and Hille 1992, Tse et al. 1993, Hille et al. 1995). Binding of GnRH to its receptor activates the phosphoinositide pathway, increasing IP_3, resulting in calcium release from intracellular endoplasmic reticulum (ER) stores. Calcium ions are then pumped back into the ER via the ATP-activated SERCA (sarcoplasmic endoplasmic reticulum calcium ATPase) pump. The system is now reprimed and subsequent GnRH binding increases IP_3 again, leading to another round of calcium release. Every rise in calcium also activates SK channels that hyperpolarize the membrane (Tse et al. 1995). This removes inactivation from voltage-gated Ca^{2+} channels on the cell surface and allows depolarization induced calcium influx.

II. Potassium Channels

In 1902 Julias Bernstein proposed that the resting membrane of the cell is permeable to potassium (Bernstein,1902). This concept implied that a potassium conductance was active when a cell is at rest and implicated an important role for potassium flux in setting the resting membrane potential. Since then recording techniques have been designed to measure potassium flux across a membrane defining many distinct differences in the potassium flux and identifying many important roles of potassium channels. Electrophysiological recordings allow potassium channels to be categorized on their biophysical parameters including (1) Voltage dependence (Kv), (2) Calcium

dependence (SK, IK, and BK), (3) Mechano-sensitivity, (4) Leak (KCNK), and (5) Inward rectification (Kir). Although many differences between potassium selective channels can be seen at the biophysical level it wasn't until their cloning that their true diversity was realized.

Potassium channel cloning

The first potassium channel cloned was a voltage-gated potassium channel from Drosophila. This landmark discovery used a Drosophila mutant, the *Shaker* fly, which displayed a neurological phenotype of rapidly shaking legs following etherisation (Kaplan and Trout, 1969). Electrophysiological recordings of a neuromuscular preparation provided a hint that electrical abnormalities were caused by a mutant channel in the *Shaker* fly (Jan and Jan, 1977). An abnormally large evoked release of transmitter from the presynaptic terminals was identified, an effect that was similar to that observed from wild type fly terminals treated with agents that blocked potassium conductances. Electrophysiological recordings from individual fly neurons were then used to electrically isolate the action potential. The action potentials were broader in *Shaker* flies than wild type flies, implicating a potassium channel involved in the repolarizing phase of the action potential as a candidate for the *Shaker* mutation (Tanouye et al. 1981). It wasn't until the voltage clamp technique was applied to flight muscle that the current was isolated as a voltage-gated potassium current (I_A A-type current) required for the fast repolarizing phase of the action potential (Salkoff and Wyman, 1981; Wu et al. 1983, Wu and Haugland 1985). Jan and colleagues used

genetic mapping and molecular biology to clone the *Shaker* gene and identified several alternatively spliced cDNAs (Kamb et. al. 1987; Papazian et al. 1987). The clone encoded a voltage-gated potassium channel that could be expressed in *Xenopus* oocytes to yield currents that recapitulated the A-type potassium current missing or altered in *Shaker* muscles (Timpe et al.1988). Interestingly the *Shaker* channel is responsible for fast presynaptic repolarization and thus *Shaker* flies have abnormally large amounts of transmitter released from neuromuscular preparations. This occurs because the depolarization following an action potential persists whithout the presende of the repolarizing *Shaker* current. The *Shaker* channel opens upon membrane depolarization due to movements in the S4 voltage sensor domain and rapidly inactivates due to pore block by an N-terminal inactivation domain. The *Shaker* polypeptide has six transmembrane domains (S1-S6) and a pore region between S5 and S6 with both the N and C terminal domains residing intracellularly. Expression studies of intact *Shaker* subunits in combinations with mutated *Shaker* subunits determined that functional channels form with a tetrameric stoichiometry (MacKinnon 1991). These studies not only provided the first sequence of a K$^+$ channel polypeptide, they described a powerful set of techniques for detailed functional analysis of cloned K+ channels.

Since the cloning of *Shaker* over 100 different potassium channels have been cloned (Coetzee et al. 1999). Using Shaker sequences as probes three more voltage dependent potassium channels were cloned: Shab, Shal, and Shaw (Butler et.al. 1990).

Although all contain six putative transmembrane (TM) domains, these subunits differ at their C and N terminal domains and form functionally distinct channels (Wei et al. 1990). The main difference between the *Shaker* (A-type) channel and the Shab, Shal, and Shaw (delayed rectifier) Kv channels is inactivation. The A-type channels inactivate following activation whereas the delayed rectifier channels are voltage dependent in their activation but don't inactivate. Heterologous expression studies in Xenopus oocytes demonstrate that Shab, Shal, and Shaw subunits form functionally distinct channels as homomeric tetramers. Therefore the voltage dependent potassium channels have been divided into subfamilies based on their amino acid sequence similarity and biophysical differences. The next potassium channel cloned was identified from another Drosophila mutant, *Slowpoke*, which showed mild leg shaking following etherisation and greatly diminished flight ability. Electrophysiological examination of *Slowpoke* flies determined that they lacked the calcium-and voltage-dependent potassium current activated following an action potential in wild type flight muscle. The channel responsible for the *Slowpoke* phenotype was cloned and displayed a large potassium specific conductance with voltage-and calcium-dependence, known as BK (Atkinson et. al. 1991). The BK channel has seven TM domains and the amino terminal of the channel is extracellular.

Inward rectifying potassium channels Kir, having very limited homology to Kv and BK channels, were the next potassium channels cloned through expression cloning in 1993 (Ho et al. 1993; Kubo et al. 1993). Kir channels have two TM domains flanking a

conserved pore loop, and also form functional channels with a tetrameric stoichiometry. Expression studies of Kir channels demonstrated many important features including inward rectification through polyamine block. Kir channels pass potassium ions into the cell when the cell is hyperpolarized from E_k and out of the cell only when the cell is slightly depolarized from E_k. Kir channels don't have a typical gate, they are blocked internally by polyamines when the cell is depolarized from E_k. In experiments on Kir channels expressed in Xenopus oocytes, block of Kir channels gradually disappeared after excision of the membrane, from the oocyte, as had been reported to occur for cardiac inwardly rectifying potassium channels (Matsuda 1988; Lopatin et al. 1994). Block of Kir channels was restored by placing excised membrane patches over the resulting hole on the surface of the oocyte, suggesting that block was caused by soluble factors exuding from the injured oocyte. Biochemical characterization identified these blocking particles as polyamines (Lopatin et al. 1994). Many other Kir channels were cloned by homology and divided into three groups: (1) classical Kir, (2) KATP or ATP sensitive Kir, and (3) G protein coupled Kir.

Recently leak and mechano-gated potassium channels that contain two pore domains (2PD) were isolated from database searches using potassium pore sequences (Lesage et al.1996). 2PD subunits contain either four or eight TM domains and form functional channels as dimers. The leak channels were first characterized as "potassium holes," due to their characteristic potassium flux without voltage dependence or block by typical potassium channel antagonists, showing potassium conductance when the cell is at

rest. As the leak channels allow potassium flux out of the cell when the cell is at rest they play an important role in setting the resting membrane potential (RMP). Leak channels are voltage insensitive however they are blocked by many independent mechanisms, including local anesthetics. The mechano-gated potassium channels are another form of 2PD channel that have specialized gating mechanisms regulated by mechanical-stress. 2PD potassium channels comprise the largest class of potassium channels cloned to date. Because of the great diversity observed with 2PD potassium channels and their widespread distribution these channels fulfill many physiological roles in addition to setting the RMP. The two pore domain K+ channels can be separated into five main functional classes: (1) the weak inward rectifiers, TWIK-1 and TWIK-2 (Lesage et al.1996; Patel et al. 2000; Pountney et al. 1999; Chavez et al. 1999); (2) the acid-sensitive outward rectifiers, TASK-1, TASK-2 and TASK-3 (Duprat et al.1997; Leonoudakis et al. 1998; Reyes et al. 1998; Kim et al. 1998; Kim et al. 2000; Rajan et al. 2000); (3) the lipid-sensitive mechano-gated K+ channels, TREK-1, TREK-2 and TRAAK (Fink et al. 1996; Fink et al. 1998; Bang et al. 2000; Lesage et al. 2000); (4) the halothane-inhibited 2 P domain K+ channel THIK-1; (Rajan et. al. 2001) and (5) the alkaline-activated background K+ channels TALK-1 and TALK-2 (Girard et al. 2001).

Six months after the cloning of the first leak channel, SK and IK channels were cloned. Using a consensus degenerate potassium pore sequence as a virtual probe, an EST (expressed sequence tag) was identified and used to screen a brain cDNA library, three full- length cDNAs were identified SK1, SK2, and SK3 (Kohler et al. 1996). Expression

studies determined that the cloned SK channels are small conductance, potassium selective, calcium activated, and voltage independent. Using the identified SK sequences as virtual probes, a database search uncovered another uncharacterized EST (Ishii et al. 1998). This EST sequence was used to probe a pancreas cDNA library and a full-length cDNA was cloned, IK. Expression studies showed that the IK clone had a slightly larger conductance than SK, was calcium activated, potassium selective, and voltage insensitive. SK and IK subunits contain six TMs with intracellular N and C terminal domains.

Sequence information and heterologous expression studies have detailed the fundamental similarities of all known potassium channels. Tetrameric assemblies of pore domains form functional potassium channels. All cloned potassium channels are potassium selective containing a similar pore sequence, which has recently been shown to confer potassium specific interactions and ion flux (Mackinnon, Science 1998). Potassium channels also fit three basic structural patterns including: (1) six transmembrane domain (TMD) proteins including voltage gated (Kv) and Ca^{2+} activated channels, with the exception of BK that contains one extra TM (2) two TMD proteins including inward rectifier (Kir) channels, and (3) two-pore subunit proteins including "leak and mechano-gated" K^+ channels. The great diversity found within potassium channels originates from the large number of genes coding for K+ channel subunits, alternative mRNA splicing, heteromeric assembly of different α-subunits, posttranslational modifications, and interaction with different β-subunits.

Alternative Splicing

BK channels are a remarkable example of fundamental diversity endowed through alternative RNA splicing. This is well demonstrated in the hair cells of the vertebrate inner ear where different variants determine tonotopic tuning. Hair cells are arranged in the cochlea on the basilar membrane, which has graded mechanical properties (Fettiplace and Fuchs, 1999). These properties allow different frequencies to displace the basolateral membrane, via the hair cell movement, maximally in different places, which results in a tonotopic map of vibration frequency. The low-frequency cell has a longer hair bundle, and a low density of slower BK channels whereas the high-frequency cell has shorter hair bundles, and a high density of faster BK channels. Differences in hair bundle length and BK channel density and splice type allow a mechanism through which different mechanical signal inputs can be sensed and converted into a specific electrical response. The mechanical signal, transmitted through the hair bundle to the basilar membrane, causes the opening of nonselective cation channels leading to a depolarization. A cascade of ionotropic movements follows the initial depolarization including: (a) activation of voltage-gated $Ca2+$ channels, causing a $Ca2+$ influx, (b) leading to activation of BK channels, hyperpolarizing the membrane (c) then $Ca2+$ channels close as the cell hyperpolarizes causing intracellular $Ca2+$ to dissipate (d) BK channels then begin to close, but due to the continued current from cation channels, the membrane becomes depolarized and initiates another cycle of calcium influx (Fettiplace and Fuchs, 1999). Different oscillation frequencies form

19

electrical signals that are communicated to the brain by the activity differences translated through 8th nerve fibers. The amount of BK and its exact mRNA type will determine how fast the cell hyperpolarizes and thus the oscillation of the cell. Modeling of BK electrical tuning using the turtle with an auditory range of, between 40–600 Hz, indicates that about five species of BK channels with different kinetics and overlapping expression could cover this range (Wu and Fettiplace, 1996). As well as having many splice variations the BK channels have modulatory beta subunits whose interactions affect both their voltage and calcium sensitivity (McManus et al. 1995; Nimigean and Magleby 1999; Wallner et al., 1999; Ramanathan et al. 1999).

Beta-subunits

Potassium channels interact with a variety of proteins that play important regulatory roles influencing channel activity and subcellular distribution. For example Kv channels interact with auxiliary beta subunits such as Kv β_1 and β_2 that have important roles in controlling channel inactivation. Kv β_1 has an inactivation ball located on its N-terminal domain and when combined with Kv alpha subunits helps regulate channel inactivation (Heinemann et. al. 1996). The Kv β_2 subunit on the other hand does not have an inactivation ball and thus increases the open probability of the Kv channels it interacts with. Beta subunits such as β_1, β_2, β_3, or β_4 also Interact with BK subunits, these interactions shift the voltage dependence of activation, to a more negative potential, and increase the calcium sensitivity of the channel (McManus et al. 1995; Nimigean and Magleby 1999; Wallner et al. 1999). SK channel activity is also affected by an important

20

beta subunit, calmodulin, which provides the calcium sensor required for SK channel function. Many auxiliary channel subunits have being identified and their additional molecular functions add to the complex nature of potassium channels.

Basis of ion selectivity

Potassium channels open and close in response to biological stimuli and selectively conduct K + ions across cell membranes. This selective permeation is achieved in the selectivity filter of the pore domain between the last two carboxyl-terminal TMs of all potassium channels, which includes a conserved GXG motif. Mutagenesis experiments have provided a great deal of information about the pore structure and location, implicating the two glycine residues (GXG) and negatively charged amino acids in potassium selectivity (Durell and Guy, 1996) and pore block. However it wasn't until the first crystal structure of a potassium channel, KcsA, was solved that a detailed understanding of potassium selectivity emerged (Doyle et al. 1998). KcsA is a potassium channel, with tetrameric stoichiometry, from Streptomyces lividans, that is potassium selective in its permeation. KcsA subunits have two TMs, intracellular N and C terminal domains, and a GYG motif in the pore domain. Four KcsA subunits form what looks like an inverted teepee, the wide part near the outside of the membrane and converging near the inside of the membrane, with ~6 angstrom diameter at the convergence. The pore region folds into the bottom of the teepee from the outside to fill most of the space in the outer part of the teepee, forming the potassium selectivity filter.

As the pore domain enters the membrane it is lined by five critical amino acids, including the GXG motif, which all have their main chain carbonyl oxygen atoms facing inward lining the pore. There are two potassium ions found in the selectivity filter of the KcsA crystal, separated by ~8 angstroms, which must be dehydrated to fit into the narrow pore (~3 angstrom diameter). To compensate for the energetic cost of dehydration, carbonyl oxygen atoms take the place of the water oxygen atoms forming multiple ion/water binding sites, and forming the basis of potassium selectivity and permeation. The potassium ion fits the selectivity filter perfectly and thus minimizes the energetic costs and gains as it travels through. However similar cations, which have different sizes, will not fit the selectivity filter well and won't be stabilized upon dehydration, therefore they will not favorably pass through potassium channels. Information on the structure and function of potassium channels are rapidly becoming available through extensive crystallization projects that have produced many new insights including mechanisms of calcium activation of potassium conductance (Schumaker et al. 2001, Jiang et al. 2002).

III. SK channels

Structure Function

Changes in intracellular calcium concentration are frequently coupled to changes in potassium flux. This concept was first introduced by Gardos in 1958 when he

observed a potassium flux from red blood cells in response to elevated internal calcium (Gardos, 1958). Meech then demonstrated that injection of calcium into an Aplasia neuron induced a potassium flux, causing the cell to become hyperpolarized (Meech, 1972). Calcium-activated potassium channels can be broadly divided into two groups: (1) large conductance voltage- and calcium-activated (BK), and (2) intermediate (IK) and small (SK) conductance calcium-activated channels. Sequence analysis suggests that SK channels contain six transmembrane (TM) domains with a potassium pore motif between the fifth and sixth transmembrane segments (Figure 3). Sharing a similar transmembrane topology as the voltage gated Kv channel it is likely that four SK subunits form a functional SK channel. The three SK subunits share around 60% sequence homology, with high homology within the TM domains and notably less conservation between the intracellular N and C domains. SK and IK channels all have a common α-helical domain in their C-terminal cytoplasmic domain required for their constitutive interaction with calmodulin. When expressed in cells as homomultimers the cloned SK channels have functional characteristics that are typical of SK channels described in skeletal muscle (Blatz and Magleby, 1986), neurons (Romey et. al. 1984), lymphocytes (Grissmer et. al. 1993), and adrenal chromaffin cells (Artalejo et. al. 1993, Park 1994). They are activated by submicromolar calcium, are potassium selective, and voltage independent.

Figure 3
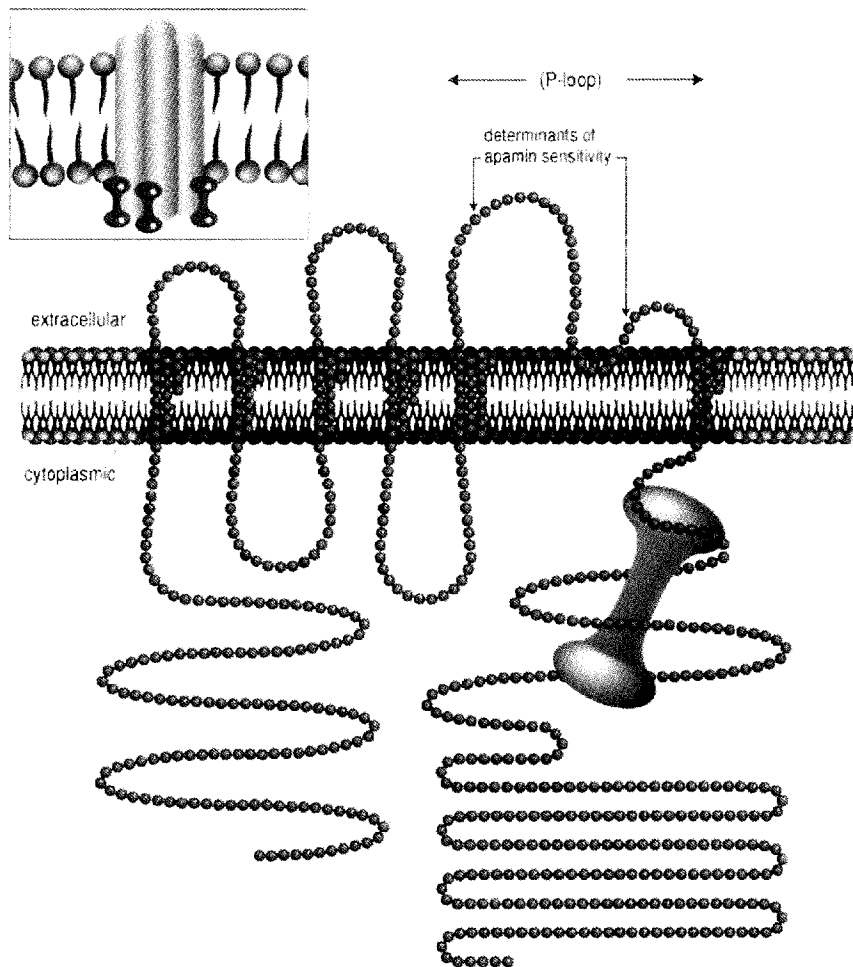
Figure 3. Structural representation of SK subunits. The main panel depicts the

putative subunit topology of a single SK subunit, with six transmembrane domains

and intracellular N- and C-termini. The dumbbell shape represents calmodulin

bound to the C-terminus of the SK subunit. The inset shows the SK channel, with

a symmetrical, tetrameric stoichiometry of SK subunits with an associated

calmodulin.

Pharmacology of SK channels

SK channels have a distinct pharmacological profile that has allowed a detailed analysis of SK function in a variety of cells including those of the CNS. Native and cloned SK channels are sensitive to the bee-venom peptide apamin, the scorpion peptide scyllatoxin, the plant alkaloids d-tubocurarine (dTC), and bicuculline, the antiseptic compound dequalinium chloride, and the bis-quinolinium cyclophane UCL 1684. However many of these compounds are not specific for SK channels. For example dTC is also blocks nicotinic acetylcholine receptors. SK channels are however the only known receptor for the bee-venom toxin and blocker apamin. SK current block measured over a range of apamin concentrations differs between the SK subtypes. Cloned SK2 and SK3 channels are highly sensitive to apamin showing an IC_{50} (half block) of ~60 pM and ~1 nM respectively (Kohler et al. 1996, Ishii et al. 1997), whereas human SK1 channels have an IC_{50} of ~12 nM. An aspartic acid and an asparagine residue, one on each side of the pore region of SK, are important for apamin sensitivity. Indeed these residues also play an important role in SK block by dTC and are likely to be involved in block by the other selective SK blockers. Apamin has been a powerful tool in the study of SK channels.

SK channel cell type expression was first characterized using apamin. I^{125} apamin binding has illustrated that these channels are found in many excitable cells including in the central nervous system (Mourre et al. 1984), erythrocytes (Brugnara et. al. 1995), colon (Hugues et al. 1982), and mouse and rat denervated skeletal muscle (Pribnow et

25

al. 1999; Schmid-Antomarchi et al. 1985). Electrophysiological studies have also characterized apamin sensitive SK channels in many cells including neoroblastoma cells (Barrett et al. 1981), rat skeletal muscle cells (Blatz and Magleby, 1986, Hugues et al. 1982) and many CNS cells (Lancaster et al. 1991).

Biophysical activity of SK channels

All cloned SK channels are (1) activated by submicromolar calcium, (2) voltage independent, (3) potassium selective, and (4) have a unit conductance of ~10 pS in symmetrical 120 mM potassium (Kohler et al. 1996). These properties were described in the following ways:

(1) Calcium dose-response relationships demonstrated that SK channels are half maximally activated by 400-800nM concentrations of calcium when expressed in cell lines or measured directly from excitable cells (Blatz and Magleby, 1986; Park, 1994). There is no measurable SK channel activity without calcium, even with changing membrane voltages, thus SK channels require only calcium for activation (Hirschberg et al. 1998).

(2) Changing the membrane voltage did not have significant affect the open probability of SK channels, measured in the presence of calcium (Hirschberg et al. 1998).

(3) The single channel conductance is ~10 pS for all three cloned SK channels recorded in symmetrical 120 mM potassium (Kohler et. al. 1996) and is

consistent with the conductance observed for native SK channels (Blatz and Magleby, 1986).

(4) Ion substitution experiments demonstrate that SK channels are highly potassium selective (Park 1994).

Although SK channels are voltage independent, they do inwardly rectify when conducting outward current. SK channels are blocked by divalent cations occluding the pore when the positively charged ions are forced toward the membrane with increasing depolarizing voltages (Soh and Park 2002, Kohler et al. 1996, Lancaster et al. 1991). A hydrophilic serine residue in the SK pore is responsible for the magnesium block (Soh and Park 2002). Therefore SK channels have a nonlinear current voltage relationship that plateaus as they are blocked by magnesium when conducting outward current.

Mechanism of calcium gating

Calcium gating of the SK channels is conferred by tightly bound calmodulin (Xia et al. 1998, Keene et al. 1999, Schumaker et al. 2001). Truncations of the C-terminal domain destroy channel activity and using a two-hybrid assay with the SK2 C-terminal domain as bait, a calmodulin interaction was identified. The SK C-terminal intracellular region following S6 is tightly bound to calmodulin, the CaM binding domain (CamBD), which contains three alpha helical domains (Xia et al. 1998). The calmodulin SK interaction is constitutive, persisting without calcium present and allowing for a rapid response to calcium. This constitutive interaction occurs between the N-terminal region of the

CamBD, involving a 63-residue region, and the C-terminal domain of CaM. Two positively charged residues, R464 and K467, are very important to this interaction and when both are mutated the constitutive interaction is lost. The interaction changes when calcium is present forming an additional interaction that includes the C-terminal domain of the CamBD, involving ~12 residues, interacting with the N terminal region of CaM. Recently the crystal structure of the Ca2+-CaM/CamBD has been solved and identified important contact points between CaM and the CaMBD that are responsible for calcium-gating (Schumaker et al. 2001). Interestingly the SK2 C-terminal end forms a dimer with CaM when crystallized in the presence of Ca2+, with two SK and two CaM molecules. However the SK2 calmodulin dimers can be arranged in a dimer of dimers formation that allows the predicted tetrameric arrangement of a functional SK channel. The binding of calcium to CaM may cause a rearrangement of the SK C-terminus leading to movements in the S6 helices and opening the SK gate. The concept of an S6 movement in response to calcium has recently been supported with studies demonstrating a state dependent access of residues in the SK2 S6 domain bundle crossing (Bruening-Wright et. al. 2002). Five residues near the S6 bundle crossing have state dependent access of an interacting molecule, indicating a movement of this S6 region in response to channel activation. There are also other important beta subunits that interact with SK subunits and their influence on SK channel activity is currently under investigation.

SK channels and the mAHP

Following an action potential the rate of repolarization and recovery to the resting membrane potential determines the ability of the neuron to fire another action potential. Action potentials were first recorded from the giant squid axon where the repolarization or falling phase was first described as a potassium conductance (Hodgkin and Huxley 1952). Since this groundbreaking discovery, many potassium conductances have been ascribed to the falling phase and hyperpolarizing phases of the action potential. Following the falling phase of an action potential, due to fast repolarization from Kv channels, there is a characteristic afterhyperpolarizing phase. Of the three kinetic components of the AHP, the medium component is clearly due to SK channel activity. The medium afterhyperpolarization influences the ability to fire another action potential. SK channels play an important role in modulating the threshold for activation of an action potential through their influence on the size of the mAHP. When a cell fires multiple action potentials the intracellular calcium levels increase thus activating more SK channels. As more SK channels are activated the mAHP becomes larger and with a burst, interspike interval is increased.

SK3 Channels

SK3 RNA and Protein Expression

Tissue specific expression of SK3 has been closely examined. In situ hybridization determined that SK3 RNA is expressed in many areas of the brain, most strongly in the:

neocortex including the enthorhinal cortex and para-/pre-/subicular cortex, basal nuclei, septum, amygdala, thalamus, habenula, and hypothalamus, raphe nuclei and serotonergic system, locus coeruleus, ventral tegmental area, and cerebellem golgi cells (Kohler et al. 1996, Stocker and Pedarzani 2000). RT-PCR showed expression in the outer hair cells of the rat cochlea (Dulon et al. 1998) where it is only expressed until early postnatal development. Similarly in skeletal muscle apamin binding and SK3 RNA levels are present at high levels in embryonic muscle and are not detectable shortly after birth (Schmid-Antomarchi et al. 1985, unpublished). SK3 RNA is also expressed in skeletal muscle following denervation (Pribnow et al. 1999). SK3 immunoreactivity has been detected in the liver, myenteric plexus, and muscular layers of the stomach, ileum, and colon (Fujita et al. 2001, Barfod et al. 2001). SK3 protein is also present at the rat neuromuscular junction in denervated but also in innervated muscles (Roncarati et al. 2001). In denervated muscle fibers, SK3 is localized to the extrajunctional as well as the junctional plasma membrane differing from innervated muscle fibers where it is only present at the presynaptic terminal of the neuromuscular junction (Roncarati et al. 2001). There are many examples of regulated SK3 expression; this thesis characterizes the SK3 promoter defining important enhancer sequences that regulate SK3 expression in response to estrogen stimulation.

SK3 regulation by estrogen

A role for estrogen in regulating SK3 transcription has recently been described through studies on gonadotropin-releasing hormone (GnRH) neurons (Wagner et al. 2001), and

vascular endothelium (unpublished). SK3 is expressed in the preoptic area (POA) of the rostral hypothalamus, which plays an important role in reproductive signaling (Kelly et al. 2002, Fleming et al. 1994; Numan and Sheehan, 1997), and contains a large proportion of GnRH neurosecretory cells that express SK3 mRNA (Silverman et al. 1979, Butler et al. 1999; Skynner et al. 1999; Hrabovszky et al. 2000). Bursts and prolonged episodes of repetitive action potentials have been associated with hormone secretion in the POA. Following repetitive action potential firing, GnRH is released into pituitary portal blood and stimulates the corresponding pulsatile secretion of the pituitary gonadotropins, follicle-stimulating hormone (FSH) and luetinizing hormone (LH) from the anterior pituitary (Ferin et al., 1984). FSH and LH are glycoproteins that stimulate estrogen release from granulosa and Sertoli cells and theca cells respectively. Estrogen, in turn, has a feedback effect on GnRH release (Ferin et al. 1984). Estrogen receptors alpha and beta are expressed in hypothalamic GnRH neurons and affect the excitability of GnRH neurons through direct influences on potassium channel activity and secondary effects on ion channel expression. Estrogen application to GnRH neurons can directly stimulate BK (White et al. 2001, Dick and Saunders 2001) causing hyperpolarization, reducing the probability of action potential firing and release of GnRH. Estrogen also elevates SK3 RNA levels in the rostral basal hypothalamus, containing GnRH neurons, of ovariectomized female guinea pigs (Bosh et al. 2002). Increased SK3 expression may result in an increased mAHP following an action potential, thus reducing the action potential firing frequency, increasing the interspike interval, and reducing GnRH release. A mechanism for transcriptional regulation of SK3

31

gene expression by estrogen, and the role of SK3 channels in the reproductive cycle is currently being investigated.

Estrogen has also been strongly associated with vascular protective effects observed in premenopausal women (Bass and Bush, 1991). Estrogen influences blood pressure through its affect on the vascular endothelium where estrogen receptors are expressed. The vascular endothelium exerts a relaxing influence on the smooth muscle cells in the arterial wall through the release of at least three factors including: (1) nitric oxide, (2) prostacyclin, and (3) Endothelium-Derived Hyperpolarizing Factor (EDHF). Following stimulation of endothelial cells, with an agonist such as acetylcholine or bradykinin, there is a transient increase in the calcium level, which leads to the activation of calcium dependent potassium channels and membrane hyperpolarization. Following endothelial stimulation NO and prostacyclin are produced and released. Endothelial hyperpolarization is also transferred to the smooth muscle through an additional molecularly undefined component termed EDHF (Campbell et al. 1996). When the smooth muscle membrane becomes hyperpolarized the calcium concentration decreases resulting in vessel dilatation. Estrogen affects the endothelium through transcriptional regulation of components that influence both NO and EDHF. Estrogen stimulates increases in nitric oxide through transcriptionally upregulating nitric oxide synthase (NOS). Estrogen also stimulates EDHF release that has recently been identified as an SK3 influenced process. Female mice without SK3 expression show dramatically increased blood pressure without the characteristic relaxing influences of

EDHF, similar to female mice without ovaries and estrogen (unpublished). These findings suggest that SK3 may then play an important role with NOS in the vascular protection observed in premenopausal women. Estrogen regulation of SK3 transcription is presented in this thesis work.

SK3 and muscle physiology

SK channels were first recorded from primary cultured rat skeletal muscle myotubes (Blatz and Magelby, 1986). A patch of membrane excised from the muscle contained a small conductance that was calcium activated, potassium selective, and voltage insensitive. A similar current has also recently been recorded from acutely dissociated mouse skeletal muscle (Neelands et. al. 2001). As the first recordings by Blatz and Magelby were performed on rat primary culture myotubes, the muscles being recorded were also denervated. Thus SK currents follow SK3 RNA expression, being expressed only in denervated skeletal muscle (Pribnow et. al. 1999). Using flexor digotorum brevis (FDB) muscle fibres from the hind-foot of a mouse, electrophysiological recordings were used to characterize SK channel activity in denervated skeletal muscle (Neelands et. al. 2001). FDB recordings are used in this thesis to identify a role for SK3 in denervation-induced skeletal muscle hyperexcitability.

(a) Denervated Skeletal Muscle

The primary function of skeletal muscle is controlled contractions through the process of excitation contraction (e-c) coupling that is achieved through a program directed by the

innervating nerve. Skeletal muscle couples the excitability mediated by release of acetylcholine at the surface membrane to the transverse tubular ion channels, and to the specialized myosin contractile apparatus using calcium as a second messenger. Muscle fibers typically repolarize through voltage-gated potassium conductances that are activated following an action potential. Ionotropic changes that affect repolarization and e-c coupling often affect muscle fibre contraction, changing the ability of the muscle to fire action potentials and thus contract (Takekura et al. 1995, Beam et al. 1986). The innervating nerve maintains normal synaptically controlled e-c coupling whereas denervation results in hyperexcitability and spontaneous contractile activity that reflects changes in the expression profile of many genes, including ion channels (Hartzell & Fambrough, 1972; Rogart & Regan, 1985; Mishina et al. 1986; Heathcote, 1989; Brenner et al. 1990; Gonoi & Hasegawa, 1991; Lupa & Caldwell, 1994). SK3 expression is one example of a change that affects skeletal muscle e-c coupling and is associated with skeletal muscle hyperexcitability. The hyperexcitability associated with denervation is blocked by apamin and SK3 RNA and protein are aberrantly upregulated in denervated skeletal muscle, and not expressed in wild type innervated skeletal muscle. The role of SK3 channels in denervation-induced skeletal muscle hyperexcitability is defined in this thesis.

(b) Myotonic Dystrophy

Myotonic Dystrophy is the most common inherited neuromuscular disease of adults, affecting 1 in 8000 people. Two forms of DM have been identified that show overlapping clinical features including the primary symptom myotonia, and other secondary symptoms including bilateral cataracts, premature balding, muscle wasting, cardiac conduction abnormalities, endocrine dysfunction, and testicular atrophy. The principle symptom of DM is myotonia, an abnormal persistent contraction of skeletal muscle following voluntary or electrical stimulation (Strumpel et al. 1981; Appel et al. 1984) and is seen upon electromyographic (EMG) examination as a repetitive discharge of muscle action potentials (Linsley and Curnen1936, Farnbach et al. 1978).

All myotonic disorders except DM stem from mutations in voltage-gated ion channels. For example recessive generalized myotonia congenita (Koch et al. 1992) and dominant myotonia (George et al. 1993) are caused by mutations in CLCN1, whereas the myotonia associated with Hyperkalemic periodic paralysis and paramyotonia congenita are caused by mutations in the voltage-gated sodium channel SCN4. In contrast DM type 1 (DM1) is caused by a CTG repeat expansion in the 3' untranslated region of a protein kinase, DMPK, on chromosome 19 (Brook et al. 1992). A similar CCTG repeat expansion in intron 1 of the zinc finger protein 9, ZNF9, on chromosome 3 has recently been linked to myotonic dystrophy-type two (Liquori et al. 2001). Recently a transgenic mouse model of DM was obtained that harbors a human skeletal actin cDNA and a CTG repeat in its 3' UTR (Mankodi et al. 2000). The mouse develops myotonia, which

35

is caused by the expanded CUG repeats shown to trigger aberrant splicing of pre-mRNA. CUG repeats, as found in DM, interact with a CUG binding protein/hNab50 and sequester it in the nucleus. As the CUG-BP participates in mRNA splicing and transport, these processes are disturbed. Recently this was demonstrated for human cardiac troponin T and the insulin receptor that both have aberrant splicing in DM1 muscle (Philips et al. 1998, Savkur et. al. 2001). The DM mouse also shows abnormal mRNA splicing which affects a chloride channel ClC1. Aberrant splicing allows only ~10% full length ClC-1 to be produced when compared to wild type levels. The lack of full length ClC-1 elevates the skeletal muscle resting membrane potential and lowers the threshold to fire an action potential, causing hyperexcitability.

The CTG repeat found in DM1 also leads to aberrant gene transcription, including expression of SK3 mRNA in skeletal muscle (Kimura et al. 2001). Apamin binds to the skeletal muscle membrane of patients with myotonic dystrophy and not to control skeletal muscle (Renaud et al. 1986). Apamin also blocks the myotonia associated with DM1 when injected into the thenar muscle of patients with myotonic dystrophy (DM1, Beherens et al. 1994). The exact role of the SK3 potassium channel, which is normally involved in hyperpolarizing the cell, causing myotonia remains unclear. However SK3 may be involved along with ClC-1 in the genesis of skeletal muscle hyperexcitability in DM1 skeletal muscle. This thesis details a role for SK3 in skeletal muscle hyperexcitability.

CHAPTER 2

SK Channels are Necessary but not Sufficient for Denervation-induced

Hyperexcitability

David Jacobson*, Paco S. Herson, James Maylie[†], John P. Adelman[#]

Vollum Institute, *Medical Genetics, and [†]Department of Obstetrics and Gynecology,

Oregon Health Sciences University, Portland, OR 97201, USA

Abstract

Skeletal muscle hyperexcitability is characteristically associated with denervation. Expression of SK3, a small conductance Ca^{2+}-activated K^+ channel, is induced by denervation and direct application of apamin, a peptide blocker of SK channels, dramatically reduces hyperexcitability. To investigate the role of SK3 channels in skeletal muscle hyperexcitability, a mouse that specifically expresses SK3 in skeletal muscle, from a muscle creatine kinase (MCK) promoter, was generated. The MCK-SK3 mouse expresses SK3 RNA and protein in skeletal muscle, however Electromyographic (EMG) recordings from skeletal muscle showed no difference in excitability from wild type animals. To further investigate the role of SK3 channels in denervation-induced hyperexcitability, SK3 expression was manipulated using a transgenic mouse that harbors a tetracycline-regulated *SK3* gene. Electromyographic (EMG) recordings from anterior tibial (AT) muscle showed that denervated muscle from transgenic or wild-type animals had equivalent hyperexcitability that was blocked by apamin. In contrast, denervated skeletal muscle from SK3tTA mice lacking SK3 channels showed little or no hyperexcitability, similar to results from wild-type innervated skeletal muscle. Similar to the MCK-SK3 mouse the innervated skeletal muscle from SK3tTA mice containing SK3 channels did not show hyperexcitability. The loss of SK3 protein was consistent with electrophysiological measurements made from dissociated fibres from flexor digitorum brevis (FDB) muscle. Depolarization of FDB fibres activated an apamin-sensitive tail current in fibres from denervated wild type or from innervated and denervated SK3tTa

38

fibres without dox, but not innervated wild type or Dox treated SK3tTA fibres. Denervated wild type fibres showed a decreased action potential threshold of ~8 mV compared to innervated wild type fibres, and application of apamin increased the action potential threshold in denervated fibres to that measured in innervated fibres. Interestingly the reversal potential of the denervated fibre tail current was elevated from the predicted value for EK. T-tubule accumulation of potassium could cause this underestimation of the reversal potential of the SK tail current, an effect that would be exacerbated at lower external potassium concentrations because the local accumulation of potassium would contribute a larger percentage of the potassium ions. A model consistent with the data is that SK3 expression in denervated muscle causes accumulation of extracellular K^+ upon contraction that does not readily diffuse from the restricted t-tubular space, resulting in a depolarized, hyperexcitable condition. The results demonstrate that SK3 channels are necessary but not sufficient for denervation-induced skeletal muscle hyperexcitability.

Introduction

Spontaneous repetitive discharges of action potentials (hyperexcitability) are characteristic of denervated skeletal muscle (Tower, 1939; Albuquerque et al. 1968; Robbins, 1977). Denervation induces changes in the expression of many genes encoding proteins that are involved in excitability (Venosa et al. 1985; Heathcote, 1989; Trimmer et al. 1990), and the *SK3* gene is a prototypic example. SK3 mRNA is minimally expressed in normal innervated skeletal muscle (Roncarati et al. 2001), but following denervation SK3 mRNA levels increase dramatically over 4 days to a maximal steady-state level (Pribnow et al. 1999). The changes in *SK3* gene expression are paralleled by the appearance of ^{125}I-apamin binding sites, and the presence of apamin-sensitive potassium conductances decrease the threshold for action potential generation (Pribnow et al. 1999; Neelands et al. 2001). Interestingly, direct injection of apamin, a blocker of small conductance Ca^{2+}-activated K^+ channels (SK channels), into denervated rat skeletal muscle (Vergara et al. 1993) dramatically suppressed the hyperexcitability.

The decreased hyperexcitability subsequent to apamin application (Vergara et al. 1993; Neelands et al. 2001) suggests an important role for SK3 channels in denervation-induced hyperexcitability. However, the many other changes in skeletal muscle associated with denervation have not permitted a clear assessment of whether SK3 channels are sufficient to induce hyperexcitability. The availability of transgenic mice in which *SK3* gene expression may be experimentally controlled (Bond et al. 2000) affords

40

a mechanism to assess the link between SK3 channels and skeletal muscle hyperexcitability. In this study, EMG recordings were employed to measure electrical activity in normal or denervated skeletal muscles from wild-type mice and *SK3* transgenic mice that either overexpressed or lacked SK3 channels. The results show that SK3 channels are necessary but not sufficient for denervation-induced skeletal muscle hyperexcitability. Electrophysiological measurements were also employed in this study to elucidate a mechanism whereby SK3 expression in denervated skeletal muscle may cause skeletal muscle hyperexcitability. The results show that SK3 in the t-tubule of denervated skeletal muscle causes a local rise in potassium, thus inducing activation of voltage gated channels leading to another contraction and thus hyperexcitability.

Results

Denervation induces apamin-sensitive hyperexcitability and SK3 protein

Adult C57/Black6 mice were denervated by surgically removing a 5 mm segment of the right hindlimb sciatic nerve; the intact left hindlimb served as a control. Electromyographic (EMG) recordings from hindlimb AT muscles were performed 7 to 10 days after denervation, measuring spontaneous EMG activity as an index of excitability. The EMG data from denervated and control muscles were quantified for comparison using power spectral density (PSD) analysis, performed over a set 1-minute interval on all EMG recordings (see Methods). In agreement with previous studies (Vergara et al. 1993; Behrens et al. 1994), innervated skeletal muscle exhibited no significant spontaneous activity, as evidenced by a low PSD ($2.0 \pm 0.3 \times 10^{-10}$ V^2/Hz, n=4, Fig. 4B). In contrast, denervated skeletal muscle exhibited robust spontaneous activity, and a 100-fold higher PSD ($1.9 \pm 0.3 \times 10^{-8}$ V^2/Hz, n=4; Fig. 4C). Apamin injection into the denervated muscle resulted in a 10-fold decrease in spontaneous activity within 3 minutes ($1.9 \pm 0.4 \times 10^{-9}$ V^2/Hz, n=4; Fig. 4D). Following EMG recordings, animals were sacrificed and SK3 protein levels in the hindlimbs were assessed by Western blot analysis. The results showed that SK3 protein was detected only in denervated muscle (Fig. 4A). These results implicate apamin-sensitive SK3 channels in denervation-induced skeletal muscle hyperexcitability.
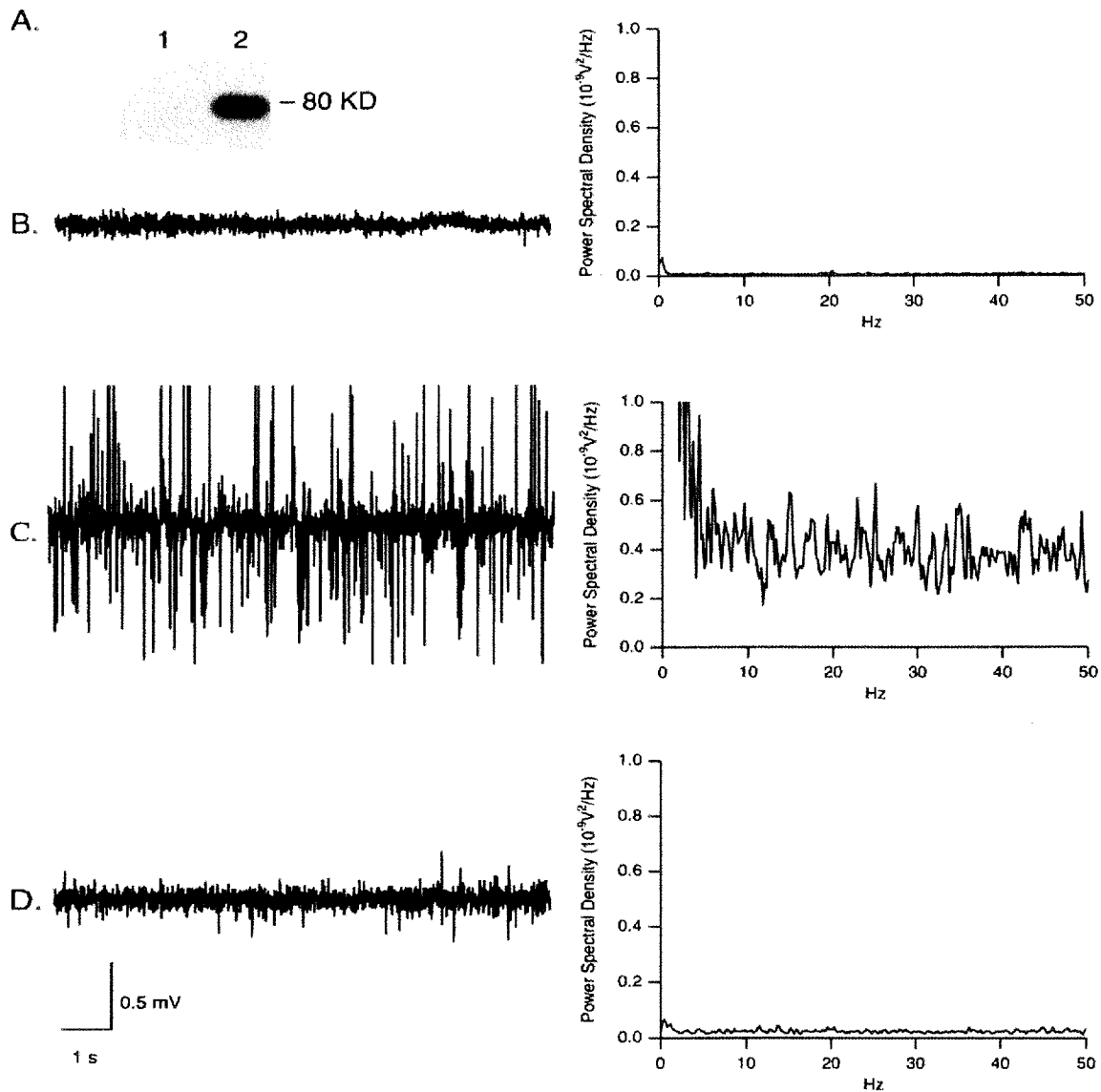
Figure 4

Figure 4. (A) Western blot of wild-type mice probed with anti-SK3 antibody. Lane 1, innervated muscle; lane 2, denervated muscle. (B-D) Representative 10-s EMG recordings from wild-type AT muscle (left),and corresponding power spectral analysis (right). (B) Innervated AT muscle; (C) denervated AT muscle;(D) denervated AT muscle, 3 min after injection of 50 µl of 10 µM apamin.

43

SK3 expression in skeletal muscle does not induce hyperexcitability

To investigate the role of SK3 expression in the generation of skeletal muscle hyperexcitability a mouse was designed that expresses SK3 specifically in skeletal muscle. A transgene was constructed using the mouse muscle creatine kinase (MCK) promoter (Johnson et al. 1989; Shield et al. 1986) to drive muscle specific expression of the mouse SK3 coding sequence. A 1200 bp piece of the MCK 5' flanking sequence with three enhancer mutations was obtained that shows skeletal muscle specific expression in mice (Shield et al. 1996). The MCK-SK3 transgene, containing the MCK piece upstream of mSK3 coding sequence and followed by a human growth hormone polyadenylation signal, was purified and injected into the male pronuclei of fertilized eggs and introduced into the oviducts of surrogate females (materials and methods). Viable pups were genotyped for the transgene using a PCR strategy (materials and methods). Seven separate founder mice were identified that harbored the MCK-SK3 DNA.

Northern blot analysis was used to determine the levels of SK3 RNA produced from the MCK-SK3 founders. Four of the seven founders expressed SK3 mRNA at different levlels (Figure 5A, lanes 1-4), some of which were higher than the levels found in denervated skeletal muscle (data not shown). Tissues including brain, heart, and liver showed no SK3 expression (data not shown) indicating that SK3 is expressed only in skeletal muscle from the MCK-SK3 mice. The SK3 expressing mice were further analyzed for protein expression and skeletal muscle hyperexcitability.

Figure 5

A.

1 Hour Exposure   Overnight Exposure

I. 1. 1. 3. 4. 5.   I. 1. 2. 3. 4. 5.

- 3 Kb

B.

- 80 KD

I. 2. 3. 4. 5. D. I.
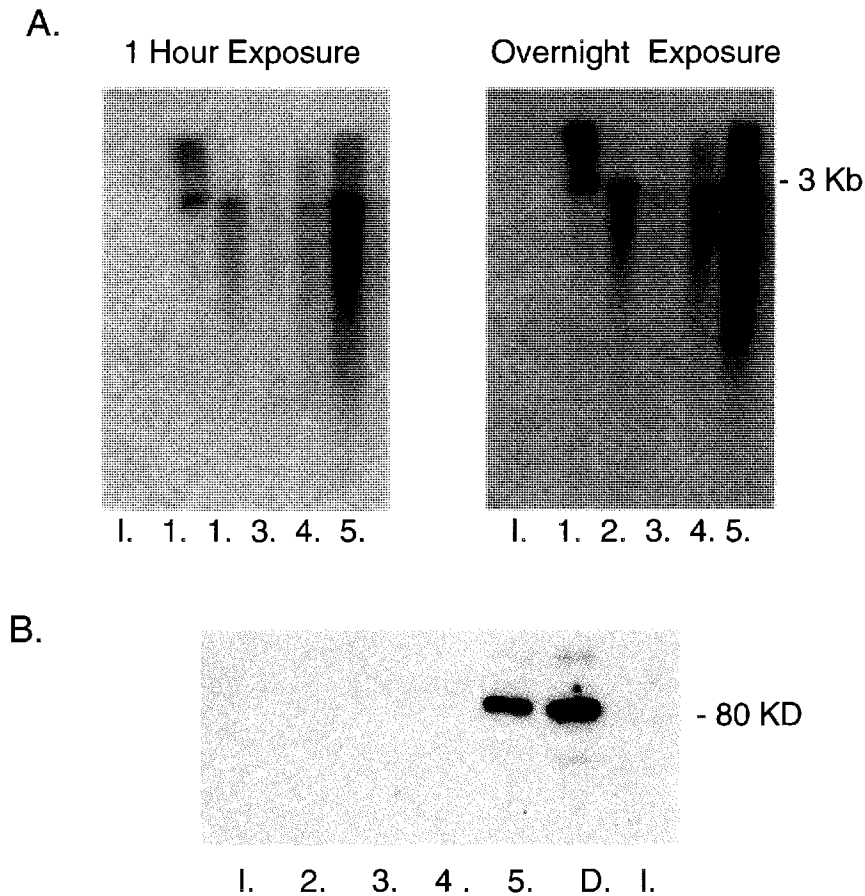
Figure 5.(A) Northern blot of MCK and wt mouse skeletal muscle RNA probed with an SK3 RNA probe. Lane I, wt innervated muscle message; ; lane,1 #1 MCK-SK3 mouse muscle; lane 2, #2 MCK-SK3 mouse muscle; lane3, #3 MCK-SK3 mouse muscle; lane 4, #4 MCK-SK3 mouse muscle; lane 5 #5 MCK-SK3 mouse muscle.

(B) Western blot of MCK-SK3 and wt mice probed with anti-SK3 antibody. Lane I, wt innervated muscle; lane D, wt denervated muscle; lane,1 #1 MCK-SK3 mouse muscle; lane 2, #2 MCK-SK3 mouse muscle; lane3, #3 MCK-SK3 mouse muscle; lane 4, #4 MCK-SK3 mouse muscle.

45

Despite the high levels of SK3 mRNA this message was poorly translated. Only the highest SK3 expressing line of the MCK-SK3 founders showed detectable levels of SK3 protein (Figure 5B). The level of SK3 protein was comparable to levels from denervated mouse muscle as seen in Figure 5. Electromyographic recordings from innervated hind limb AT muscle of the MCK-SK3 mice, expressing SK3 protein, were used to analyze skeletal muscle hyperexcitability. EMG recordings demonstrated that the AT muscle from the MCK-SK3 animal has no spontaneous activity, which resemble recordings taken from wild-type innervated AT muscle (Figure 6 A and B). Therefore SK3 is not sufficient by itself to cause skeletal muscle hyperexcitability in innervated skeletal muscle.

SK3 expression is necessary but not sufficient for denervation-induced hyperexcitability

The role of SK3 channels was examined in more detail using transgenic mice (SK3tTA) in which the murine *SK3* gene has been altered by homologous recombination to include a tetracycline-sensitive gene switch (Bond et al. 2000). In the absence of experimental intervention SK3 is overexpressed, whereas administration of tetracycline or analogs such as doxycycline (dox) into the drinking water abolishes SK3 expression (Bond et al. 2000). Therefore, SK3tTA mice with or without dox treatment were denervated and examined for SK3 expression levels and skeletal muscle hyperexcitability. Western blot analysis showed that in the absence of dox treatment SK3 protein was present in AT muscle obtained from innervated or denervated SK3tTA mice (Fig. 7A, lanes 1 and 2). Expression levels in innervated muscle were comparable

Figure 6

A.

B.

0.5 mV

1 s
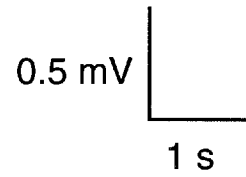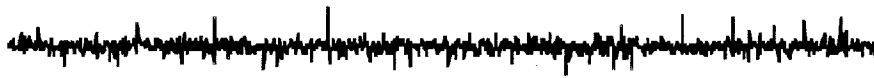
Figure 6. (A)10s EMG recording from wild type mouse innervated anterior tibial skeletal muscle; (B) 10s EMG recording from MCK-SK3 #4 mouse innervated anterior tibial skeletal muscle.

47

Figure 7

A.

B.

C.

D.

E.

0.5 mV

1 s
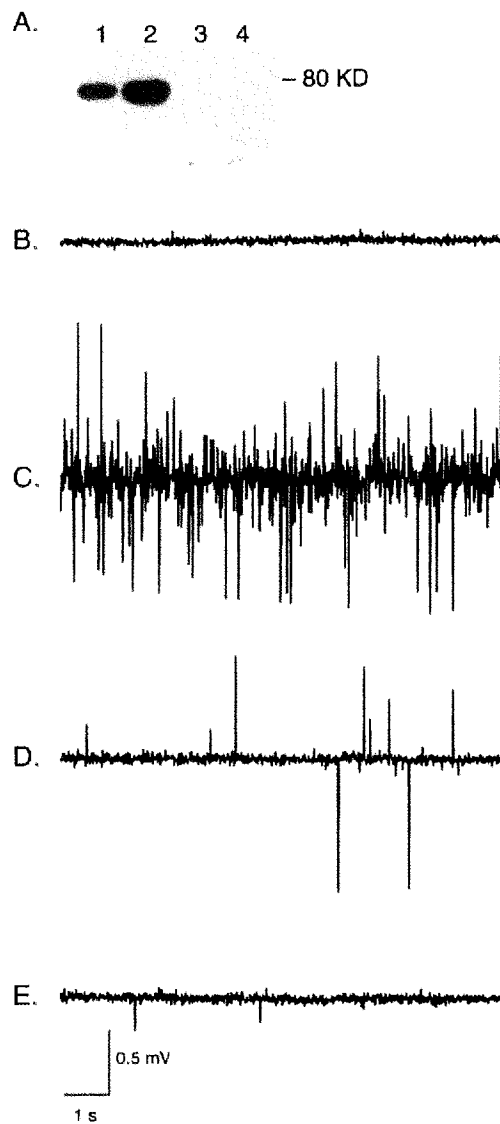
Figure 7. (A) Western blot of SK3tTA mice probed with anti-SK3 antibody.

Lane 1: innervated AT muscle; lane 2: denervated AT muscle; lane 3:innervated

AT muscle from dox-treated animal; lane 4: denervated AT muscle from dox-

treated animal. (B-E) Representative 10-s EMG recordings from SK3tTA mice.

(B) Innervated AT muscle without dox administration; (C) denervated AT muscle;

(D) denervated AT muscle 3 min after injection of 50μ l of 10 μM apamin; (E)

denervated AT muscle from a dox-treated animal.

48

to those seen in denervated wild-type muscle (see Fig. 4A), and denervation resulted in substantially elevated levels. Dox treatment abolished SK3 expression in innervated or denervated AT muscle (Fig. 7A, lanes 3 and 4).

The loss of SK3 protein was consistent with electrophysiological measurements. Currents were recorded from FDB muscle fibers isolated from innervated and denervated wild type or SK3tTa mice with and without dox treatment (Fig. 8A and B). FDB fibers were voltage clamped at -50 mV and depolarized to 40 mV for 10 ms to activate sarcoplasmic reticulum Ca^{2+} release and muscle contraction. Following repolarization to -40 mV, a slowly decaying outward tail current was observed in denervated wild type and innervated or denervated SK3tTA FDB fibres but not in innervated wild type or innervated and denervated SK3tTA dox treated FDB fibres, which reflects SK3 channel activation (Fig. 8A and B). The outward tail current was suppressed by both apamin and dialysis with 20 mM EGTA in the patch pipette solution, to buffer Ca2+ below 1 nM, confirming that it truly represents an SK current (Fig. 9). The mean amplitude of the maximum outward current measured between 50 and 100 ms following repolarization was 0.78 ± 0.05 nA (n = 72) and 0.13 ± 0.01 nA (n = 8) for denervated and innervated wild type fibres, respectively. The mean tail current measured 50-100 ms following repolarization in innervated and denervated SK3tTa mice was 1.07±0.34 nA (n=8) and 1.97±0.717 nA (n=4), respectively. Dox treatment reduced the tail current recorded from the innervated and denervated SK3tTa mice to 0.04±0.01 nA (n=8) and 0.09±0.01 nA (n=6), respectively. Currents from the SK3tTA

Figure 8
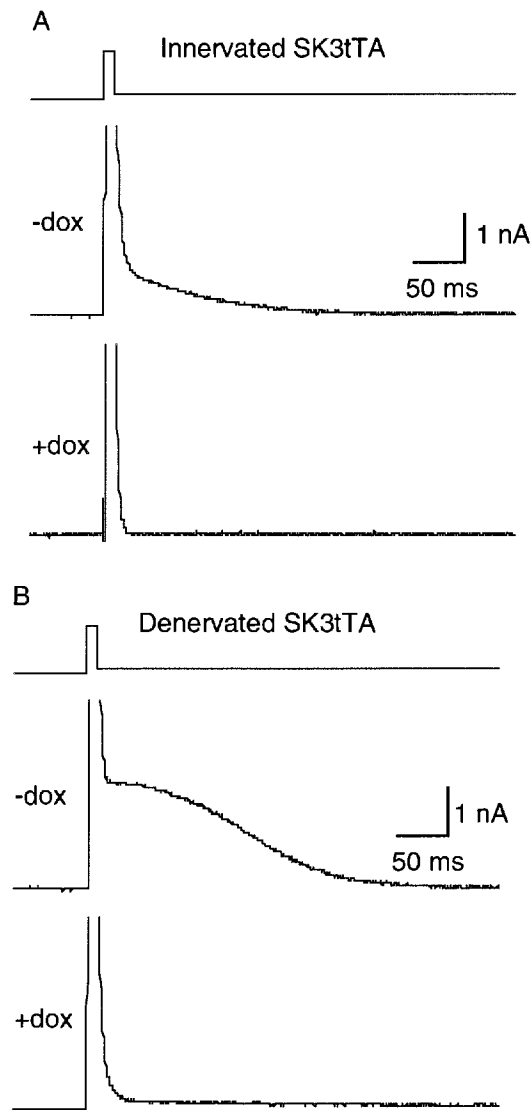
Figure 8. Currents measured from innervated and denervated SK3tTa and wild-type mice. (A) Current recording from innervated SK3tTa FDB isolated from a mouse without (-dox) and with dox treatment (+dox). Currents evoked by a 10-ms depolarization to 40 mV from a holding potential of -50 mV (top trace). Tail currents were recorded on repolarization to -40 mV. Currents during the 10-ms depolarizing pulse to 40 mV were off-scale. (B) Current recordings from denervated SK3tTa FDB without (-dox) and with dox treatment (+dox).

Figure 9

A.

B.
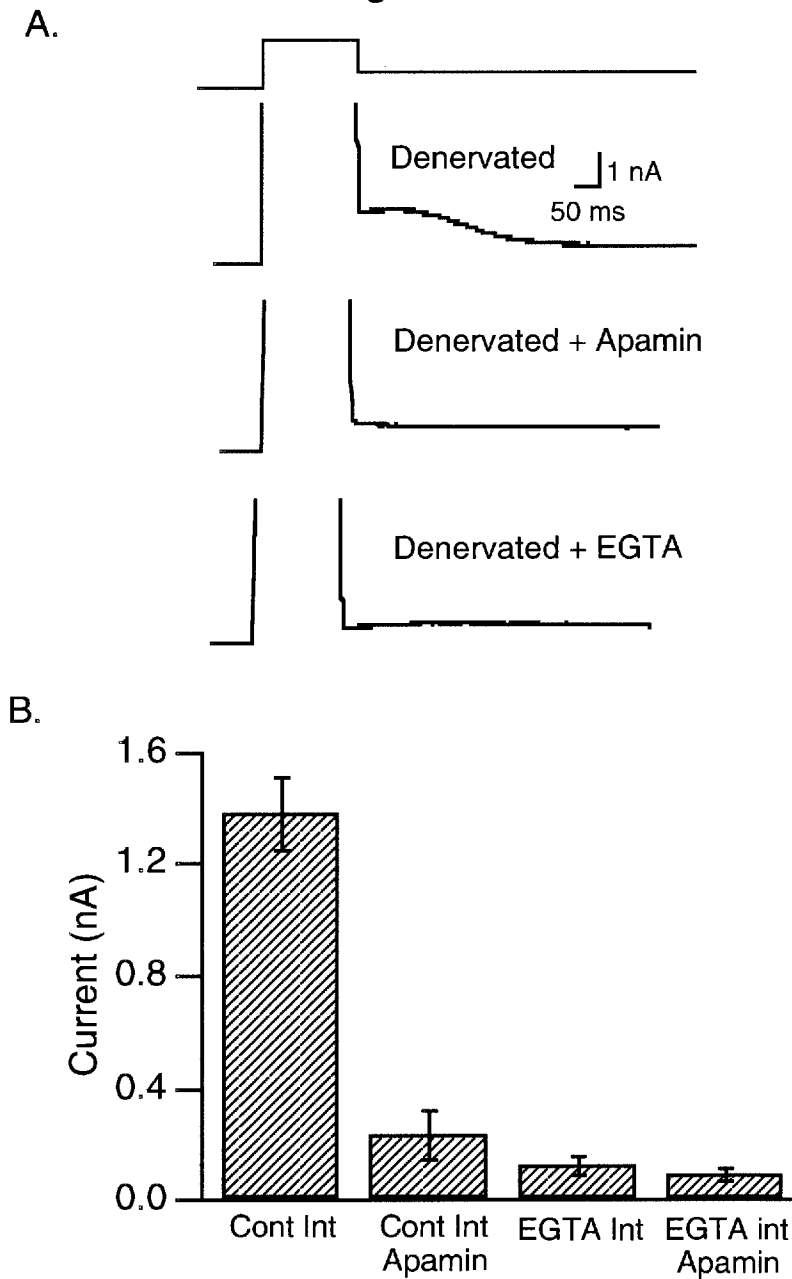
Figure 9: (A) Current recording from denervated wild-type FDB alone or in the

presence of apamin or EGTA. (B) bar graph of mean maximum tail current measured

between 50 and 200 ms in control bath solution or control bath solution containing

1 µM apamin in fibres dialysed with either control internal solution (Cont Int, n = 6) or

EGTA-containing internal solution (EGTA Int, n = 4). Data are means ± S.E.M.

51

dox-treated mice are similar to those recorded from wild-type innervated mice, indicating that expression of SK3 is responsible for the SK tail current, and is completely suppressed by dox.

Despite the presence of SK3 protein and its resulting current, EMG recordings from innervated AT muscle in the absence of dox treatment did not show spontaneously activity (2.0 ± 0.1 x10^{-10} V^2/Hz, n=3; Fig. 7B). In SK3tTA mice, denervation induced higher levels of SK3 expression and hyperexcitability that were not quantitatively different from the denervation-induced hyperexcitability in wild-type muscles (1.6 ± 0.3 x10^{-8} V^2/Hz, n=5; Fig. 7C). As for wild-type denervated muscle, the hyperexcitability in denervated SK3tTA mice was blocked by direct application of apamin (1.1 ± 0.2 x10^{-9} V^2/Hz, n=5; Fig. 7D). In contrast, denervation of SK3tTA mice that had been treated with dox failed to induce hyperexcitability (6.0 ± 2.0 x10^{-10} V^2/Hz, n=5; Fig. 7E). The results from WT and SK3tTA mice are summarized in Fig. 10, and demonstrate that SK3 channels are necessary but not sufficient for generating denervation-induced hyperexcitability.

T-Tubule accumulation of potassium

The role of SK3 in skeletal muscle hyperexcitability was defined through electrophysiological measurements of FDB fibres from wild type C57Blk6 mice. The denervated SK3 tail current was sensitive to apamin, however apamin block took a very long time, ~15 minutes, to develop and this may be due to the narrowed mouth of the T-

Figure 10
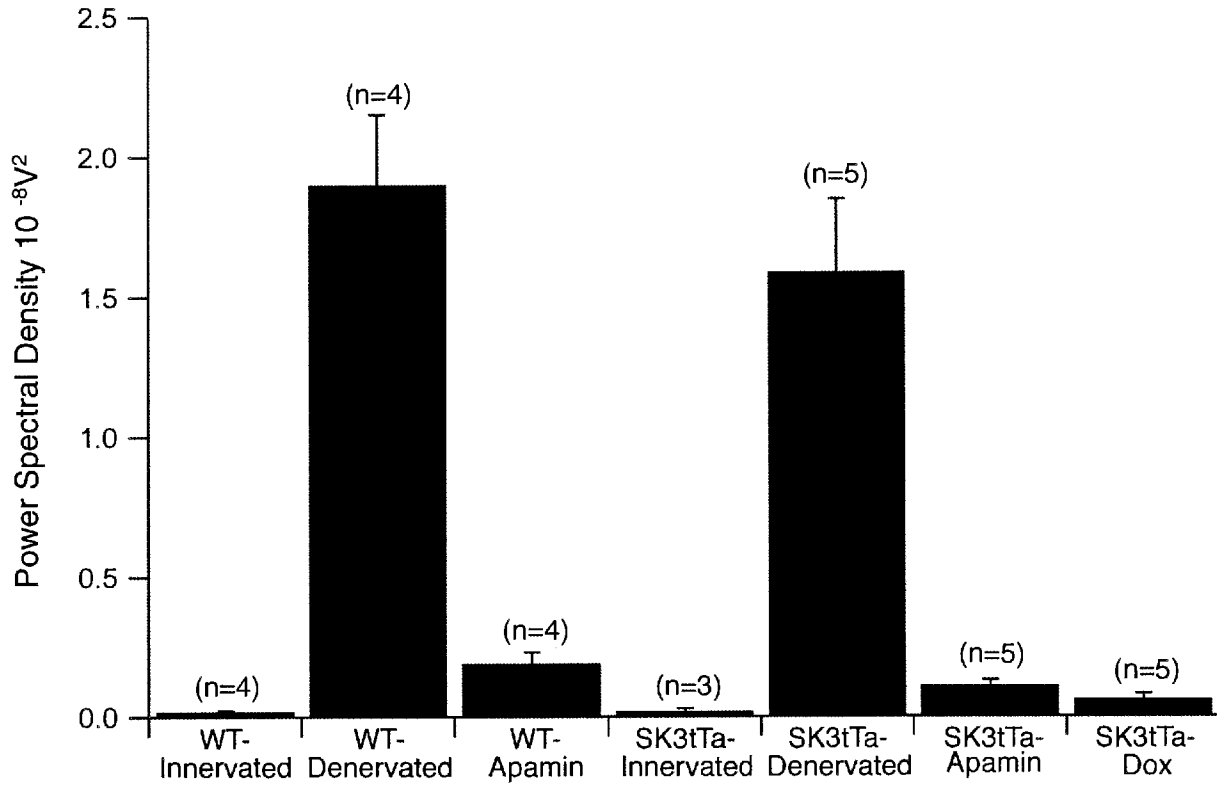
Figure 10. Bar graph of the power spectral density analysis applied to 60-s

EMG recordings taken from the indicated groups. Error bars are ± SEM.

tubule, which could slow the diffusion of apamin into the tubular lumen and affect the time course of SK block. Looking at SK reversal potentials in denervated skeletal muscle provided support for this concept. The reversal potential is the membrane potential that results in no net current flowing through an open receptor. The reversal potential of a channel is greatly affected by the ionic concentration on each side of the polarized membrane, the driving force, which affects the net current flow with a set voltage. The SK3 reversal potential from FDB fibres was determined with increases in the concentration of external K+ from 5 to 50 mM. Currents were activated by a 20 ms depolarizing command to 40 mV from a holding potential of -50 mV, and tail currents were measured over a range of voltages that the cells were returned to, from -80 to -10 mV. To deactivate the voltage-gated currents the end voltage clamp protocol was preceded by a gap potential back to -50 mV for 20 ms (Fig. 11A). The slopes of decaying phase of the tail current measured from 0.14 to 0.2 s (Fig. 11A, vertical lines) were plotted as a function of voltage for each concentration of external K+ and the reversal potential calculated from the voltage intercept of a line fitted to the data points by linear regression. Increasing the external K+ concentration increased the reversal potential (Fig. 11B). Mean reversal potentials changed from -72 ± 2.9 mV in 5 mM K+ to -31.7 ± 2.3 mV in 50 mM K+ (n = 4, Fig. 11C). The mean values were plotted as a function of the K+ concentration and fitted with a logarithmic regression, yielding a slope of 40.7 mV per decade (Fig. 11C). Although these results are consistent with a K+-selective ion channel, the slope was slightly less than that predicted for a purely K+-selective channel (dashed line, Fig. 11C). The measured reversal potential deviated

Figure 11
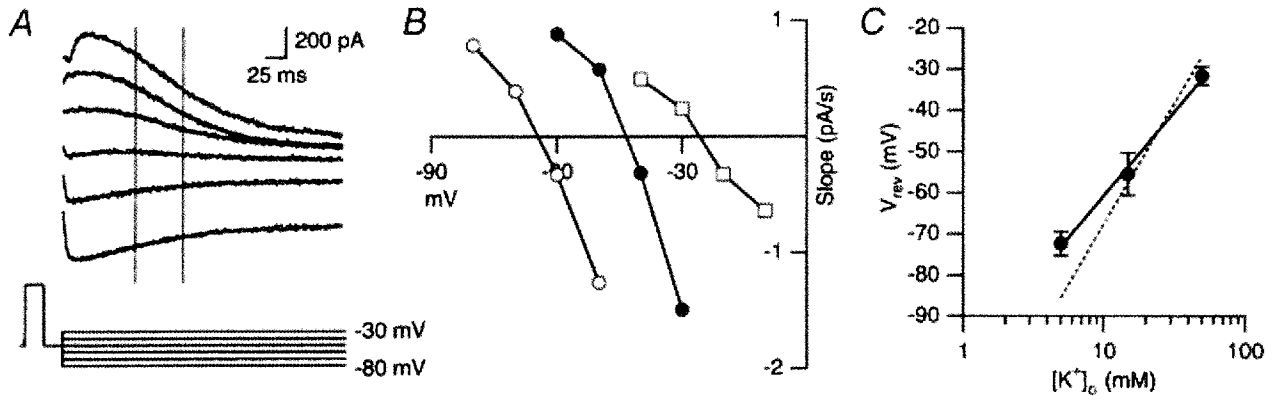
Figure 11. A, family of tail currents measured at tail potentials between -30 and -80 mV

(10 mV increments) in 5 mM external K+. From a holding potential of -50 mV the fibre

was depolarized to 40 mV for 20 ms, repolarized to -50 mV for 20 ms and

subsequently stepped to potentials between -30 and -80 mV (bottom panel). B, the

slope of the decaying phase of the tail currents (measured between the vertical lines in

A) plotted as a function of voltage for a single fibre bath perfused with either 5 m(white

circles), 15 mM (black circles) or 50 mM (white squares) external K+. The reversal

potential was determined by interpolation between points on either side of zero for

each K+ concentration. C, mean reversal potential () plotted versus the log of the

external K+ concentration. Data are means ± S.E.M. (n = 4). The slope of the

continuous line was 40.7 mV per decade. The dashed line represents the relation for a

purely K+-selective channel with a slope of 55 mV per decade.

from the predicted value primarily in low (5 mM) K+. The change in reversal potential in low potassium may be a direct result of potassium accumulation in the t-tubule, which shifts the reversal potential to a more positive voltage similar to the measurement predicted for SK with higher external potassium.

SK3 channels reduce the action potential threshold in denervated skeletal muscle

The propensity to fire an action potential may be altered with t-tubule potassium accumulation as the membrane is more depolarized. Therefore the initiation of action potentials was analyzed between innervated and denervated fibres. FDB fibres were current clamped at −70 mV and given current depolarizing pulses (1 s duration) of increasing amplitude in ~3 mV increments until an action potential was fired. The steady-state potential measured at the end of the pulse at which the first action potential was initiated was taken as the action potential threshold. Figure 11 shows voltage records from innervated and denervated FDB muscles in response to increasing depolarizing current pulses. The action potential threshold was reached at -50 mV in the innervated fibre in Figure 9A. However, the threshold was reduced to -53 mV in the denervated fibre (Fig. 12B). The mean action potential threshold in denervated muscle of -55.6 ± 0.5 mV (n = 21) was significantly less than that measured in fibres obtained from innervated FDB muscle, -47.4 ± 1.2 mV (n = 10, P < 0.01, ANOVA; Fig. 12E). Application of apamin (1 μM) increased the action potential threshold in denervated fibres to -48.2 ± 1.8 mV (n= 6; Fig. 12E), similar to that measured in innervated fibres. Suppression of the SK tail current in denervated fibres by dialysis with 20 mM EGTA in

56
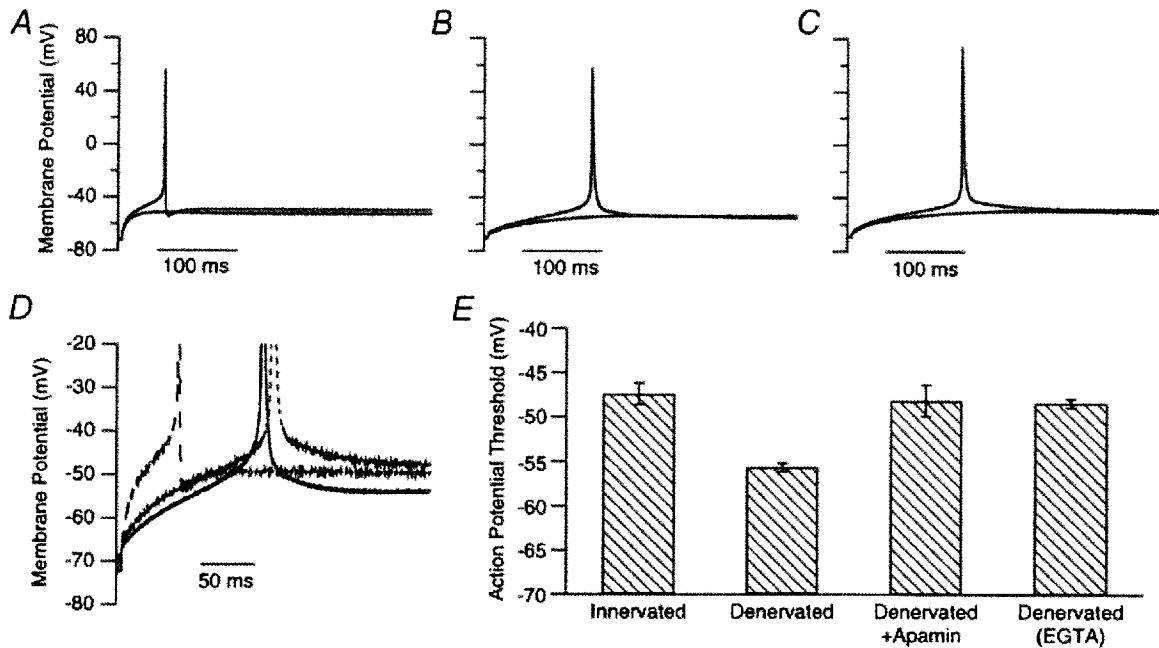
Figure 12

Figure 12. A, action potentials recorded in an innervated fibre in current clamp

mode. A holding current was applied to set the resting membrane potential at -70

mV. Superimposed traces are shown for a subthreshold and threshold level of

current injection that just initiates an action potential. B, voltage records for

subthreshold and threshold current injection in a denervated fibre. C, voltage

records from the same fibre as in B perfused with 1 μM apamin. D, overlay of

action potentials recorded in innervated fibres (long-dash trace), denervated

fibres (continuous trace) and denervated fibres perfused with apamin (short-dash

trace). E, bar plot of mean threshold for innervated fibres (n = 10), denervated

fibres (n = 21), denervated fibres perfused with 1 μM apamin (n = 6) and

denervated fibres dialysed with 20 mM EGTA (n = 6). Data are means ± S.E.M.

57

the patch pipette solution, to buffer Ca2+ below 1 nM, also yielded on average an action potential threshold of -48.4 $\pm$ 0.5 mV (n = 6) similar to that of innervated fibres and denervated fibres exposed to apamin (Fig. 12E). These results show that expression of SK channels in denervated skeletal muscle fibres alters the action potential threshold, consistent with an increase in excitability of the denervated fibres.

Methods

Denervation

Animal care and handling were in accordance with Institutional Animal Care and Use Committee guidelines. Mice between the ages of P8-P10 were anesthetized with an isoflourane-oxygen mix. In one hindlimb, a section of the sciatic nerve (5 mm) was excised through a small (3-5 mm) incision over the hip. The incision was sutured with a single stitch and formulated Cyanoacrylate (Vetbond, 3M, St. Paul, MN) was applied to the wound. For tissue harvest, animals were humanely sacrificed 4-10 days after denervation by deep isoflourane anesthesia and cervical dislocation.

Electrophysiology

An aliquot of the muscle fibres was plated in a recording chamber perfused with Ca^{2+}-free Tyrode solution containing (mM): 140 NaCl, 5 KCl, 2.8 $MgCl_2$, 10 dextrose, 10 Hepes, pH 7.35. The whole-cell recording configuration was established with 2-4 M electrodes filled with (mM): 145 potassium aspartate, 3.5 NaCl, 1 $MgCl_2$, 6.5 NaOH, 0.05 EGTA, 10 Hepes, 5 MgATP, pH 7.1. Following whole-cell formation, the external bath solution was switched to Tyrode solution containing 1.8 mM Ca^{2+}. The majority of fibres contracted in response to membrane depolarization in the absence of external Ca^{2+}, consistent with skeletal muscle E-C coupling, and only these fibres were studied. All experiments were performed at room temperature. Fibre length and width were

measured using an ocular micrometer with 100 μm divisions. Fibres were observed with a 40x objective yielding an optical resolution of 2.5 μm between divisions. Half the distance between divisions was easily resolved giving a measured error of $\pm$1.25 μm. Sarcomere spacing, determined from the number of sarcomeres over 10 divisions, was routinely 2-2.5 μm. Only fibres with a sarcomere spacing greater than 2 μm were considered relaxed and used in these experiments.

Whole-cell recordings were performed using an EPC9 (HEKA Elektronik) or Axopatch 200B (Axon Instruments) amplifier and Pulse software (HEKA Elektronik) interfaced to a Macintosh Power PC computer. In voltage clamp mode, series resistance and whole-cell capacitance were electronically compensated; 50-80 % of the series resistance was electronically compensated. Constant current clamp mode was used for action potential measurements. The resting membrane potential was set to -70 mV. Series resistance, measured as an instantaneous jump in membrane potential to an applied current pulse, was nullified by applying series resistance compensation with the percentage compensation set at 100 (Axopatch 200B).

In experiments investigating reversal potential, equimolar KCl was substituted for NaCl. The pipette solution for testing the effects of high internal EGTA

comprised (mM): 120 potassium aspartate, 10 NaCl, 1 $MgCl_2$, 0.7 $CaCl_2$, 20 EGTA, 10 Hepes, 5 MgATP, pH adjusted to 7.1 with KOH; the free Ca^{2+}

concentration was ~10 nM.

Data analysis was performed off-line using PulseFit (HEKA Elektronik) and IGOR software (WaveMetrics, Inc., Lake Oswego, OR, USA). Statistical comparisons were performed with either Student's paired t tests or one-way ANOVAs with Tukey HSD post hoc tests to determine which combinations differed. Post hoc tests were performed only on data sets in which the P value of the ANOVA was less than 0.05. Data sets with $P <$ 0.05 were considered significant. All statistical tests were performed with the Instat program (Graphpad) and IGOR. Data are presented as means $\pm$ S.E.M. (n, number of fibres). SK currents were examined in muscle fibers from the flexor digitorum brevis muscle (FDB) as previously described.[16] Whole-cell recordings were performed using an EPC9 (Heka Elektronik, Mahone Bay, Nova Scotia) or Axopatch 200B (Axon Instruments, Union City, CA) amplifier and Pulse software (Heka Elektronik) interfaced to a Macintosh Power PC computer (Apple Computer, Cupertino, CA); series resistance (50-80 %) and whole-cell capacitance were electronically compensated. Data analysis was performed off-line using PulseFit (Heka Elektronik) and IGOR software (WaveMetrics, Lake Oswego, OR).

Electromyography

EMG recordings were performed under isoflourane anesthesia using 30-gauge concentric needle electrodes (Meditech, Westwood, MA) with sampling of at least three separate locations within the anterior tibial (AT) muscle. The signal was amplified through a DAM 50 amplifier (World Precision Instruments, Sarasota, FL) and digitally

recorded using a Mac Lab chart recorder. Analysis was performed using the data recorded during the first minute and the fourth minute following injection of either apamin (Alomone Laboratories, Jerusalem, Israel; 50μl of 10μg/ml) or saline. EMG activity was analyzed using power spectral density analysis and significance was determined using both paired t-test and analysis of variance (ANOVA). Fast Fourier transforms, applied to 1024-point segments, were performed on EMG traces over a 60-second interval. The magnitude of the fast Fourier transforms, sum of the squares of the real and imaginary parts, was averaged to produce a power spectral density. The power spectral density was integrated over a frequency range of 5 to 50 Hz for each trace.

Transgenic Mouse Design (Pronuclear Microinjection)

Eggs were harvested from superovulated females and fertilized in vitro. Holding the fertilized egg in place many copies of linearized MCK-SK3-HghPA DNA was injected into the male pronucleus. These eggs were then introduced into the oviducts of surrogate females (Hogan et al. 1994). Seven separate lines from individually injected ponuclei were obtained all containing varying transgene copy number and chromosome insertion points.

The transgene was produced using the skeletal muscle specific MCK promoter, (Johnson et al. 1989) which was fused to the mouse SK3 coding sequence (Kohler et al. 1996; Bond et al. 2000), and followed by the human growth hormone polyadenylation (PA) signal (Bond et al. 2000). 1200 bp of the MCK promoter were used that contain

62

three e-box mutations allowing skeletal muscle specific transcription (Johnson et al. 1989). The mouse coding sequence was obtained through RT PCR, sequenced, and tested in cells to ensure proper expression and channel function.

Isolation of FDB fibres

FDB muscle, isolated from the hindfoot, was pinned out in a 35 mm dish coated with Sylgard (Dow Corning, MI, USA). The muscles were incubated in Dulbecco's modified Eagle's medium (DMEM) containing 10 % fetal calf serum, 100 μg ml-1 penicillin-streptomycin and 0.05 % collagenase 1A (Sigma, St Louis, MO, USA) for 1.5-2 h in an incubator at 5 % CO_2 and 37 °C. Single muscle fibres were dislodged by gentle trituration in DMEM and were studied within 6 h.

Western Blot Analysis

Membrane proteins were prepared from cultured cells or muscle tissue. Briefly, cells were dounce-homogenized in 10mM Tris (pH 7.5) with protease inhibitors and debris was pelleted at 1000xg for 10 minutes. The membranes were pelleted from the supernatant at 50000xg for 10 minutes, resuspended in 0.6M potassium iodide, repelleted for 10 minutes, washed twice in 10mM Tris (pH 7.5), and resuspended in 20mM Tris (pH 7.5) with protease inhibitors. Following electrophoresis through an 8% denaturing polyacrylamide gel, 10 μg of protein were prepared as a Western blot on nitrocellulose. SK3 antibody (Alomone Laboratories, Jerusalem, Israel) was used to probe the membranes (1:1000 dilution), washed with phosphate-buffered saline

containing 0.1% Tween, and incubated with goat anti-rabbit horseradish peroxidase-coupled secondary antibody (Santa Cruz Biotechnology, Santa Cruz, CA; 1:25,000 dilution). Horseradish peroxidase was illuminated using Pico-signal (Pierce, Rockford, IL) and exposed on Kodak X-omat Blue film (Kodak, Rochester, NY).

Discussion

The primary function of skeletal muscle is controlled contractions through the process of excitation-contraction (e-c) coupling, achieved by coupling excitability mediated by surface and transverse tubular ion channels to the specialized myosin contractile apparatus. The second messenger that couples membrane excitation and contraction is Ca^{2+}. Therefore, aberrant ion channel function due to mutations in ion channel genes, altered levels of expression, or subcellular mislocalization of ion channels may result in abnormal e-c coupling (Beam et al. 1986; Takekura et al. 1995). The innervating nerve maintains normal synaptically controlled e-c coupling, whereas denervation results in hyperexcitability and spontaneous contractile activity that reflects changes in the expression profile of many genes, including ion channels (Hartzell & Fambrough, 1972; Rogart & Regan, 1985; Mishina et al. 1986; Heathcote, 1989; Brenner et al. 1990; Gonoi & Hasegawa, 1991; Lupa & Caldwell, 1994). Among the changes consequent to denervation is induction of the gene encoding the small conductance Ca^{2+}-activated K^+ channel, SK3 (Pribnow et al. 1999). Expression of SK3 channels has been implicated in denervation-induced hyperexcitability because direct application of apamin, a selective blocker of SK channels, greatly reduces the hyperexcitability (Vergara et al. 1993).

The results presented here show that SK3 channel expression is necessary for denervation-induced hyperexcitability, but it is not sufficient. In SK3tTA mice, selectively abolishing SK3 expression abolished denervation-induced hyperexcitability. However, overexpression of SK3 in normal innervated muscle in the MCK-SK3 and SK3tTA mice,

65

at levels similar to those seen after denervation in wild-type muscle, did not result in hyperexcitability. This suggests that other alterations in skeletal muscle gene expression consequent to denervation are required to unlock the effects of SK3 channels. The resting membrane potential of skeletal muscle is close to the potassium equilibrium potential (E_K; Albuquerque and Thesleff, 1968; Almers, 1980; Neelands et al. 2001) suggesting that expression of SK3 channels alone may have little impact on excitability, consistent with the lack of hyperexcitability observed in the SK3tTA mice overexpressing SK3 channel activity in innervated skeletal muscle. This is due to the activation of inward rectifier potassium channels near E_K that counter the potassium flux by SK. However, the array of alterations consequent to denervation results in a significantly depolarized resting membrane potential (from -79 mV to -57 mV; Albuquerque and Thesleff, 1968; Almers, 1980), substantially removed from E_K. Under these circumstances, SK3 expression will alter excitability. Indeed, SK3 channels in denervated mouse skeletal muscle cause a decrease in the action potential threshold. Therefore, changes in the levels or functions of another ion channel following denervation, that induce a decreased resting membrane potential are necessary for the SK3-mediated hyperexcitability. Although the proteins underlying the decreased resting membrane potential have not yet been identified, lower expression levels of chloride channels, inwardly rectifying potassium channels, or sodium channel isoform switches are possible candidates (Heathcote, 1989; Venosa and Kotsias, 1985; Trimmer et al. 1990).

66

Potassium channel activity generally causes a hyperpolarizing effect on membrane potential, raising the apparent paradox of K^+ channel-mediated hyperexcitability: why do SK3 channels make skeletal muscle hyperexcitable? This may reflect the unique cytoarchitecture of skeletal muscle. Expression of SK3 channels in the transverse tubules may result in an accumulation of extracellular K^+ that does not readily diffuse from the restricted tubular space, resulting in a depolarizing, hyperexcitable condition. Support for this model comes from measurements of SK current reversal potentials in denervated skeletal muscle in different extracellular K^+ concentrations.

Many different inherited myotonic disorders result in skeletal muscle hyperexcitability. However, only the myotonia associated with myotonic dystrophy exhibits apamin sensitivity (Behrens et al. 1994) and increased SK3 expression (Kimura et al. 2000). Interestingly, patients with that disorder develop varying degrees of neuropathy (Coers, 1955; Mac Dermot 1961; Mondelli et. al. 1993). Therefore it is possible that compromised nerve function or nerve death consequent to myotonic dystrophy may lead to hyperexcitability that mirrors the changes induced by acute denervation.

CHAPTER 3

Determinants Contributing to Estrogen-Regulated Expression of SK3

David Jacobson, David Pribnow, Paco S. Herson,

James Maylie[#], John P. Adelman[*]

[#] Department of Obstetrics and Gynecology and Vollum Institute

Oregon Health & Sciences University, Portland, Oregon

Abstract

The rat SK3 gene encodes a small conductance Ca2+-activated K+ channel that is transcriptionally regulated by estrogen. To examine determinants of rSK3 gene expression, the CAP site was defined and the promoter was identified. A 33 base pair sequence adjacent to the promoter was shown to act as an enhancer in L6 cells that express SK3 and estrogen receptor alpha (ERα). The 33 bp enhancer was unable to stimulate transcription in Cos7 cells that don't express SK3 or ERα. However when cotransfected with ERα and stimulated with 17β-estradiol (E2) the enhancer was activated. Interestingly, expression of ERα in Cos7 cells and E2 treatment was sufficient to induce expression of the endogenous SK3 gene. Only Sp1 and Sp3 specifically bound to the enhancer from Cos7 and L6 nuclear extracts, however ERα increased Sp1s affinity for the enhancer. The stimulation of SK3 transcription agrees with the increase of SK3 RNA found in the rostral hypothalamus in response to estrogen injection. However when ovariectomized mice were stimulated with E2 injections the levels of SK3 transcription were reduced 10 fold in uterus tissue, when compared to tissue harvested from animals given mock injections. The estrogen regulation observed in uterus is the opposite of that seen in Cos7 cells and in the rostral hypothalamus (Bosch et al. 2002), but may be important in respect to estrogen regulation working through an Sp motif, which can have both positive and negative affects on transcription. Indeed the levels of internally translated short Sp3, which lead to decreased transcription, are only expressed in estrogen

69

treated uterus tissue. A model consistent with the data is that immediately following estrogen stimulation ERα increases the binding of Sp1 to the SK3 33 bp enhancer, stimulating transcription, whereas continued E2 stimulation leads to accumulation of the short isoforms of Sp3 which competes with Sp1, reducing SK3 transcription.

Introduction

SK channels are important regulators of excitability. Activated by elevated levels of intracellular Ca^{2+}, such as occur in neurons during an action potential, K^+ efflux through SK channels hyperpolarizes the membrane. Three SK channels, SK1, 2 and 3, and a related intermediate conductance channel, IK1, have been cloned (Kohler et al. 1996; Ishii et al. 1997; Joiner et al. 1997). They are all Ca^{2+}-activated, voltage-independent, and K^+-selective and form a distinct lineage within the diverse K^+ channel superfamily. Functional channels are heteromeric complexes of four pore-forming a subunits, and the Ca^{2+} sensor protein, calmodulin which mediates Ca^{2+}-gating (Xia et al. 1998; Keen et al. 1999; Schumacher et al. 2001).

A role for SK3 in reproductive endocrinology is emerging. SK3 is expressed in many areas of the brain including the preoptic area (POA) of the rostral hypothalamus (Fleming et al. 1994; Numan et al. 1997; Wagner et al. 2001; Bosch et al. 2002), a region that contains a large proportion of GnRH neurosecretory cells that also express estrogen receptors (ERs; Silverman et al. 1979; Butler et al. 1999; Skynner et al. 1999; Hrabovszky et al. 2000). Pulsitile GnRH release from these cells likely reflects endogenous, rhythmic excitability; action potentials increase intracellular Ca^{2+} that induces exocytosis while also activating SK channels that hyperpolarize the membrane and terminate

71

excitability. GnRH secretion is also modulated by a feedback loop mediated by gonadal steroids such as estrogen (Ferin et al. 1984), and estrogen directly affects SK channel function (Wagner et al. 2001). In addition, estrogen mediates classical actions on SK3 gene expression. SK3 mRNA levels in the rostral hypothalamus were elevated by injection of E2 into ovariectomized female guinea pigs (Bosch et al. 2002).

SK channels are also important in gonadotropes. Episodic GnRH release results in rhythmic release of gonadotropins from anterior pituitary gonadotropes. The rhythmic exocytosis is caused by underlying oscillations in the levels of intracellular Ca^{2+}. Binding of GnRH to its receptor activates the phosphoinositide pathway and release from intracellular Ca^{2+} stores; each round of Ca^{2+} elevation induces a burst of exocytosis. The elevated Ca^{2+} levels also activate apamin-sensitive SK channels that hyperpolarize the cell membrane. This removes inactivation from voltage-gated Na^+ and Ca^{2+} channels and allows action potential firing that terminates the hyperpolarization and initiates a new round of oscillation (Tse and Hille 1992; Tse et al. 1993; Tse et al. 1995, Hille et al. 1995).

SK3 channels are also implicated in the rhythmic uterine contractions required during birth. In SK3 transgenic mice, parturition was compromised when gene expression was higher than normal, and this condition was reversed upon down-

regulation of SK3 (Bond et al. 2000). The problems giving birth are likely due to SK3 expression in uterine smooth muscle, a tissue that is subject to hormonal regulation during the female cycle, particularly through the actions of estrogen (Bond et al. 2000).

Coronary smooth muscle shows profound gender-specific differences in diameter that are related to estrogen (Wellman et al. 1996; Knot et al. 1999). SK3 is expressed in smooth muscle endothelial cells where SK3 channels appear to modulate the release of EDHF that regulates myogenic tone (submitted). Endothelial smooth muscle SK3 expression also affects arterial and bladder development (Herrera et al. 2000; Hasegawa et al. 2001; Burnham et al. 2002). In addition, SK3 is expressed in embryonic skeletal muscle (Pribnow et al. 1999), and skeletal myoblasts express functional estrogen receptors that mediate increased growth upon exposure to estrogen (Kahlert et al. 1997).

L6 is a rat skeletal muscle cell line that expresses SK3 and ERs (Pribnow et al. 1999; Kahlert et al. 1997), while neither are expressed in Cos7 cells, derived from monkey kidney epithelium. These cell lines were used to investigate transcriptional regulation of the rSK3 gene.

Results

Identification of the mouse SK3 transcriptional start site

Nucleotide sequence comparisons from multiple independent rSK3 cDNA clones implicated a region of genomic DNA that might contain the transcriptional start site for rSK3. Therefore, a 6 kb sequence of rat genomic DNA including this area was determined (Genbank accession number AC133222.1). Initial experiments to identify the start site for rSK3 transcription used rt-PCR with RNA extracted from L6 cells, which express SK3. The PCR was performed with a single 3' oligonucleotide directed to a sequence within the second exon in conjunction with a series of 5' oligonucleotides directed to sequences progressively 5' from the coding sequence (Figure 13A). When oligonucleotides 3 or 4 were employed, a product was obtained that was consistent with the size predicted by cloned cDNA sequences. However, when oligonucleotides 1 or 2 were employed, residing slightly farther 5' in the genomic DNA sequence, no product was detected (Figure 13B). Identical results were obtained using cDNA derived from denervated skeletal muscle that also expresses the SK3 gene (Pribnow et al. 1999; not shown), suggesting that transcription initiates between oligonucleotides 2 and 3. The CAP site was precisely defined by results obtained from RNA ligase-mediated RACE (RLM-RACE; Schaefer et al. 1995). RNAs from L6 myotubes, denervated skeletal muscle, and Cos7 cells that do not express SK3, were dephosphorylated and decapped prior to ligation of an RNA oligonucleotide onto

Figure 13

A

AGCGCCAACGTTCATCCCGGATTGCTGTGGGCATCAGTTATCCTGACCATACCTCCAAGAGGAAAGAAGG

CAGCTGCTCAGCTCGGGGGCGGAGTGTGGAAGGGTCGGAGTGGTAGTGGTCTTGGAGCAAAAACTACA

GTTCCCAGTCCTCGTTGCGCTGCCTCCCGGCGAGGAGCGAAGGATGGCAGGCCCCTTCTTTGAGGCGG

AGCCTGATTGGGAGGCGGAGTTAGGAGGGGGGTTGGAGAGTTAAGCTAAGCCAATGAAACTGCTGGCTAA
1   2

TAAGTGGGCTTGGCTTGCCATATAACAGTGTCAGGAGGAGGAGAGCGAAGCGATTGAGCCAGCGAGGAG
3   CAP

TGAAGCTGAGTCTGCCTCATTCACTCCTAGAGGACCGCCTTCAGAATAGAGTTCTTTTCGCCCCTTCCTC
4

CTTCTCCCAGCTCCTCTCCTGGCTTTTCTATCCGCCCAATACAATGCACACTCGAGTGGCAGCCCCAGAG

AACTGAAGCAAACCAAAGAGAGAGGACTGGAGCCAAGACACTTCTGGTGGGGAAGCTTGGATGCCTGG

CTTTCTTTGAGGTCATCTTTGGAACGAGGGTGGCTTTGGGGTGGAGGGTCGTGCTGCAGGGAACCCAG

CCAGGCCCCAAGATGGACACTTCTGGGCACTTCCATGACTCGGGGGTGGGG

B   C   D

Figure 13. Nucleotide sequence and CAP site localization in the 5' flanking region of the rSK3 gene. A) Schematic showing the 5' flanking region and the exon (boxes) intron (lines connecting boxes) mosaic of the first two exons. Arrows (1-4) depict the positions of primers used in the PCR in conjunction with primer 5 for localizing the CAP site. The nucleotide sequence extends 258 nucleotides 5' from the CAP site determined by RLM-RACE. TATA and CAAT boxes, and Sp consensus binding sites are boxed. The 33 bp enhancer (see text) is over lined. B) Identification of the CAP site for rSK3 transcription using rt-PCR analysis with cDNA derived from L6 cells. Products of the predicted size were generated using primers 3 or 4 but not with 1 or 2, in conjunction with primer 5. C) RLM-RACE products from denervated rat skeletal muscle (D), L6 myotube (T) and Cos7 (C) RNAs. D) Northern blots of L6 myotube (T), Cos7 (C), and denervated (D) skeletal muscle. The blot was probed with rSK3 5' untranslated region sequences. Relative loading was determined by reprobing the blot with a radiolabeled oligonucleotide specific for 18S RNA (below).

the 5' termini. The RNAs were then reverse transcribed using an oligonucleotide directed to a sequence 3' of the rSK3 translation start site. The resulting cDNA was used to amplify the rSK3 5' end with 3' and 5' specific oligonucleotides, yielding a single product from myotube and denervated muscle cDNA; no product was detected from Cos7 cells (Figure 13C; see methods). The nucleotide sequences of 20 clones derived from each of the positive cDNAs were identical, and identified a CAP site for rSK3 transcription (see Figure 13A). Previous Northern blot analysis of denervated skeletal muscle or L6 myotube RNA using the SK3 coding sequence as a probe detected two hybridizing species of ~3 and ~10 kb (Pribnow et al. 1999). Nucleotide sequences derived from 3' RACE strongly suggested that the differences in the two classes of transcripts reside entirely in alternative polyadenylation sites ~7 kb apart (unpublished data). This is consistent with the single transcription initiation site identified by rt-PCR and RLM-RACE. Further support for this conclusion was obtained from Northern blots probed with 5' untranslated region sequences that detected both rSK3 RNAs (Figure 13D). Taken together, the results identify a start site for rSK3 transcription 305 nucleotides 5' from the translational initiator codon.

Examination of the genomic DNA sequences 5' to the identified CAP site suggested potential promoter elements, a TATA-box 28 nucleotides from the transcriptional start site and a CCAAT-box an additional 35 nucleotides in the 5' direction. Three other consensus sites for transcription factors were identified

76

within 341 nucleotides of the CAP site, two Sp motifs (-103 to -107 and -121 to -125; Kadonaga et al. 1987) and one binding site for the muscle developmental factor, MyoD (-249 to -259; Pinney et al. 1988).

Reporter assays identify the SK3 promoter and a cell type-specific enhancer sequence

L6 myotubes (ATCC CRL-1458; 39) express SK3 mRNA and protein whereas Cos7 cells do not (Figure 13D). To identify the rSK3 minimal promoter and test for enhancer sequences, two series of luciferase reporter plasmids were constructed and transfected into L6 or Cos7 cells. One series of plasmids, promoter-reporter constructs, contained fragments of rSK3 genomic DNA fused directly to luciferase (Figure 14A), while a second series of plasmids, enhancer-reporter constructs, contained rSK3 genomic DNA fragments cloned 5' to the prolactin (PRL) minimal promoter that directed luciferase expression (Figure 15A).

Results from promoter-reporter constructs showed that the rSK3 minimal promoter was contained within the proximal 82 bp of 5' flanking sequence. Extracts from L6 cells transfected with reporters harboring a 72 bp fragment (beginning 10 bp 5' of the CAP site; P2) showed a 62-fold increase in luciferase activity compared to cells transfected with the parent plasmid (Figure 14B, inset), and reversing the orientation of the 72 bp fragment virtually eliminated luciferase

Figure 14

A

Promoter Reporters

B
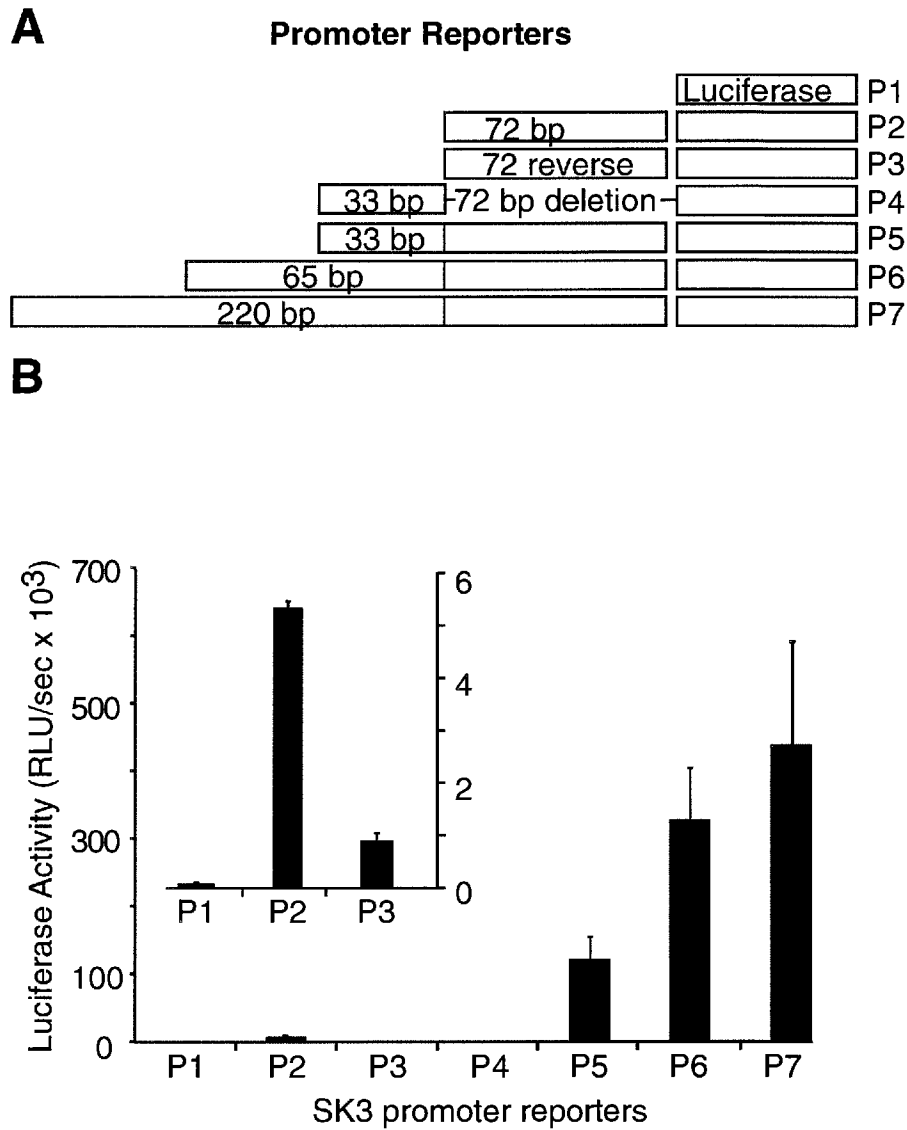
Figure 14. Identification of the rSK3 minimal promoter. A) Promoter-reporter constructs with rSK3 5' flanking sequences fused to the luciferase coding sequence. The indicated 72 bp of 5' rSK3 flanking sequence begins 10 bp 5' of the identified CAP site. B) Luciferase expression levels from L6 cells transfected with the indicated rSK3 promoter-reporter constructs. Inset shows rescaled comparisons for constructs 1, 2, and 3 identifying the minimal rSK3 promoter. Results are presented as ±SEM for n≥6.

Figure 15

A

Enhancer Reporters

B
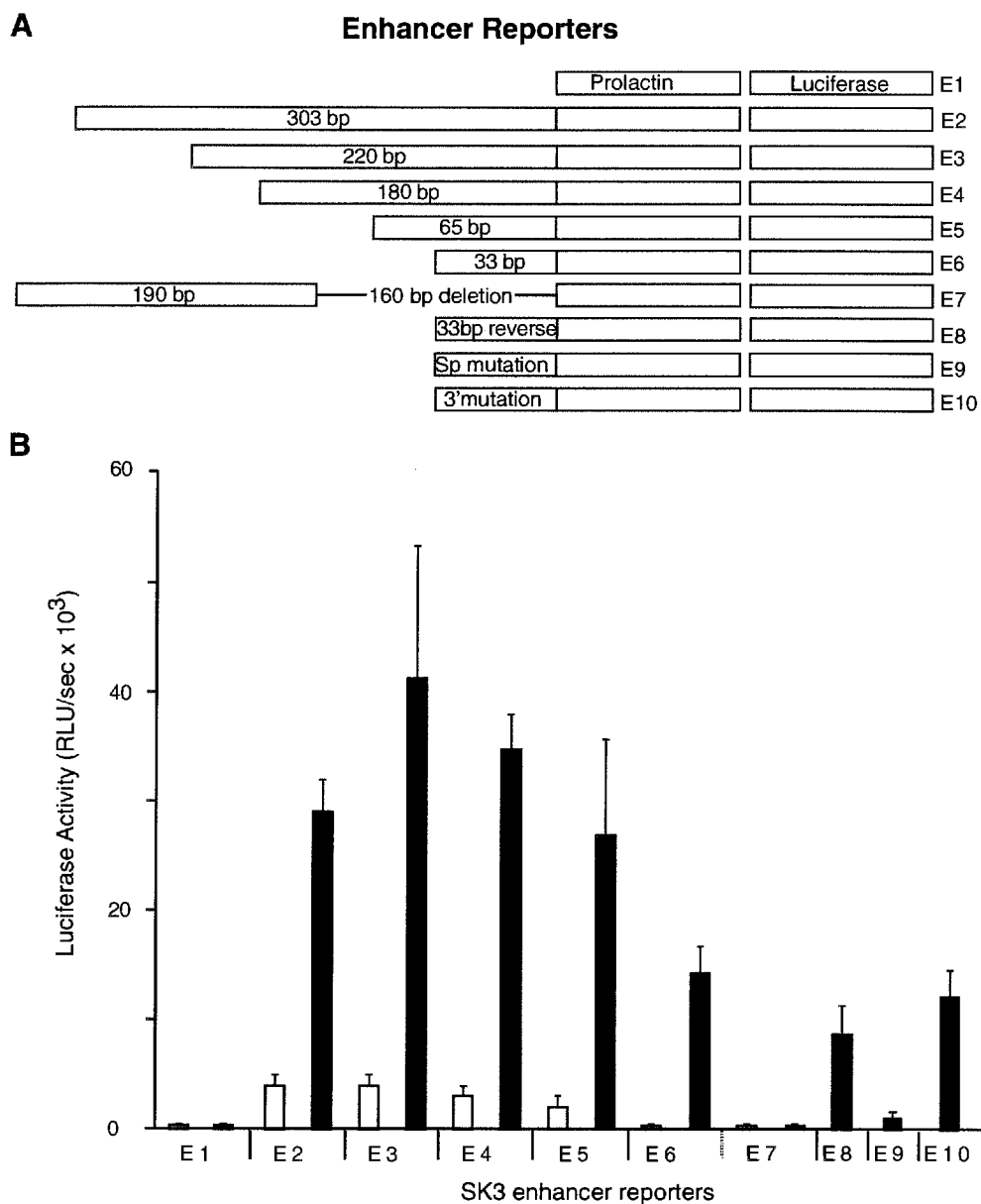
Figure 15. Identification of rSK3 enhancer sequences. A) Enhancer-reporter constructs fusing the indicated rSK3 sequences to the prolactin minimal promoter that directs luciferase expression. B) Luciferase expression levels from L6 cells (black bars) and Cos7 cells (white bars) transfected with the indicated rSK3 enhancer-reporter plasmids. Results are presented as ±SEM for n≥6.

activity (Figure 14B, inset). Extending the genomic sequence by an additional 33 bp (P5) endowed an additional 25-fold increase in luciferase activity, and further extending the fragment by an additional 220 bp (P7) did not significantly increase activity (P=0.11). In contrast, transfections into Cos7 cells that do not express SK3 yielded levels of luciferase activity that were not significantly different from empty vector controls for all reporter plasmids tested (not shown). These results identify the rSK3 minimal promoter and implicate the adjacent 33 bp sequence as a transcriptional enhancer.

The ability of 5' flanking sequences to act as a cell type specific enhancer was investigated using the enhancer-reporter constructs (Figure 15A). The results show that in L6 myotubes, inclusion of the 33 bp fragment increased expression from the PRL minimal promoter by 300-fold (Figure 15B, black bars; E6). Extending the sequence of 5' genomic DNA sequence did not significantly increase expression levels (E2-5, E3 P>0.10). Deleting the 33 bp sequence from a longer fragment (E7), resulted in a loss of enhancing activity. Transcriptional enhancers function independently of orientation and reversing the orientation of the 33 bp fragment yielded equivalent luciferase activity (E8). In contrast to L6 cells, transfections into Cos7 cells yielded only low levels of luciferase activity for all of the enhancer-reporter constructs (Figure 15B, white bars). The 33 bp sequence contains a consensus Sp factor binding motif (GGCGG) in its 5' domain, and mutations in this motif significantly decreased enhancer activity (E9;

P=0.02), while mutations in the 3' domain of the 33 bp sequence did not alter enhancing ability (E10; P=0.73).

Sp1 and Sp3 bind to the 33 bp enhancer

To investigate nuclear proteins that bound to the 33 bp enhancer, electrophoretic mobility shifts were performed using radiolabeled 33 bp fragments incubated with nuclear protein extracts prepared from Cos7 or L6 cells (Figure 16). The results show that nuclear extracts from both sources induced gel-shifts of three bands. The interactions were specific as all three bands were competitively inhibited by nonradiolabeled 33 bp DNA but not by nonspecific 33 bp DNA. In addition, all three bands were competitively inhibited by a consensus Sp binding site (Figure 16, lanes 1-4 for Cos7, lanes 7-10 for L6), but were not shifted by a 33 bp competitor fragment with a mutated Sp binding site (not shown). The results suggest that all of the bound proteins are members of the Sp family (Figure 16, lanes 1-4 for Cos7, lanes 7-10 for L6). To distinguish among the Sp factors that bound to the 33 bp rSK3 enhancer supershift assays were performed using Sp-specific antibodies. Incubation of Sp3 antibodies with the 33-bp enhancer and L6 or Cos7 nuclear extracts supershifted two of the three bands (Figure 16, lanes 6, 12, respectively), while incubation with Sp1 antibodies supershifted the other band (Figure 16, lane 5, 11, respectively).

Figure 16
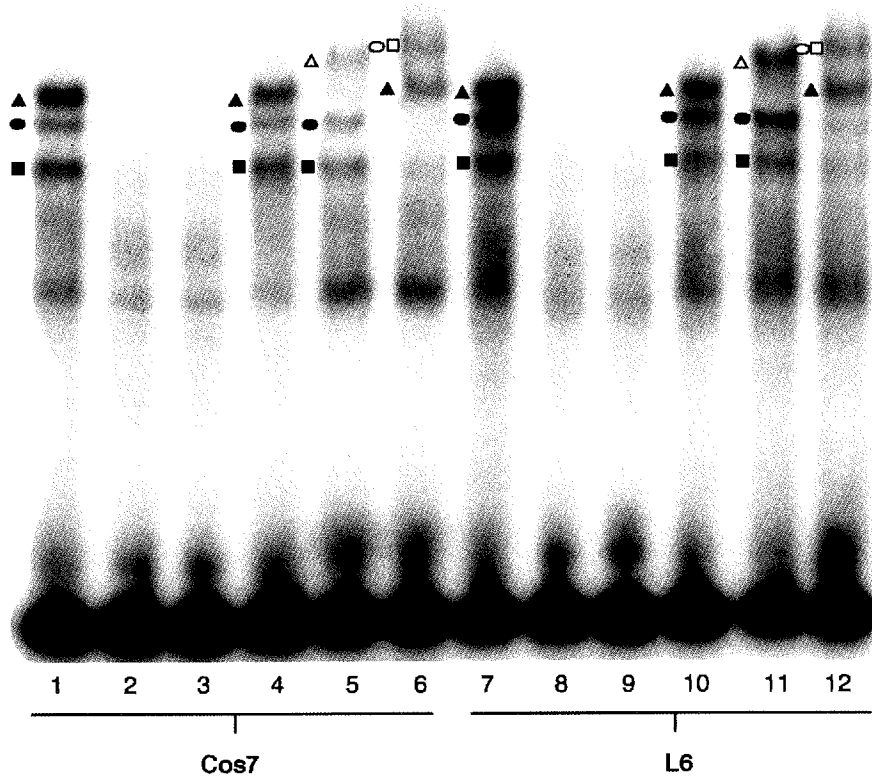
Figure 16. Identification of transcription factors that bind to the 33 bp SK3 enhancer. Electrophoretic mobility shift assay performed with nuclear extracts from Cos7 cells (lanes 1-6) or L6 myotubes (lanes 7-12). The three bands observed from both Cos7 and L6 nuclear extracts with the 33 bp probe are denoted by the square, oval, and triangle. Lanes 1, 7: no competitor; lanes 2, 8: rSK3 33 bp enhancer competitor; lanes 3, 9: Sp1 competitor; lanes 4, 10: nonspecific 33 bp competitor. Lanes 5, 6 (Cos7) and 11, 12 (L6) are supershift assays performed using Sp1 and Sp3 antibodies. The filled shapes indicate specific bands that are not shifted, and the open shapes indicate supershifted bands. Lane 5: Cos7 + Sp1 antibody; lane 6: Cos7 + Sp3 antibody; lane 11: L6 + Sp1 antibody; lane 12: L6 + Sp3 antibody.

82

The 33 bp fragment mediates enhanced transcription in response to estrogen

The results presented above show that a combination of Sp1 and Sp3 present in L6 and Cos7 nuclear extracts bind to the 33 bp rSK3 enhancer. However, they do not reveal cell-type specific factors that might explain why SK3 is expressed in L6 but not Cos7 cells. One difference between the two cell lines is that L6 cells, but not Cos7 cells, express ERα (Kahlert et al. 1997). Therefore, the ability of the 33 bp sequence to mediate differences in expression induced by ERα was investigated by cotransfecting Cos7 or L6 cells with ERa and enhancer-reporter constructs. The results showed that with cotransfected ERa, the enhancer now functioned in Cos7 cells; cotransfected Cos7 cells treated with E2 showed a 15-fold increase in luciferase activity compared to cells transfected with only the enhancer-reporters followed by E2 stimulation (Figure 17A). Similarly L6 cells showed a significant increase in luciferase activity in response to E2 (Figure 18A, E6, p=0.02). Interestingly, E2-mediated enhanced expression was abolished for reporter plasmids with the 33 bp sequence harboring a mutation in the Sp binding motif, indicating that an intact Sp binding site is necessary for E2-stimulated expression. To examine whether ERα bound directly to the 33 bp motif, electrophoretic mobility shift assays were performed with either nuclear extracts from Cos7 cells transfected with the ERa, or purified ERa protein. Neither assay detected direct ERa binding to the 33 bp sequence (not shown).

83
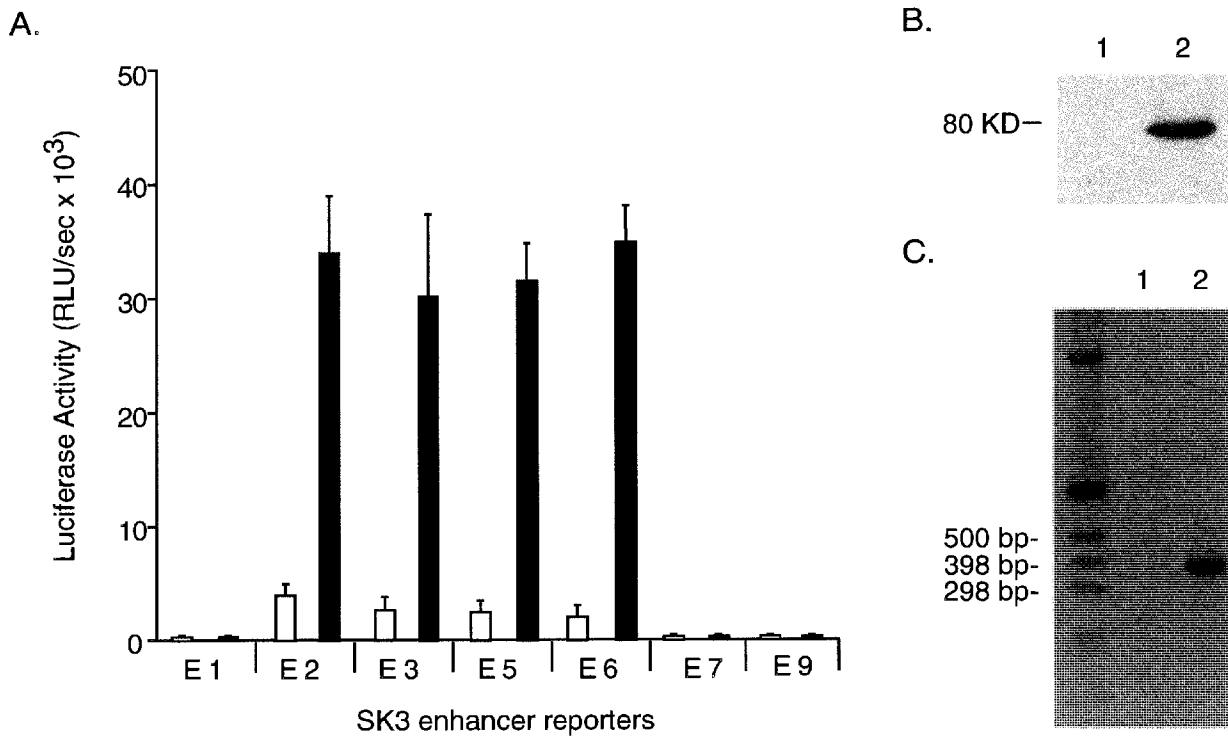
Figure 17

Figure 17. ER-alpha endows expression in Cos7 cells through the 33 bp enhancer and activates the endogenous SK3 gene. A) Enhancer-reporter constructs as depicted in Figure 3 were transfected into Cos7 cells alone (white bars) or together with ERa (black bars). Cells were stimulated with E2 and assayed for luciferase expression. Results are presented as ± SEM for n≥6. B) Western blot analysis of Cos7 membranes prepared from Cos7 cells alone (lane 1) or Cos7 cells expressing ER-alpha and stimulated with E2 (lane2) using an SK3-specific antibody. C) RLM-RACE products produced from RNA isolated from untransfected Cos7 cells (lane 1) or Cos7 cells expressing ERa and stimulated with E2 (lane 2).

84
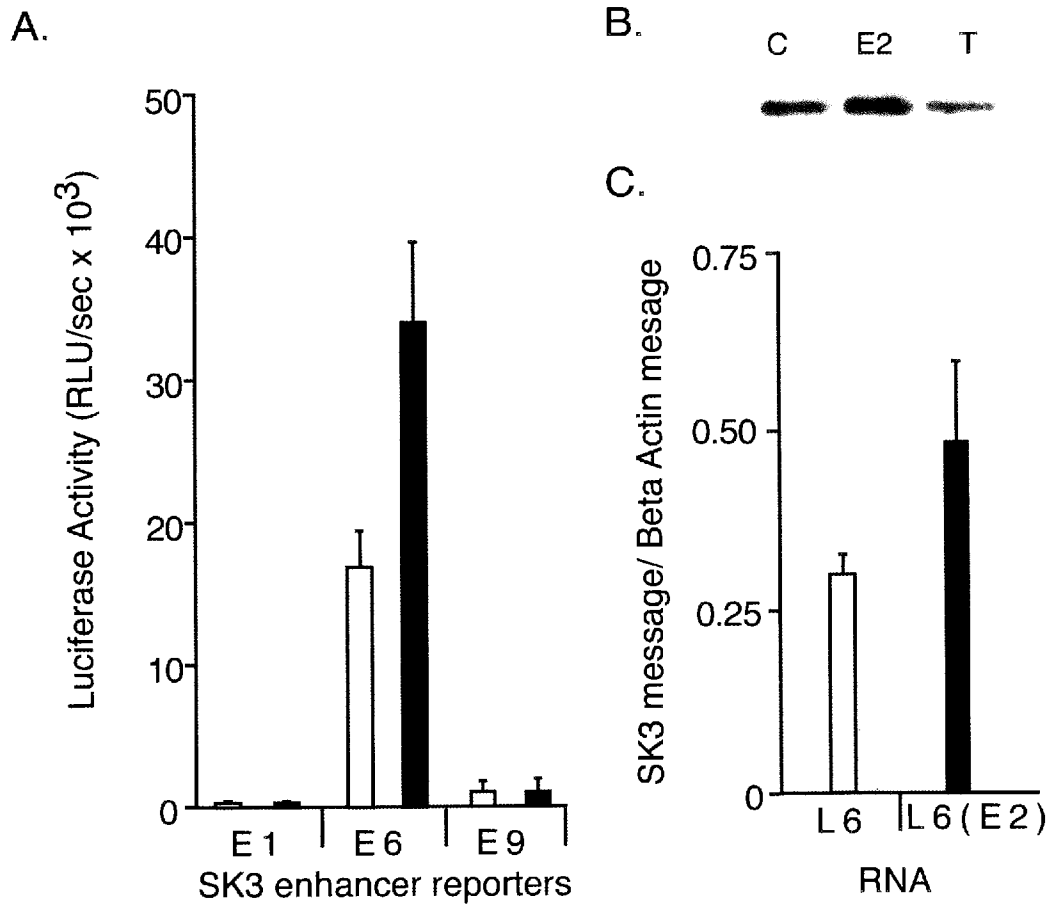
Figure 18

Figure 18. Estrogen enhances SK3 expression in L6 cells.

A) Enhancer-reporter constructs as depicted in Figure 3 were transfected into

L6 cells with or without ERα and E2 stimulation.

B) Westem blot analysis of L6 membranes prepared from L6 cells stimulated

with (E2) or without (C) E2 and Tamoxifen(T).

C) Quantitative real time PCR on RNA prepared from L6 cells with (E2) or

without (C) E2 and tamoxifen(T).

Taken together, the results indicate that the 33 bp enhancer sequence is important for cell-type specific rSK3 gene expression, that it binds Sp1 and Sp3, and mediates the effects of E2 without direct binding of ERα. Since L6 cells express the endogenous SK3 gene while Cos7 cells do not, and nuclear extracts from both cell lines yielded similar mobility shift results, the ability of E2 to stimulate endogenous SK3 expression through ERα was examined in L6 and Cos7 cells. L6 cells showed increased SK3 expression in response to E2 stimulation (Figure 6B and 6C). Protein from L6 cells treated with E2, Tamoxifen (an ERα inhibitor), and vehicle for 6 hours were prepared as a western blot and probed with an SK3 specific antibody (Figure 18B). The results showed a clear increase in SK3 protein in response to E2. Similarly for RNA levels, quantitative real time PCR, using cDNA prepared from L6 cells treated with vehicle or E2 for 2 hours, showed a significant increase in SK3 RNA levels in response to E2 (Figure 18C, p=0.03). SinceCos7 cells do not express ERs, the ability of heterologous ERα expression to activate the endogenous SK3 gene was also examined. Western blot analysis (Figure 17B) showed that Cos7 cells transfected with ERα and treated with E2 robustly expressed SK3. RLM-RACE confirmed that the ERα-induced expression of the endogenous SK3 gene occurred from the same region of genomic DNA as in L6 cells and denervated skeletal muscle (Figure 17C). Therefore, expression of ERa and stimulation with E2 is sufficient to induce SK3 gene expression in Cos7 cells.

ERα enhances the interaction of Sp1 to the SK3 33 bp fragment

The results are consistent with a model in which the 33 bp fragment mediates the effects of ERα yet this affect occurs in the absence of DNA binding. Previous studies have shown that ERα can interact with Sp1 and increase the binding of Sp1 to its DNA binding motif (Porter et al. 1997; Duan et al. 1998; Wang et al. 1998; Sun et al. 1998; Qin et al. 1999; Samudio et al. 2001). Therefore the SK3 33 bp enhancer was used in mobility shift assays to assess if ERα increased Sp1 binding. *In vitro* synthesized Sp1 bound to the 33 bp probe and the Sp1 specific band was inhibited by nonradiolabeled 33 bp DNA but not by nonspecific 33 bp DNA (Figure 19, lanes 1-3). The Sp1-shifted bands were quantified by densitometry and, normalizing the data to 1 μl of Sp1, 0.5 μl and 0.25 μl yielded 0.6 and 0.4, respectively. When 800 $f$moles of ERα and 20nM E2 were incubated with these same amounts of Sp1 the binding to the SK3 enhancer was increased for each concentration, 3.3±1.0-fold, 3.3±1.3-fold, and 3.4±1.4-fold, respectively (n=3; Figure 19, compare lanes 4 and 7, lanes 5 and 8, and lanes 6 and 9).

Estrogen Regulation in vivo

To further address the importance of SK3 regulation by estrogen mouse SK3 transcription in response to estrogen stimulation was analyzed. C57 BLK6 mice, six week-old overiectamized females, were injected subcutaneously with soybean oil or 40 μg/g 17ß-estradiol. The mice had been overiectamized
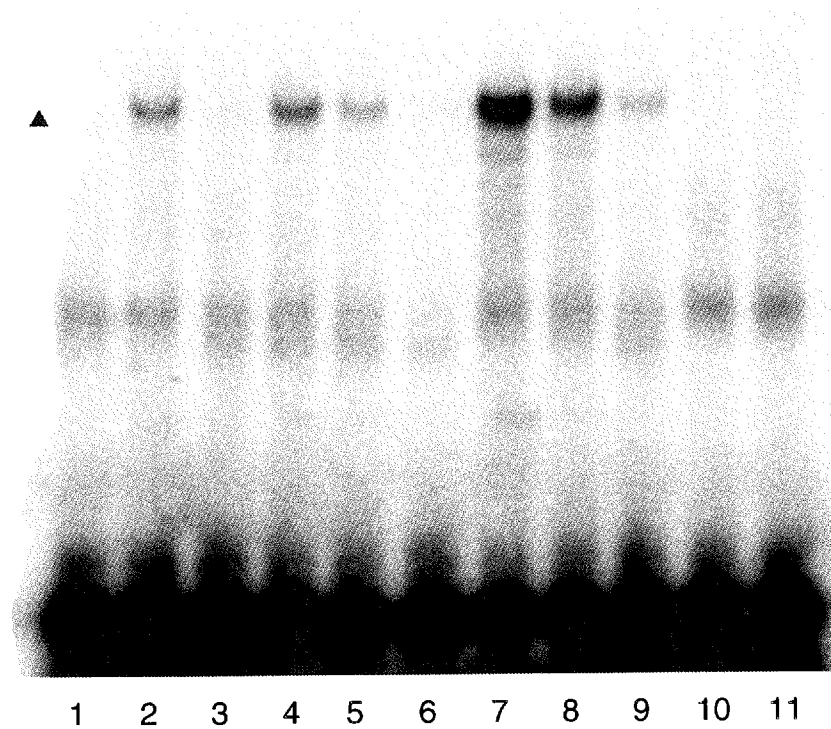
Figure 19

Figure 19. ERα enhances the interaction of Sp1 to the SK3 33 bp enhancer.Electrophoretic mobility shift assay performed with *in vitro* translated Sp1 and the 33 bp enhancer; the Sp1-specific band is denoted by the triangle. Where indicated, 800 ƒmoles ERα were included, and *E2* was used at 20 nM. Lane 1: unprogrammed *in vitro* translation lysate; lane 2: 1μL Sp1 + 100x nonspecific competitor; lane 3: 1μL Sp1 + 100x rSK3 33 bp enhancer competitor; lane 4: 1μL Sp1; lane 5: 0.5 μL Sp1; lane 6: 0.25μL Sp1; lane7: 1μL Sp1 + ERα and E2; lane8: 0.5μL Sp1 + ER α and E2; lane9: 0.5μL Sp1 + ERα and E2; lane10: 1μL unprogrammed lysate + ERα and E2; lane11: 1μL unprogrammed lysate + ERα and E2 + 100x ERE competitor.

88

for two weeks prior to treatment and were given injections of 17ß-estradiol

and or soybean oil every 24 hours for four consecutive days. On the fourth

day the mice were euthenized and estrogen sensitive tissues including:

mammary, pituitary, bladder, and uterus were harvested. Quantitative real-

time PCR was used to address transcriptional effects of the estrogen on SK3

transcription within the harvested tissues. Interestingly there was little change

in the SK3 mRNA levels observed in pituitary, mammary, and or bladder

when normalized to β-actin RNA levels. However Sk3 transcription in the

uterus was profoundly altered in response to estrogen and dropped 10 fold

with 17ß-estradiol injections (Figure 20).

Estrogen affects uterine SP3 levels

As the estrogen response on SK3 transcription in mouse uterus was opposite

that observed in Cos7 cells the mechanisms for the difference was

investigated. The motif responsible for estrogen regulation in Cos7 cells is an

SP motif in the SK3 5'flanking sequence. Therefore the levels of SP1 and

SP3 were determined from harvested uterus tissues using western blot

analysis. The levels of SP1 protein were similar between estrogen treated

and control animals (Figure 21A). However there was a strong induction of

the internally translated small SP3 isoform in the uterus from animals treated

with estrogen (Figure 21A). Thus the difference in SK3 levels may be related

to the levels of the short SP3 isoform which only contains the GC DNA

Figure 20
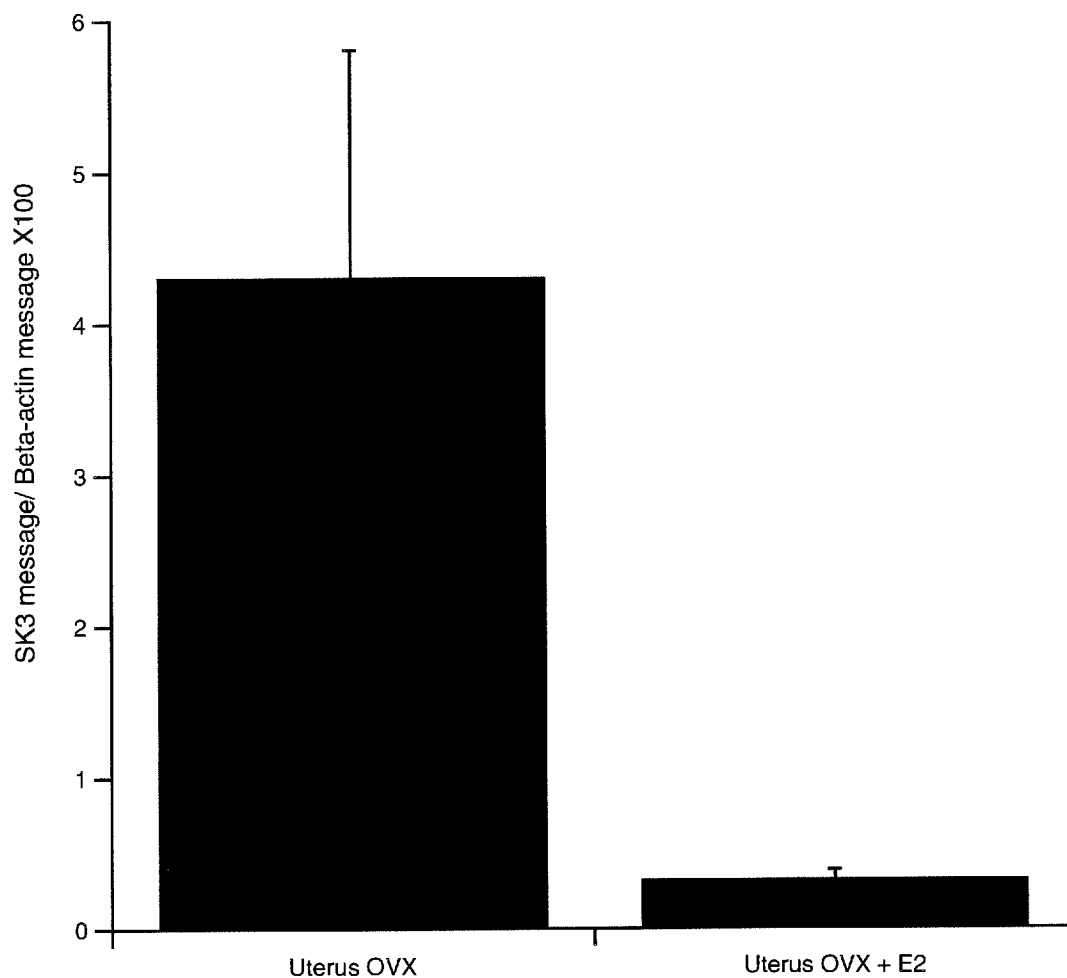
Figure 20. Quantitative real-time PCR performed on RNA harvested from

uterus tissue from ovariectomized (OVX) mice with and without estrogen (E2)

injections 40 µg/g x 4 days. The SK3 message was normalized to beta-actin

message from the same RNA samples. Error bars are ± SEM (n=4).

Figure 21

A.

Sp3

- 94 kD
- 68 kD

1 2   3 4

Sp1

- 94 kD

1 2   3 4

B.

- Sp1
- Sp3

- Sp3

1   2   3   4
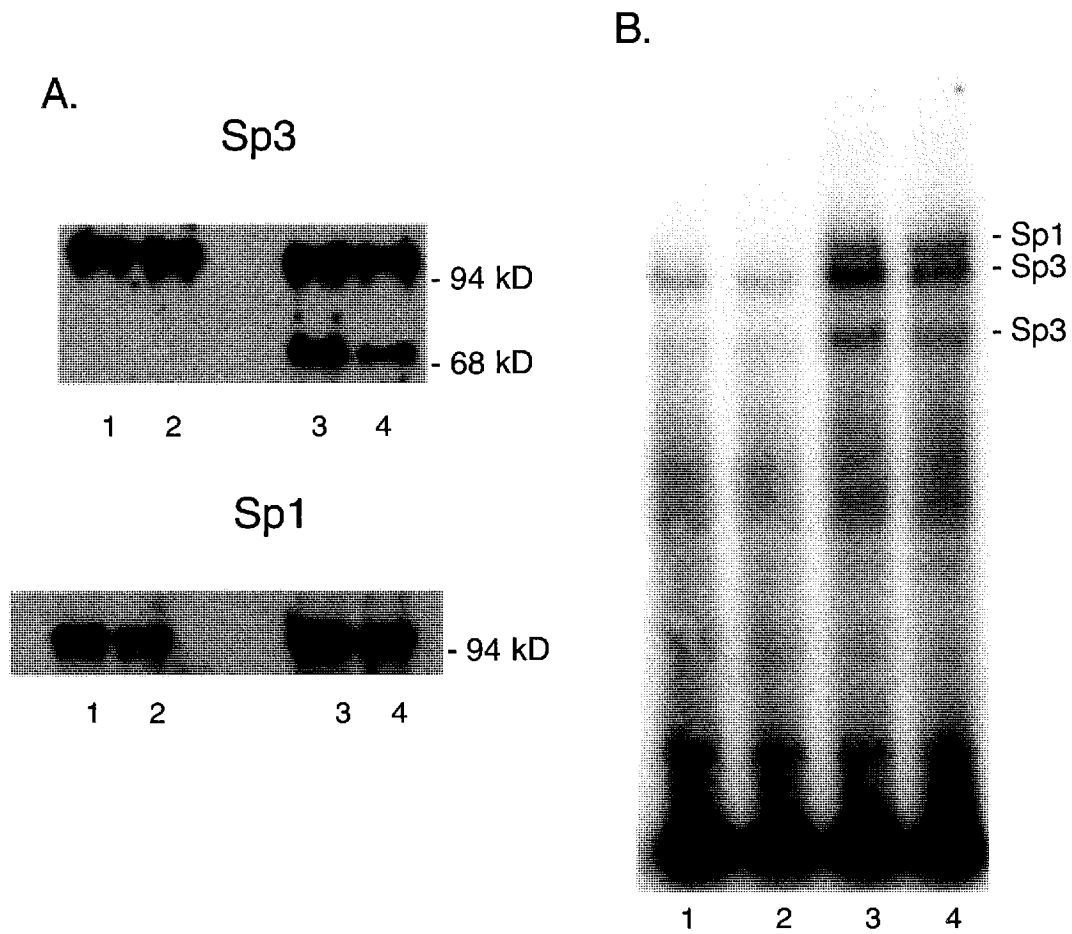
Figure 21. A. Western blot analysis of nuclear extracts prepared from uterus from ovariectomized mice Lanes 1 and 2, and OVX mice given estrogen injection lanes 3 and 4with Sp3 (top) or Sp1 (bottom) antibodies. B. Electrophoretic mobility shift assay performed with uterus nuclear extracts using the 33 bp enhancer as a probe with extracts from OVX lanes 1 and 2 or from OVX + estrogen injections lanes 3 and 4

91

binding activity and does not enhance transcription.

Estrogen affects uterine transcription factor binding to the SK3 33bp enhancer

Elecrophoretic mobility shifts were also employed to test the effects of 17ß-estradiol on transcription factor binding to the SK3 33bp enhancer. Nuclear extracts were prepared from 17ß-estradiol treated uterus and soybean oil treated uterus from two independent animals each. The shifts observed with incubation of the uterine extracts with the 33bp probe were the same corresponding SP bands as those observed with Cos7 and L6 extracts. As dictated by the differences in SP protein levels observed from the treated and untreated uterus the shifts show much more SP3 binding with the 17ß-estradiol treated extracts (Figure 21, compare lanes 1 and 2 with lanes 3 and 4). The differences in Sp bands observed with estrogen treatment may also be a consequence of the enhanced binding of SP1 and SP3 transcription factors in the presence of activated ER∝.

Materials and methods

Reverse transcription-PCR

Reverse transcriptions were performed as described (Bond et al. 2000). For amplifications to identify the CAP site, the PCR was performed with the following primers: reverse primer from exon 2 (Figure 13A, #5): GCTCTACTTCCCTTGTGTGATAGG, forward primers from 5' to 3' of the CAP site, 1: TGGCTAATAAGTGGGCTTGGC; 2: CTTGCCATATAACAGTGTCAG; 3: TGAGCCAGCGAGGAGTGAAGCTGAGT; 4: ATACAATGCACACTCGAGTGGC. The reactions used Taq polymerase (Promega, Madison, WI), with 2mM $MgCl_2$, 1XTaq buffer (Promega), 0.3µM of each oligonucleotide, 0.2µM dNTPs, in a 50µl volume. Cycling conditions: 96°, 30"; 55°, 30"; 72°, 1.5'; X 30 cycles. Twenty microliters of the PCR were electrophoresed through a 1% agarose gel, stained with ethidium bromide, and photographed under UV illumination.

5' RNA ligase–mediated rapid amplification of 5' cDNA ends (RLM-RACE)

5' RLM-RACE (Schaefer et al. 1995) was performed using the GeneRacer kit, according to the manufacturer's instructions (Invitrogen, Carlsbad, CA). Total RNA from denervated skeletal muscle and from L6 myotubes was dephosphorylated with calf intestinal phophatase and decapped with tobacco acid pyrophosphatase. An RNA oligonucleotide was ligated to the decapped RNA and reverse transcription was performed using an SK3 specific oligonucleotide (CTGTACTTCCCTTGTGTGGTAGG) located in the second exon

93

of rSK3 (AF292389). Nested PCR amplified the resultant cDNAs using outer and inner GeneRacer 5' primers and a primer 3' to the SK3 translation start site (GAGTCATGGAAGTGCCCAGAAGTG). The resulting PCR products were cloned and the nucleotide sequences determined.

Northern Blots

TriReagent (Sigma, St. Louis, MO) was used to prepare total RNA from tissue homogenized with a polytron, or from cell culture and 10μg were prepared as a Northern blot using Genescreen Plus (Dupont NEN, Boston, MA) nylon membranes. The antisense riboprobe was made from a linearized DNA template using ^{32}P-UTP (Dupont NEN, Boston, MA). The blot was hybridized in 50% formamide, 5% SDS, 0.4M NaPO$_4$, 1mM EDTA at 60°C for 12 h and then washed at 62°C in 0.05 x SSC. Relative loading was assessed by reprobing blots with a ^{32}P-5'end-labeled oligonucleotide complimentary to 18S rRNA (Levallet et al. 2001). Hybridization signals were visualized using a Phosphorimager 445 SI (Molecular Dynamics, Sunnyvale, CA).

Cell Culture

Cells were maintained in a humidified incubator at 37°C with 5% CO$_2$. L6 rat myoblasts (ATCC CRL-1458) were grown in DMEM + 15% Fetal Calf Serum. For differentiation into myotubes, the media was shifted to DMEM + 2% Horse Serum. L6 cells were harvested after 10 days for nuclear extract preparations

94

and after 2 days for gene expression reporter assays. Cos7 cells (ATCC CRL-1651) were grown in DMEM + 10% fetal calf serum and harvested after 2 days froe nuclear extract preparations and gene expression reporter assays.

Real Time PCR

Quantitative PCR was performed on the DNA Engine Opticon[TM] Continuosu Flourescence Detection System and the respective software. The principle of the method has been described elsewhere (e.g. Holland and Becker). The PCR product is measured via a fluorescent signal during the PCR. The cycle number Ct, at which the fluorescence signal crosses a certain threshold (in correlation to the background fluorescence of the assay), is noted. This Ct value is proportional to the logarithm of the target concentration in the assay. From dilution series of a standard with known concentration of target sequences, running in parallel assays, a calibration curve is created (Ct versus logarithm of the starting concentration).

The signal in this study was generated by the binding of the fluorophore SybrGreen[TM] (SG, Molecular Probes, Eugene, OR) to double-stranded DNA. Baseline and threshold calculations were done with the OPTICON software. The chemical composition of the PCR assays was according to the descriptions of the Taq polymerases using random hexamer rt-PCR reaction material prepared from homogenized mouse uterus RNA. The amplification followed a three-step PCR

Reporter Assays

L6 or Cos7 cells were transfected using lipofection (Polyfect; Quiagen, Valencia, CA) with a 9:1 mixture of luciferase reporter and pCMV-LacZ plasmid DNAs. L6 cells were switched to low serum conditions (2% Horse Serum) 12 hours after transfection and in all cases luciferase assays were conducted 48 hours after transfection. Where indicated, a CMV-based ERα expression plasmid (generous gift from Dr. Gail Clinton, OHSU, Portland, OR) was transfected into Cos7 cells. Twenty-four hours following ERα transfection the cells were incubated in media containing 20 nM E2 (Sigma, St. Louis, MO) for an additional 24 hours. Cells were then harvested in ATP buffer (0.1M $NaPO_4$, 4mM ATP, 1mM PPi, and 6mM $MgCl_2$) with 0.2% TritonX-100; 5-15μl of lysate were used as described (Levallet et al. 2001), on an AutoLumat LB 953 luminometer (EG&G, Berthold Analytical Instruments, Nashua, NH). The data were normalized to β-galactosidase activity (Impey et al. 1996), as measured on the same luminometer, grouped for each reporter and cell type, and presented as ± S.E.M. Significant differences (P<0.05) between the data sets were determined using an unpaired t-test.

Electrophoretic Mobility and Super Shift Assays

Cell extracts were prepared as described (Dignam et al. 1983) and dialyzed twice for 3 hours in 20mM HEPES (pH7.6), 20% glycerol, 100mM KCl, 1.5mM $MgCl_2$, 0.2mM EDTA, with a protease inhibitor cocktail (Sigma, St. Louis, MO). For Cos7

and L6 nuclear extracts, electrophoretic mobility shift assays were performed as described (Vinals et al. 1997). For assays using purified Sp1 protein, the Sp1coding sequence (Genbank accession number NM_012655) was transcribed and translated *in vitro* using a rabbit reticulocyte lysate kit (Pro-mega, Madison, WI). Synthesized protein was used (1μL, 0.5μL, and 0.25μL) in electrophoretic mobility shifts, with or without 800 *f*moles of ERα (Pan Vera, Madison, WI) and *E2* (20 nM), as described (Wang et al. 1998). Three independent mobility shifts were performed and DNA binding was quantified by densitometry using ImageQuant software (Molecular Dynamics, Sunnyvale, CA). Double stranded oligonucleotides were radiolabeled at the 5' termini using γ-^{32}P-ATP and T4 polynucleotide kinase, and purified using Qiagen DNA columns. Unlabeled competitor DNAs, all double stranded and 33bp in length, were used to test the specificity of the shifted bands (mutations in bold) 1: nonspecific, 5'GTGGAGGGGTTGGAGTGGTAGTGGTCTTGGAGC$^{3'}$; 2: wild type: 5'ATTGGGAGGCGGAGTTAGGAGGGGGTTGGAGAG$^{3'}$; 3: Sp specific, 5'ATTCGATCGGGGCGGGGCGAGC$^{3'}$; 4: Sp mutant, 5'ATTGGGATTTGGAGTTAGGAGGGGGTTGGAGAG$^{3'}$; 5: ERE 5'GTCCAAAGTCAGGTCACAGTGACCTGATCAAAGTT$^{3'}$. The mobility shift mixtures were electrophoresed through non-denaturing 3% polyacrylamide gels at 100V for at least four hours. The gels were then vacuum-dried and signals were visualized using a Phosphorimager 445 SI (Molecular Dynamics, Sunnyvale, CA). For supershift assays, reactions were performed in the

presence of 4μg of Sp1 or Sp3 antibodies (Santa Cruz Biotechnology, Santa Cruz, CA).

Western Blots

SK3

Membrane proteins were purified from Cos7 cells as described (Alamone Labs, Jerusalem, Israel) and prepared as a Western blot on nitrocellulose membranes after electrophoresis through an 8% denaturing polyacrylamide gel. SK3 antibody (Alamone Labs, Jerusalem, Israel) was used to probe the membrane at a 1:1000 dilution in PBS, 0.1% TWEEN, and 5% powdered dry milk, followed by goat anti-rabbit horseradish peroxidase (HRP)-coupled secondary antibody (Santa-Cruz Biotechnology) at 1:25,000 in the same solution. The membranes were washed between and after antibody incubations in PBS containing 0.1% TWEEN; HRP was illuminated using Pico-signal (Pierce, Rockford, IL) and exposed on Kodak X-omat Blue film (Kodak, Rochester, NY).

SP3 and SP1

Ten micrograms of nuclear extract proteins were prepared as a Western blot on nitrocellulose membranes after electrophoresis through an 8% denaturing polyacrylamide gel. Sp3 or SP1 antibody (Santa-Cruz Biotechnology) was used to probe the membrane at a 1:1000 dilution in PBS, 0.1% TWEEN, and 5% powdered dry milk, followed by goat anti-rabbit horseradish peroxidase (HRP)-

coupled secondary antibody (Santa-Cruz Biotechnology) at 1:25,000 in the same

solution. The membranes were washed between and after antibody incubations

in PBS containing 0.1% TWEEN; HRP was illuminated using Pico-signal (Pierce,

Rockford, IL) and exposed on Kodak X-omat Blue film (Kodak, Rochester, NY).

Discussion

The results presented here identify a transcriptional start site for SK3 expression, the minimal rSK3 promoter, and a 33 bp enhancer adjacent to the minimal promoter. The enhancer endows upon a heterologous minimal promoter the ability to achieve high levels of expression in L6 myotubes but not in Cos7 cells. However when Cos7 cells express ERα and are stimulated with E2, the 33 bp motif becomes a strong transcriptional enhancer. Remarkably, ERα expression and exposure to E2 activate the otherwise silent endogenous SK3 gene in Cos7 cells and stimulate SK3 expression in L6 cells. Taken together with the results from reporter experiments, it is likely that ER-mediated activation of the SK3 gene in Cos7 and L6 cells occurs through the 33 bp enhancer, implying that this sequence is conserved in the simian SK3 gene, and is sufficient for inducing SK3 expression in Cos7 cells.

The 33 bp sequence contains a consensus Sp binding motif (GGCGG), binds Sp1 and two forms of Sp3, and also mediates the effects of ERα on estrogen-stimulated SK3 gene expression but is not directly bound by ERα. Indeed, gel-shift assays suggest that Sp1 and Sp3 account for all of the nuclear proteins from L6 or Cos7 cells that interact directly with the 33 bp enhancer. Consistent with these observations, the 33 bp enhancer does not contain an ERE (Klein-Hitpass et al. 1988) and shows no estrogen-mediated enhancing activity when mutations

are introduced into the Sp motif. Thus ERα seems to be enhancing transcription through the Sp proteins bound to the Sp motif. The interaction between these two transcriptional regulatory pathways has been previously demonstrated by elegant studies showing that ERα binds to both Sp1 and Sp3 and enhances Sp1 binding to an Sp consensus motif (Porter et al. 1997; Duan et al. 1998; Wang et al. 1998; Sun et al. 1998; Wang et al. 1999; Qin et al. 1999; Saville et al. 2000; Xie et al. 2000; Samudio et al. 2001). The results presented here are consistent with these studies and show that ERα increases the binding of Sp1 to the SK3 33 bp enhancer.

Sp1 and Sp3 are ubiquitously expressed transcription factors yet molecular, genetic, and biochemical analyses have demonstrated that the Sp factors are not functionally redundant. Sp1 and Sp3 generate diversity in both binding and transcriptional effects through translational and post-translational modification. For example, Sp1 may undergo a proteolytic cleavage to generate an alternative protein, while three distinct Sp3 translation products arise from the use of alternative translational start codons (Rao et al. 1998; Kennett et al. 1997). The two smaller forms of Sp3 lack much of the glutamine-rich domains important for transcriptional enhancement and can act as negative transcriptional regulators (Kennett et al. 1997). Moreover, the smaller forms of Sp3 can compete for Sp1 binding, preventing Sp1-mediated enhancement of transcription, or inhibiting the activity of DNA-bound Sp1 (Stoner et al. 2000). In general, Sp1 functions as a

101

transcriptional activator while Sp3 decreases transcription through interfering with Sp1 binding. ERα may shift the ratios of the Sp factor binding, resulting in transcriptional stimulation.

Estrogen regulation of SK3 expression is emerging as an important physiological influence in reproductive and smooth muscle tissues (Bond et al. 2000; Bosch et al. 2002; submitted) and the effects of ERα expression in Cos7 cells suggest that at least in some cell types, SK3 expression may depend only on ERα expression. Yet, SK3 is not expressed in every cell that expresses ERα (not shown), and it is likely that a dynamic balance between the different forms and levels of Sp1 and Sp3, regulated expression of ERα itself, and additional transcriptional regulatory elements that have not yet been identified engender physiologically responsiveness upon the levels of SK3 gene expression.

The stimulation of SK3 transcription agrees with the increase of SK3 RNA found in the rostral hypothalamus in response to estrogen injection. However the *in vivo* data presented here describe a reduction in SK3 transcription within the uterus in response to estrogen. The estrogen regulation observed in uterus is the opposite of that seen in Cos7 cells and in the rostral hypothalamus (Bosch et al. 2002), but may be important in respect to estrogen regulation working through an Sp motif, which can have both positive and negative affects on transcription. Indeed the levels of the short isoforms of SP3 were increased in the uterine

tissue treated with estrogen. As described the short forms of SP3 do not stimulate transcription but can bind to Sp motifs and thus reduce transcription from the motifs they bind. A model consistent with the data is that immediately following estrogen stimulation ERα increases the binding of Sp1 to the SK3 33 bp enhancer, stimulating transcription, whereas continued E2 stimulation leads to accumulation of the short isoforms of Sp3 which competes with Sp1, reducing SK3 transcription.

In addition to transcriptional effects, estrogen affects the activity of SK3 channels in the plasma membrane, such as seen in GABAergic POA neurons, where estrogen enhanced the ability of a-1 adrenergic receptor agonists to inhibit SK channels, increasing cell excitability (Wagner et al. 2001). Therefore, estrogen regulation of SK3 transcription may be crucial in the reproductive axis as the levels of SK3 channels will have profound consequences for excitability in specific populations of neurons, and for secretory capability in gland cells as a function of hormonal status.

CHAPTER 4

DISCUSSION

This thesis work focuses on the physiological role of the small conductance

calcium activated potassium channel, SK3, in skeletal muscle hyperexcitability,

and its transcriptional regulation by estrogen. SK3 channels influence many

important cellular processes through calcium-dependent potassium flux.

Transcription of the SK3 gene is regulated by the muscle-nerve status of skeletal

muscle and hormonal control through estrogen. Expression of SK3 in skeletal

muscle is associated with skeletal muscle hyperexcitability, observed with both

patients with myotonic dystrophy and in denervated skeletal muscle (Vergara et

al. 1993, Behrens et al. 1994). Where as SK3 expression and regulation by

estrogen helps regulate the release of gonadotropin releasing hormone (GnRH)

in the preoptic hypothalamus, and affects LH and FSH release from pituitary

gonadtrophs. (Bosh et al. 2002).

I. Transcriptional regulation of the SK3 gene

Sp factor regulation of SK3 gene expression

Skeletal muscle develops and maintains its unique architecture, excitability, and contractile apparatus through an exquisite coordination of gene expression networks. The SK3 gene is expressed as part of the prenatal program that is switched off upon innervation, and re-expressed following denervation. In addition, the SK3 gene is aberrantly expressed in DM muscle. For two pathological conditions, denervation (Vergara et al. 1993) and DM (Behrens et al. 1994), the associated symptom of hyperexcitability may be reduced or abolished by direct application of apamin, a blocker of SK channels (Blatz et al. 1986). SK3 is also expressed in the L6 rat skeletal muscle cell line, which reflects SK3 expression in denervated skeletal muscle (Pribnow et al. 1999), and the factors responsible for expression of the rat SK3 gene were thus investigated in L6 cells. After identifying the minimal promoter sequence of the SK3 gene, a sequence of 33 bp 5' proximal to the promoter was shown to enhance expression from the basic SK3 promoter. The short enhancing sequence that contains a consensus Sp factor binding motif endows upon a heterologous minimal promoter the ability to achieve high levels of expression in L6 myotubes but not in Cos7 cells, where SK3 is not expressed. Therefore, the 33-bp enhancer participates in determining SK3 gene expression specifically in L6 cells and may play an important role in denervation-induced SK3 expression.

Interestingly Sp1 and Sp3 both bound the 33 bp enhancer from bothL6 myotube

and Cos7 extracts, however they may not be equivalent in the two cell types.

The Sp factors bind to a consensus motif (GGCGG), present in the SK3 33-bp

enhancer, and influence transcriptional activity by protein-protein interactions

with components of the basic transcriptional apparatus. These interactions

influence the recruitment or stabilization of other transcription factors to the

promoter complex (Lania et al. 1997; Martin et al. 1991). All four Sp family

members, Sp1-4, contain a highly conserved C-terminal DNA-binding domain

composed of three zinc finger motifs, and serine/threonine- and glutamine-rich

domains in their N-terminal regions (Suske, 1999; Berg et al. 1992). Molecular,

genetic, and biochemical analyses have demonstrated that the Sp factors are not

functionally redundant. Sp1 and Sp3 generate diversity in both binding and

transcriptional activity through translational and post-translational modification.

For example, Sp1 may undergo a proteolytic cleavage to generate an alternative

to the full-length protein, while three distinct Sp3 translation products arise from

the use of internal translational start codons (Rao et al. 1998; Kennett et al.

1997). Sp1 has multiple phosphorylation sites and phosphorylation reduces the

affinity of Sp1 for its DNA target sequences (Jackson et al. 1990; Leggett et al.

1995; Haidweger et al. 2001). Sp3 post-translational modification has not been

as extensively examined although there is evidence that phosphorylation also

modifies DNA binding affinity (Zhu et al. 2000). The two smaller forms of Sp3

lack much of the glutamine-rich domains important for transcriptional

enhancement and can act as negative transcriptional regulators (Kennett et al. 1997). Moreover, the smaller forms of Sp3 can compete for Sp1 binding, preventing Sp1-mediated enhancement of transcription, or inhibiting the activity of DNA-bound Sp1 (Stoner et al. 2000). Indeed, negative regulation by Sp3 has been suggested for denervation-induced changes in the levels of the glucose transporter, Glut-1 (Fandos et al. 1999). Therefore, the ratios of the various forms of Sp factors will determine the integrated consequences for transcription. However the translational and post-translational differences between Sp1 and Sp3 in Cos7 and L6 cells were minimal (not shown), thus other mechanisms of SK3transcriptional regulation were pursued.

Estrogen regulation of SK3 gene expression

A role for SK3 in reproductive endocrinology and smooth muscle tone is emerging and in both tissues expression is regulated by estrogen. In the hypothalamus, estrogen regulates GnRH release, influencing hypothalamic-pituitary-gonadal reproductive axis balance (Ferin et al. 1984). Coronary smooth muscle also shows profound gender-specific differences in diameter that are related to estrogen. Recently estrogen has been shown to affect the levels of SK3 in both the rostral hypothalamus of the reproductive axis and in vasculature endothelium (Bosh et al. 2002, unpublished). SK3 levels in turn influence both hormone release from the reproductive axis and vasodilation (Wagner et al. 2001, Murphy et al. 1995, Corriu et al. 1996, Doughty et al. 1999, Lagaud et al.

1999, unpublished).

The information obtained from L6 cells about SK3 transcriptional regulation was valuable in pursuing transcriptional regulation of SK3 by estrogen. The SK3 promoter and enhancer constructs were used to define determinants responsible for estrogen regulation of SK3 transcription. Cos7 cells were employed to test for an estrogen response on SK3 transcription, as Cos7 cells don't express SK3 or estrogen receptors. Therefore an estrogen receptor alpha (ERα) expression construct allowed these constructs to be tested for an estrogen response element (ERE). Using the Cos7 system an estrogen sensitive motif was identified as the same motif that was identified as being important in L6 cell type specific expression of SK3. The use of an Sp motif in estrogen receptor mediated transcription has been well characterized. Although the Sp motif is not an ERE, the interaction between Sp1and ERα has been shown to enhance Sp1 DNA binding (Porter et al. 1997; Duan et al. 1998; Wang et al. 1998; Sun et al. 1998; Wang et al. 1999; Qin et al. 1999; Samudio et al. 2001). Thus estrogen-mediated enhancement of the SK3 gene may be due to previously described protein-protein interactions between Sp1 factors and the ERα.

Several genes are transcriptionally stimulated by estrogen through one or more Sp motifs in their promoters, including cathepsin D, E2F1, bcl-2, c-fos, adenosine deaminase, insulin like growth factor binding protein 4, and retinoic acid receptor alpha

1 (Porter et al. 1997; Duan et al. 1998; Wang et al. 1998; Sun et al. 1998; Wang et al. 1999; Qin et al. 1999; Saville et al. 2000; Xie et al. 2000; Samudio et al. 2001). Sp1 has been linked to estrogen sensitive enhancement of transcription through a direct interaction with ERα (Duan et al. 1998). ERα interacts with the DNA binding domain and also with the transcriptional transactivation domains of Sp1. The current understanding is that ERα interacting with Sp1 stimulates the Sp1 GC motif interaction. This can clearly be seen with a mobility shift that illustrates the enhancement of Sp1 binding to a labeled GC containing fragment as well as to the SK3 33bp enhancer fragment with ERα present in the reaction (Figure18; Porter et al. 1997; Duan et al. 1998; Wang et al. 1998; Sun et al. 1998; Wang et al. 1999; Qin et al. 1999; ; Samudio et al. 2001). Therefore the 33 bp enhancer identified within the SK3 5' flanking sequence endows estrogen sensitive transcriptional regulation in part through interactions of ERα and Sp1. Interestingly estrogen stimulated transcription through an Sp motif within the 33 bp SK3 enhancer may also explain the differences in SK3 expression between L6 and Cos7 cells. L6 cells express estrogen receptors and Cos7 cells are devoid of the estrogen receptors (Kahlert et al. 1997). Stimulation of Sp1 DNA interactions in L6 cells through the endogenous estrogen receptor may be involved in enhancing SK3 expression in L6 cells. Remarkably ERα expression in Cos7 cells and stimulation with estrogen results in endogenous SK3 RNA and protein expression. Therefore the expression of estrogen receptors in Cos7 cells seems to shift the negative interactions of Sp factors within the 33 bp SK3 Sp motif stimulating transcription through increased

109

Sp1 GC interactions and may be similar to the mechanism of estrogen enhanced SK3 expression in the rostral hypothalamus.

Estrogen enhancement of SK3 transcription may have profound consequences on the reproductive axis. The upregulation of SK3 in the rostral hypothalamus will have important affects on the release of GnRH. As SK3 is found presynaptically (Roncarati et al. 2001) an increase of this hyperpolarizing potassium conductance will reduce the voltage change following an action potential at the nerve terminal, thus reducing GnRH release from GnRH neurons in the POA. By reducing GnRH release estrogen negatively feeds back on the reproductive axis causing a reduction in hormone release.

SK3 enhanced transcription also has important influences in vasodilation. An apamin sensitive SK conductance in the vascular endothelium enhances EDHF induced dilation of vascular smooth muscle (Nelson). Estrogen also increases vasodilation and stimulates SK3 transcription in the vascular endothelium (unpublished). Estrogen provides a cardiovascular protective affect in premenopausal women who develop cardiac disease later then men. However when men undergo an orchiectomy, there is an associated decreased prevalence of coronary disease (Slater et al. 1986). Similarly cirrhosis of the liver causes a deficiency of testosterone levels and increase of estrogen (Baker et al. 1976), which has been associated with a decreased prevalence of coronary disease in men. Experimental studies show that long-term estrogen therapy improves vascular function (New et al. 1997) and it is associated with enhanced arterial

reactivity in male to female transsexuals (McCrohon et al. 1997). In both male and female dogs, estrogen stimulates increases in myocardial protection from an experimentally induced cardiac infarction (Lee et al. 2000). Estrogen may stimulate vasodilation through SK3 expression and might be used in the male population at risk for cardiovascular disease. Interestingly testosterone is aromatized to estrogen and may also affect SK3 transcription. Indeed vasodilation is also caused by epoxyeicosatrienoic acid, which dramatically affects aromatase levels in vascular smooth muscle (Snyder et al. 2002). Thus the levels of aromatase may also play an important role in cardiac protection in males.

SK3 expression is dramatically affected by an Sp motif in its 5' flanking sequence. A role for the Sp motif in both estrogen regulated expression and cell type specific expression of SK3 have clearly been demonstrated. The role of the Sp motif is obviously important however mechanisms of gene regulation in immortalized cells are typically different than that found *in vitro*, as was clearly demonstrated by Hauschka's work on the muscle creatine kinase promoter (Johnson et al. 1989; Jaynes et al. 1986). Therefore the regulation of SK3 transcription was the next logical step to deciphering important determinants of SK3 gene regulation.

Along with being important in GnRH release and in vasodilation, SK3 has also been implicated in the rhythmic uterine contractions required during

111

Parturition. In SK3 transgenic mice, parturition was compromised when gene expression was higher than normal, and this condition was reversed upon down-regulation of SK3 (Bond et al. 2000). The problems observed in the transgenic mice giving birth are likely due to SK3 expression in uterine smooth muscle, a tissue that is subject to hormonal regulation during the female cycle, particularly through the actions of estrogen (Bond et al. 2000). Therefore estrogen regulation of SK3 in the uterus was addressed, testing if the SK3 regulation observed in Cos7 cells and in the rostral hypothalamus are maintained in the uterus.

To address *in vivo* regulation of SK3, ovariectomized mice were obtained and given either mock vehicle injections or injections of 17β-estradiol (outlined in Chapter 3) and uterus tissue was harvested. Quantitative PCR was employed to examine SK3 transcription within this tissue. SK3 message levels from uterus were 10-fold lower in the animals given 17β-estradiol injections. The estrogen regulation observed in uterus is the opposite of that seen in Cos7 cells and in the rostral hypothalamus (Bosch et al. 2002), but may be important in respect to estrogen regulation working through an Sp motif, which can have both positive and negative affects on transcription. This could help explain why estrogen stimulates SK3 expression in the rostral hypothalamus for only the first 24 hours and the transcriptional stimulation declines and returns to baseline at 48 hours following estrogen stimulation (Bosch et al. 2002). The experiments outlined in

this thesis used uterus tissue harvested at 96 hours following 17β-estradiol injections with all of the Cos7 experiments being done 24hours following estrogen stimulation. Thus estrogen may stimulate SK3 transcription at first, through the characterized increase in SP1 SK3 enhancer interactions, which may eventually reverse because of the affects of estrogen on other Sp transcription factors that have negative influences on transcription.

The reductions in SK3 levels in response to estrogen are important with respect to parturition and rhythmic uterine contraction. SK3 is expressed in the circular and longitudinal layers of the uterus (Bond et al. 2000). When over expressed in uterine smooth muscle mice develop complications during parturition and fail to deliver viable pups, however when the SK3 is reduced in uterine smooth muscle parturition proceeds normally (Bond et al. 2000). Interestingly Kv4.3 and BK are also expressed in the uterine circular and longitudinal muscle layers and are dramatically down regulated in response to the increases in estrogen observed near the end of gestation (Song et al. 1999; Song et al. 2001). Thus SK3 down-regulation in response to estrogen agrees with the reported down-regulation of potassium currents in late pregnant myometrium (Wang et al. 1998). Although an apamin sensitive current has not been reported from myometrium, SK3 expression has been observed within the small intestine and proximal colon circular and longitudinal smooth muscles. Potassium channel activity regulates myometrium contractility, and the reduced expression of potassium channels

reduces the hyperpolarizing influences on the muscle, which allows for increased uterine contractility (Anwer et al. 1993). Therefore estrogen may lower the levels of SK3 along with other potassium channels as a directed program eventually leading to labor and parturition.

The molecular mechanisms that cause reductions in the level of SK3 transcription, found in the uterus in response to estrogen, are important as they may also influence other potassium channels gene expression and or other important gene transcription during pregnancy. Following from the work done in Cos7 cells the estrogen sensitive Sp motif was a possible target for the estrogen-induced reduction of transcription observed in uterus. The differences in Sp3 protein levels and DNA binding were first analyzed because Sp3 has well characterized negative influences on transcription as described above (Kennett et al. 1997). Interestingly the internally translated short Sp3 isoforms were only observed in uterine tissue harvested from the animals given estrogen injections and not in mock injected animals (Figure 20). The short Sp3 isoforms only have negative influences on transcription as they lack the transcriptional transactivation domains but retain the DNA binding domain (Kennett et al. 1997). Thus the reduced levels of SK3 transcription observed in estrogen stimulated uterus might result from increases in the short isoform of Sp3 competing for Sp1 and reducing SK3 transcription. ERα also interacts with Sp3, an interaction that increases Sp3s affinity for GC motifs causing down regulation of pVEGF6 in endometrial cells (Stoner et al. 2000). Therefore estrogen may also cause a higher affinity of the negative Sp3 isoform for GC

114

motifs, which could affect SK3 transcription. A model consistent with the data is that immediately following estrogen stimulation ERα increases the binding of Sp1 to the SK3 33 bp enhancer, stimulating transcription, whereas continued E2 stimulation leads to accumulation of the short isoforms of Sp3 which competes with Sp1, reducing SK3 transcription.

This is the first time that increased internally translated SP3 in response to estrogen has been shown. However this mechanism of transcriptional down regulation may be important with respect to other hormonally controlled genes. The estrogen sensitive short Sp3 isoform may occur because of a change in Sp3 transcription and or translation. As the Sp3 gene has many Sp motifs in its 5' flanking sequence it would be interesting to study the changes in SP3 transcription in response to estrogen. One possibility is that the SP1/ERα interactions stimulate both SK3 and SP3 transcription at first and that when SP3 levels increase they compete for the SP1 interactions and reduce transcription.

II. SK3 is necessary but not sufficient for denervation-induced skeletal muscle hyperexcitability

Skeletal muscle cells couple calcium release, activated during the action potential, to the muscle contraction. Calcium gated SK3 channels have been implicated in the genesis of hyperexcitable skeletal muscle resulting from denervation or the inherited myotonic disorder, myotonic dystrophy. Aberrant

115

expression of SK3 mRNA is found in both denervated and DM skeletal muscle (Pribnow 1999, Kimura 2000). Apamin also binds to the membranes of denervated and DM skeletal muscle and blocks the muscle hyperexcitability observed in both conditions (Behrens & Vergara, 1992; Behrens et al. 1994). Therefore a link between SK3 and skeletal muscle hyperexcitability was investigated in mice with denervation-induced skeletal muscle hyperexcitability, to determine a role for SK3 in skeletal muscle hyperexcitability.

Denervated skeletal muscle has high levels of spontaneous electrical activity measured by EMG (Vergara et. al. 1993) whereas innervated skeletal muscle shows very low spontaneous activity (Figure 4). Following previous reports we used EMG recordings to measure denervation-induced skeletal muscle hyperexcitability and show that it was apamin sensitive (Figure 4, Beherens et al. 1994). EMG recordings were then employed to measure the electrical activity in mouse denervated skeletal muscle with and without SK3 protein. Selectively abolishing SK3 expression abolished denervation-induced hyperexcitability in the SK3tTa mouse (Figure 7), resembling innervated levels with minimal spontaneous activity (Figures 4 and 7). Unlike the wild-type mouse however, the SK3tTa mouse also shows SK3 expression in innervated skeletal muscle. However innervated Sk3tTa skeletal muscle shows no spontaneous activity and thus SK3 is not sufficient by itself to cause skeletal muscle hyperexcitability.

These results demonstrate that SK3 is necessary but not sufficient to cause denervation-induced skeletal muscle hyperexcitability.

SK3 channel activity is generally associated with membrane hyperpolarization; therefore a role in skeletal muscle hyperexcitability is contradictory its normal hyperpolarizing influence. This may be due to the location of SK3 channels in the unique membrane architecture of skeletal muscle. SK3 is located in the transverse tubules of skeletal muscle, which form invaginations into the muscle fibres that limit diffusion of ions such as potassium (Almers, 1980). T-tubular localization of SK channels was first postulated when apamin block took a very long time to develop in skeletal muscle, which could be due to the narrowed mouth of the T-tubule slowing diffusion of apamin into the tubular lumen. This observation was confirmed with measurements of SK reversal potentials taken from denervated skeletal muscle fibres, which varied from the predicted values of a purely potassium selective channel, and could be a direct result of potassium accumulation from SK activity in t-tubules of denervated skeletal muscle (Figure 11, Neelands et. al.). T-tubule accumulation of potassium would cause an underestimation of the reversal potential of the SK current, an effect that would be exacerbated at lower external potassium concentrations because the local accumulation of potassium would contribute a larger percentage of the potassium ions. A local depolarization due to potassium accumulation in the t-tubule could account for the lower action potential threshold seen with denervated fibres

117

(Figure 12), as the membrane will require less of a depolarizing pulse to reach the action potential firing threshold. This was confirmed through SK channel block that returned the threshold for activation of an action potential back to innervated levels. SK3 t-tubule activity would lead to a local buildup of potassium that would cause a local depolarization, which might trigger another action potential, thus causing hyperexcitability.

SK3 expression in skeletal muscle is unable to cause skeletal muscle hyperexcitability when expressed in innervated skeletal muscle (Figures 6 and 7), suggesting that other alterations consequent to denervation are required to unlock the effects of SK3 channels. As expected there are many changes following denervation some of which result in a significantly depolarized resting membrane potential (RMP), from -80mV to -60 mV (Hartzell & Fambrough, 1972; Rogart & Regan, 1985; Mishina et al. 1986; Heathcote, 1989; Brenner et al. 1990; Gonoi & Hasegawa, 1991; Lupa & Caldwell, 1994). The lower RMP in denervated muscle is due to many changes including lower expression levels of chloride channels, inwardly rectifying potassium channels, or sodium channel isoform switches (Heathcote, 1989; Trimmer et al. 1990; Venosa and Kotsias, 1985). As well as depolarizing the membrane the lower RMP changes the membrane potential from a value close to the equilibrium potential of potassium, -80 mV, where there would not be much SK3 activity, to a potential that increases open probability of SK3 channels, -60 mV. A model consistent with the

118

data is that activation of SK3 in the t-tubule of denervated skeletal muscle leads to a local buildup of potassium that together with a lower RMP induces enough of a local depolarization to fire another action potential thus causing hyperexcitability.

Although many inherited myotonic disorders result in skeletal muscle hyperexcitability, only the myotonia associated with DM exhibits apamin sensitivity and increased SK3 expression. Patients with DM also develop varying degrees of neuropathy (Coers, 1955; Mac Dermot 1961; Mondelli et. al. 1993) that reflects the nerve resection in denervated skeletal muscle. Therefore it is possible that compromised nerve function or nerve death consequent to myotonic dystrophy may lead to hyperexcitability that mirrors the changes induced by acute denervation. Interestingly male patients with DM also develop pituitary-gonadal abnormalities and have reduced testosterone levels and increased LH and FSH production (Takeda et al. 1977; Pizzi et al. 1985). The reduced testosterone levels result from aberrant gonadal Lydig cell function, which don't produce normal levels of testosterone in response to LH (Lou et al. 1994). As described estrogen affects SK3 levels in the rostral hypothalamus, which regulate FSH and LH release from gonadotropes. Testosterone can be aromatized to estrogen and activate the estrogen receptors (Ogawa et al. 1998), which will increase SK3 expression in the rostral hypothalamus. Therefore diminished testosterone levels may reduce SK3 transcription in the rostral

119

hypothalamus, which would increase the probability of GnRH release and cause increased FSH and LH release. However the uterus differs in its response to estrogen, which when elevated leads to decreased SK3 levels in the circular a longitudinal muscle layers. SK3 levels may be affected in skeletal muscle by estrogen as in the uterine smooth muscle, which could increase SK3 transcription with decreased estrogen receptor stimulation. Thus SK3 levels in DM may also be directly affected through hormonal changes and account for the gonadal-pituitary and skeletal muscle discrepancies that have been observed with DM.

III. Future Studies

This thesis defines important transcriptional regulatory sequences, involved in SK3 gene expression, found within the SK3 5' flanking sequence. Using the Sp estrogen regulated motif studies could be designed to elucidate the positive and negative roles of estrogen on SK3 transcription in different estrogen sensitive tissues with different E2 stimulation times. SK3 adenovirus promoter reporters could be used to infect primary cultures treated with and without estrogen and help define the importance of SK3 regulation by estrogen in vivo.

SK3 plays an important role in vascular tone and studies on mice have recently shown that SK3 is expressed predominantly in the vascular endothelium of mice (Nelson, in press). SK3 could be important in vascular protection observed with

premenopausal females and if so its transcription via estrogen is an important regulatory mechanism that may be exploited as a therapeutic target for heart disease. Studies could be designed to define the mechanisms of SK3 transcriptional regulation by estrogen in vascular endothelium addressing the effects of hormone replacement on its expression.

A role for SK3 in skeletal muscle hyperexcitability has been clearly demonstrated by this thesis work, however further proof of transverse tubule location in denervated skeletal muscle is needed. Therefore electron microscopy could be used to identify the location of SK3 in the membrane of denervated skeletal muscle. It would also be interesting to look at SK3 expression in DM type 2, if it is also aberrantly expressed in skeletal muscle SK3 transcriptional regulation with respect to a CTG repeat could be addressed.

References

Albuquerque, E. X. & Thesleff, S. (1968). A comparative study of membrane properties of innervated and chronically denervated fast and slow skeletal muscles of the rat. Acta Physiologica Scandinavica 73, 471-480

Almers W. (1980). Potassium concentration changes in the transverse tubules of vertebrate skeletal muscle. Fed Proc 39, 1527-1532

Anwer K, Oberti C, Perez GJ, Perez-Reyes N, McDougall JK, Monga M, Sanborn BM, Stefani E, Toro L. (1993). Calcium-activated K+ channels as modulators of human myometrial contractile activity. Am J Physiol. 265(4 Pt 1), C976-85

Artalejo AR, Garcia AG, Neher E. (1993). Small-conductance Ca(2+)-activated K+ channels in bovine chromaffin cells. Pflugers Arch 423(1-2), 97-103

Ashcroft FM, Gribble FM. (1998). Correlating structure and function in ATP-sensitive K+ channels. Trends in Neuroscience 21(7), 288-94

Atkinson NS, Robertson GA, Ganetzky B. (1991) A component of calcium-activated potassium channels encoded by the Drosophila slo locus. Science 2;253(5019), 551-5

Bang H, Kim Y, Kim D. (2000). TREK-2, a new member of the mechanosensitive tandem pore K+ channel family. Journal of Biological Chemistry 275, 17412–17419

Barfod ET, Moore AL, Lidofsky SD. Cloning and functional expression of a liver isoform of the small conductance Ca2+-activated K+ channel SK3. American Journal of Cell Physiology. 2001 Apr;280(4), C836-42

Barrett JN, Barrett EF, Dribin LB. (1981). Calcium-dependent slow potassium conductance in rat skeletal myotubes. Developmental Biology 82(2), 258-66

Bass KM, Bush TL. (1991). Estrogen therapy and cardiovascular risk in women. J La State Medical Society 143(5), 33-9.

Berg, J. M. (1992). Sp1 and the subfamily of zinc finger proteins with guanine-rich binding sites. Proceedings of the National Academy of Sciences USA 89(23), 11109-10.

Beam KG, Knudson CM, Powell JA. (1986). A lethal mutation in mice eliminates the slow calcium current in skeletal muscle cells. Nature 320(6058),168-70

Behrens MI, Jalil P, Serani A, Vergara F, Alvarez O. (1994). Possible role of apamin-sensitive K+ channels in myotonic dystrophy. Muscle Nerve 17(11),1264-70

Bernstein J. (1902). Untersuchungen zur Thermodynamik der bioelektrischen Strome. Erster Theil. Pflugers Arch 92, 521-562

Blatz,AL, and Magleby KL.(1986).Single apamin-blocked Ca- activated K+ channels of small conductance in cultured rat skeletal muscle. Nature 323 ,718 –720.

Brenner, H. R., Witezmann, V. & Sakmann, B. (1990). Imprinting of acetylcholine receptor messenger RNA accumulation in mammalian neuromuscular synapses. Nature 344, 544-547

Bilbrey GL, Herbin L, Carter NW, Knochel JP. (1973). Skeletal muscle resting membrane potential in potassium deficiency.
Journal of Clinical Investigation 52(12), 3011-8

Blatz, A. L. and K. L. Magleby (1986). Single apamin-blocked Ca-activated K+ channels of small conductance in cultured rat skeletal muscle. Nature 323, 718-720

Bond CT, Sprengel R, Bissonnette JM, Kaufmann WA, Pribnow D, Neelands T, Storck T, Baetscher M, Jerecic J, Maylie J, Knaus HG, Seeburg PH, Adelman JP. (2000). Respiration and parturition affected by conditional overexpression of the Ca2+-activated K+ channel subunit, SK3. Science 289(5486),1942-6

Bosch MA, Kelly MJ, Ronnekleiv OK. (2002) Distribution, neuronal colocalization, and 17beta-E2 modulation of small conductance calcium-activated K(+) channel (SK3) mRNA in the guinea pig brain. Endocrinology 143(3),1097-107

Brenner HR, Witzemann V, Sakmann B. (1990). Imprinting of acetylcholine receptor messenger RNA accumulation in mammalian neuromuscular synapses. Nature 344, 544-547

Brook JD, McCurrach ME, Harley HG, Buckler AJ, Church D, Aburatani H, Hunter K, Stanton VP, Thirion JP, Hudson T, et. al. (1992). Molecular basis of myotonic dystrophy: expansion of a trinucleotide (CTG) repeat at the 3' end of a transcript encoding a protein kinase family member.
Cell 68(4), 799-808.
Bruening-Wright A, Schumacher MA, Adelman JP, Maylie J. (2002) Localization of the activation gate for small conductance Ca2+-activated K+ channels.
Journal of Neuroscience 22(15), 6499-506

Brugnara C, Armsby CC, De Franceschi L, Crest M, Euclaire MF, Alper SL. (1995). Ca(2+)-activated K+ channels of human and rabbit erythrocytes display distinctive patterns of inhibition by venom peptide toxins. Journal of Membrane Biology 147(1), 71-82

Burnham MP, Bychkov R, Feletou M, Richards GR, Vanhoutte PM, Weston AH, Edwards G. (2002). Characterization of an apamin-sensitive small-conductance Ca(2+)-activated K(+) channel in porcine coronary artery endothelium: relevance to EDHF, Br. J. Pharmacol.135, 1133-1143

Butler A, Wei A, Salkoff L. (1990). Shal, Shab, and Shaw: three genes encoding potassium channels in Drosophila. Nucleic Acids Research 18(8), 2173-4

Butler JA, Kallo I, Sjoberg M, Coen CW. (1999). Evidence for extensive distribution of oestrogen receptor alpha-immunoreactivity in the cerebral cortex of adult rats. Journal of Neuroendocrinology 11(5), 325-9

Butler JA, Sjoberg M, Coen C. (1999). Evidence for oestrogen receptor alpha-immunoreactivity in gonadotrophin-releasing hormone-expressing neurones (see comments). J. Neuroendocrinol. 11, 331-335

Campbell WB, Gebremedhin D, Pratt PF, Harder DR. (1996). Identification of epoxyeicosatrienoic acids as endothelium-derived hyperpolarizing factors. Circulation Research 78(3), 415-23

Chavez RA, Gray AT, Zhao BB, C.H. Kindler, Mazurek MJ, Mehta Y, Forsayeth JR,Yost CS. (1999) TWIK-2, a new weak inward rectifying member of the tandem pore domain potassium channel family. Journal Biological Chemistry 274, 7887–7892

Coers C. (1955). Les variations structurelles normales et pathologiques de la junction neuromusculair. Acta Neurological Psychiatry Belgium 55, 741-866

Coetzee WA, Amarillo Y, Chiu J, Chow A, Lau D, McCormack T, Moreno H, Nadal MS, Ozaita A, Pountney D, Saganich M, Vega-Saenz de Miera E, Rudy B. (1999). Molecular diversity of K+ channels. Annals of the New York Academy of Sciences 868, 233-85

Corriu C, Feletou M, Canet E, Vanhoutte PM. (1996). Endothelium-derived factors and hyperpolarization of the carotid artery of the guinea-pig. British Journal of Pharmacology 119(5), 959-64

Dick GM, Sanders KM. (2001) (Xeno)estrogen sensitivity of smooth muscle BK channels conferred by the regulatory beta1 subunit: a study of beta1 knockout mice. J Biol Chem. 276(48), 44835-40

Dignam JD, Lebovitz RM, Roeder RG. (1983). Accurate transcription initiation by RNA polymerase II in a soluble extract from isolated mammalian nuclei. Nucleic Acids Research 11(5),1475-89

Doughty JM, Plane F, Langton PD. (1999). Charybdotoxin and apamin block EDHF in rat mesenteric artery if selectively applied to the endothelium. American Journal of Physiology 276(3 Pt 2), H1107-12

Doyle DA, Morais Cabral J, Pfuetzner RA, Kuo A, Gulbis JM, Cohen SL, Chait BT, MacKinnon R. (1998) The structure of the potassium channel: molecular basis of K+ conduction and selectivity. Science 280, 69-77

Duan R, Porter W, Safe S. (1998). Estrogen-induced c-fos protooncogene expression in MCF-7 human breast cancer cells: role of estrogen receptor Sp1 complex formation. Endocrinology 139, 1981-1990

Dulon D, Luo L, Zhang C, Ryan AF. (1988). Expression of small-conductance calcium-activated potassium channels (SK) in outer hair cells of the rat cochlea. European Journal of Neuroscience 10(3), 907-15

Duprat F, Lesage F, Fink M, Reyes R, Heurteaux C, Lazdunski M. (1997). TASK, a human background K+ channel to sense external pH variations near physiological pH. EMBO Journal 16, 5464–5471

Durell SR, Guy HR. (1996). Structural model of the outer vestibule and selectivity filter of the Shaker voltage-gated K+ channel. Neuropharmacology 35(7), 761-73

Fandos C, Sanchez-Feutrie M, Santalucia T, Vinals F, Cadefau J, Guma A, Cusso R, Kaliman P, Canicio J, Palacin M, Zorzano A. (1999). GLUT1 glucose transporter gene transcription is repressed by Sp3. Evidence for a regulatory role of Sp3 during myogenesis. Journal of Molecular Biology 294(1), 103-19

Farnbach GC, Brown MJ, Barchi RL. (1978). A maturational defect in passive membrane properties of dystrophic mouse muscle. Experimental Neurology 62(3), 539-54

Ferin M, Van Vugt D, Wardlaw S. (1984). The hypothalamic control of the menstrual cycle and the role of endogenous opioid peptides. Recent. Prog. Horm. Res. 40, 441-485

Fettiplace R, Fuchs PA. (1999). Mechanisms of hair cell tuning. Annual Review of Physiology 61, 809-34

Fink M, Duprat F, Lesage F, Reyes R, Romey G, Heurteaux C, Lazdunski M. (1996). Cloning, functional expression and brain localization of a novel unconventional outward rectifier K+ channel. EMBO Journal 15, 6854–6862

Fink M, Lesage F, Duprat F, Heurteaux C, Reyes R, Fosset M, Lazdunski M. (1998) A neuronal two P domain K+ channel activated by arachidonic acid polyunsaturated fatty acid. EMBO Journal 17, 3297–3308

Fleming, A. S., Suh, E. J., Korsmit, M., and Rusak, B. (1994) Behavioral Neuroscience 108(4), 724-34

Fojas de Borja P, Collins NK, Du P, Azizkhan-Clifford J, Mudryj M. (2001). Cyclin A-CDK phosphorylates Sp1 and enhances Sp1-mediated transcription. EMBO Journal 20(20), 5737-47

Franzini-Armstrong C, Protasi F. (1997). Ryanodine receptors of striated muscles: A complex channel capable of multiple interactions. Physiology Review 77, 699-729

Fujita A, Takeuchi T, Saitoh N, Hanai J, Hata F. (2001). Expression of Ca(2+)-activated K(+) channels, SK3, in the interstitial cells of Cajal in the gastrointestinal tract. American Journal Physiology Cell Physiology 281(5), C1727-33

Gardos G. (1958). The function of calcium in the potassium permeability of human erythrocytes. Biochim Biophys Acta 30, 653-654

Ge Y, Matherly LH, Taub JW. (2001). Transcriptional regulation of cell-specific expression of the human cystathionine beta -synthase gene by differential binding of Sp1/Sp3 to the -1b promoter. Journal of Biological Chemistry 276(47), 43570-9

George, A. L. Jr, Crackower, M. A., Abdalla, J. A., Hudson, A. J. & Ebers, G. C. (1993). Molecular basis of Thomsen's disease (autosomal dominant myotonia congenita). Nature Genetics 3, 305-310

Girard C, Duprat F, Terrenoire C, Tinel N, Fosset M, Romey G, Lazdunski M, Lesage F. (2001). Genomic and functional characteristics of novel human pancreatic 2P domain potassium channels. Biochemistry and Biophysical Research Communications23, 249–256

131

Gonoi, T. & Hasegawa, S. (1991). Postnatal induction and neural regulation of inward rectifiers in mouse skeletal muscle. Pflügers Archive 418, 601-607

Grissmer S, Lewis RS, Cahalan MD. (1992). Ca(2+)-activated K+ channels in human leukemic T cells. Journal General Physiology 99(1),63-84

Grissmer S, Nguyen AN, Cahalan MD. (1993). Calcium-activated potassium channels in resting and activated human T lymphocytes. Expression levels, calcium dependence, ion selectivity, and pharmacology. Journal of General Physiology 102(4), 601-30

Haidweger E, Novy M, Rotheneder H. (2001). Modulation of Sp1 activity by a cyclin A/CDK complex. Journal of Molecular Biology 306(2), 201-12

Hartzell, H. C. & Fambrough, D. M. (1972). Acetylcholine receptors. Distribution and extrajunctional density in rat diaphragm after denervation correlated with acetylcholine sensitivity. Journal of General Physiology 60, 248-262

Hasegawa H, Kurasawa T, Ohtake Y, Matsukawa H, Ezure Y, Koike K, Shigenobu K, Imai T. (2001). Effects of different types of K+ channel modulators on the spontaneous myogenic contraction of guinea-pig urinary bladder smooth muscle. Biol. Pharm. Bull. 24, 897-901

132

Heathcote RD. (1989). Acetylcholine-gated and chloride conductance channel expression in rat muscle membrane. Journal of Physiology 414, 473-97

Heinemann SH, Rettig J, Graack HR, Pongs O. (1996). Functional characterization of Kv channel beta-subunits from rat brain. Journal of Physiology 493 (Pt 3), 625-33

Herrera GM, Heppner TJ, Nelson MT. (2000) Regulation of urinary bladder smooth muscle contractions by ryanodine receptors and BK and SK channels. Am. J. Physiol. Regul. Integr.Comp. Physiol. 279, R60-68

Hille B, Tse A, Tse FW, Bosma MM. (1995) Siganlling mechanisms during the response of pituitary gonadotropes to GNRH. Recent Prog. Horm. Res. 50, 75-95

Hille B. (2001). Ion Channels of Excitable Membranes Third Edition.

Hirschberg B, Maylie J, Adelman JP, Marrion NV. (1998). Gating of recombinant small-conductance Ca-activated K+ channels by calcium. Journal of General Physiology111(4), 565-81

Ho K, Nichols CG, Lederer WJ, Lytton J, Vassilev PM, Kanazirska M V,

Hebert SC. (1993). Cloning and expression of an inwardly rectifying

ATP-regulated potassium channel. Nature 362, 31-37

Hodgkin AL, and Huxley AF. (1952). Currents carried by sodium and potassium

ions through the membrane of the giant squid axon of Loligo. Journal of

Physiology 116, 473-496

Hogan B, Beddigton R, Costantini F, Lacy E. (1994). Manipulating the mouse

embryo: a laboratory manual. 2nd edition. Cold Spring Harbor, NY: Cold Spring

Harbor Laboratory Press

Hrabovszky E, Shughrue PJ, Merchenthaler I, Hajszan T, Carpenter CD, Liposits

Z, Petersen SL. (2000) Detection of estrogen receptor-beta messenger

ribonucleic acid and 125I-estrogen binding sites in luteinizing hormone-releasing

hormone neurons of the rat brain. Endocrinology 141, 3506-9

Hugues M, Duval D, Kitabgi P, Lazdunski M, Vincent JP. (1982). Preparation of a pure monoiodo derivative of the bee venom neurotoxin apamin and its binding properties to rat brain synaptosomes. Journal of Biological Chemistry 257(6),2762-9

Hugues M, Schmid H, Romey G, Duval D, Frelin C, Lazdunski M. (1982). The Ca^{2+}-dependent slow K^+ conductance in cultured rat muscle cells: characterization with apamin. EMBO Journal 1(9), 1039-42

Impey S, Mark M, Villacres EC, Poser S, Chavkin C, Storm DR. (1996). Induction of CRE-mediated gene expression by stimuli that generate long- lasting LTP in area CA1 of the hippocampus. Neuron 16(5), 973-82

Ishii TM, Silvia C, Hirschberg B, Bond CT, Adelman JP, Maylie J. (1997). A human intermediate conductance calcium-activated potassium channel. Proceedings of the National Academy of Sciences USA 94, 11651-11656

Jackson SP, MacDonald JJ, Lees-Miller S, Tjian R. (1990). GC box binding induces phosphorylation of Sp1 by a DNA-dependent protein kinase. Cell 63(1), 155-65

Jan YN, Jan LY. (1977). Two mutations of synaptic transmission in Drosphila. Proceedings of the Royal Society of London Biological Sciences 198, 87-108

Jaynes JB, Chamberlain JS, Buskin JN, Johnson JE, Hauschka SD. (1986). Transcriptional regulation of the muscle creatine kinase gene and regulated expression in transfected mouse myoblasts. Mol Cell Biol. 6(8), 2855-64

Jiang Y, Lee A, Chen J, Cadene M, Chait BT, MacKinnon R. (2002). Crystal structure and mechanism of a calcium-gated potassium channel. Nature 417(6888), 515-22

Johnson JE, Wold BJ, Hauschka SD. (1989). Muscle creatine kinase sequence elements regulating skeletal and cardiac muscle expression in transgenic mice. Mol Cell Biol. 9(8), 3393-9

Joiner WJ, Wang LY, Tang MD, Kaczmarek LK. (1997). HSK4, a member of a novel subfamily of calcium-activated potassium channels. Proceedings of the National Academy of Sciences USA 94, 11013-11018

Kadonaga JT, Carner KR, Masiarz FR, Tjian R. (1987). Isolation of cDNA encoding transcription factor Sp1 and functional analysis of the DNA binding domain. Cell 51, 1079-1090

Kahlert S, Grohe C, Karas RH, Lobbert K, Neyes L, Vetter H. (1997). Effects of estrogen on skeletal myoblast growth, Biochem. Biophys. Res. Comm. 232, 373-378

Kamb A, Iverson LE, Tanouye MA. (1987). Molecular characterization of Shaker, a Drosophila gene that encodes a potassium channel. Cell 50(3), 405-13

Kandel ER, Schwartz JH, Jessel TM. (2000). Principles of Neural Science fourth edition.

Kaplan WD, Trout WE 3rd. (1969). The behavior of four neurological mutants of Drosophila. Genetics 61(2), 399-409

Keen JE, Khawaled R, Farrens DL, Neelands T, Rivard A, Bond CT, Janowsky A, Fakler B, Adelman JP, Maylie J. (1999). Domains responsible for constitutive and Ca(2+)-dependent interactions between calmodulin and small conductance Ca(2+)-activated potassium channels. Journal Neuroscience 19(20), 8830-8

Kelly MJ, Ronnekleiv OK, Ibrahim N, Lagrange AH, Wagner EJ. (2002). Estrogen modulation of K+ channel activity in hypothalamic neurons involved in the control of the reproductive axis. Steroids 67(6), 447-56

Kennett SB, Udvadia AJ, Horowitz JM. (1997). Sp3 encodes multiple proteins that differ in their capacity to stimulate or repress transcription. Nucleic Acids Research 25(15), 3110-7

Kim D, Fujita A, Horio Y, Kurachi Y. (1998). Cloning and functional expression of a novel cardiac two-pore background K+ channel (cTBAK-1). Circulation Research 82, 513–518

Kim Y, Bang H, Kim D. (2000). TASK-3, a new member of the tandem pore K+ channel family. Journal of Biological Chemistry 275, 9340–9347

Kimura T, Takahashi MP, Okuda Y, Kaido M, Fujimura H, Yanagihara T, Sakoda S. (2000). The expression of ion channel mRNAs in skeletal muscles from patients with myotonic muscular dystrophy. Neuroscience Letter 295(3), 93-6

Klein-Hitpass L, Ryffel GU, Heitlinger E, Cato AC. (1988). A 13 bp palindrome is a functional estrogen responsive element and interacts specifically with estrogen receptor. Nucleic Acids Res. 16, 647-663

Knot HJ, Lounsbury KM, Brayden JE, Nelson MT. (1999). Gender differences in coronary artery diameter reflect changes in both endothelial Ca2+ and ecNOS activity, Am. J. Physiol. 277, H1178-1188

Koch, M.C., Steinmeyer, K., Lorenz, C., Ricker, K., Wolf, F., Otto, M., Zoll, B., Lehmann-Horn, F., Grzeschik, K.H., and Jentsch, T.J. (1992). The skeletal muscle chloride channel in dominant and recessive human myotonia. Science 257, 797–800

Kohler M, Hirschberg B, Bond CT, Kinzie JM, Marrion NV, Maylie J, Adelman JP. (1996). Small-conductance, calcium-activated potassium channels from mammalian brain. Science 273(5282), 1709-14

Kubo Y, Baldwin TJ, Jan YN, Jan LY. (1993) Primary structure and functional expression of a mouse inward rectifier potassium channel. Nature 362(6416), 127-33

Lagaud GJ, Skarsgard PL, Laher I, van Breemen C. (1999). Heterogeneity of endothelium-dependent vasodilation in pressurized cerebral and small mesenteric resistance arteries of the rat. Journal of Pharmacological Experimental Therapy 290(2), 832-9

Lancaster B, Adams PR. (1986) Calcium-dependent current generating the afterhyperpolarization of hippocampal neurons. Journal of Neurophysiology 55(6),1268-82

Lancaster B, Nicoll RA, Perkel DJ. (1991). Calcium activates two types of potassium channels in rat hippocampal neurons in culture. Journal of Neuroscience 11(1), 23-30

Lania L, Majello B, De Luca P. (1997). Transcriptional regulation by the Sp family proteins. International Journal Biochemistry Cell Biology 29(12), 1313-23

Latorre R, Oberhauser A, Labarca P, Alvarez O. (1989). Varieties of calcium-activated potassium channels. Annual Review of Physiology 51, 385-99

Leggett RW, Armstrong SA, Barry D, Mueller CR. (1995). Sp1 is phosphorylated and its DNA binding activity down-regulated upon terminal differentiation of the liver. Journal of Biological Chemistry 270(43), 25879-84

Leonoudakis D, Gray AT, Winegar BD, Kindler CH, Harada M, Taylor DM, Chavez RA, Forsayeth JR, Yost CS. (1998) An open rectifier potassium channel with two pore domains in tandem cloned from rat cerebellum. Journal of Neuroscience 18, 868–877

Lesage F, Lazdunski M. (2000). Molecular and functional properties of two-pore-domainpotassium channels. Americal Journal of Physiology Renal Physiology 279, F793–F801

Lesage F, Guillemare E, Fink M, Duprat F, Lazdunski M, Romey G, Barhanin J. (1996). TWIK-1, a ubiquitous human weakly inward rectifying K + channel with a novel structure. EMBO Journal 1996, 15, 1004-1011

Lesage F, Terrenoire C, Romey G, Lazdunski M. (2000). Human TREK2, a 2P domain mechano-sensitive K+ channel with multiple regulations by polyunsaturated fatty acids, lysophospholipids, and Gs, Gi, and Gq protein-coupled receptors. Journal of Biological Chemistry 275, 28398–28405

Levallet J, Koskimies P, Rahman N, Huhtaniemi I. (2001). The promoter of murine follicle-stimulating hormone receptor: functional characterization and regulation by transcription factor steroidogenic factor 1. Molecular Endocrinology 15(1), 80-92

Lindsley DB, and Curnen EC. (1936). An electromyographic study of Myotonia. Arch Neurological Psychiatry 35, 522-535

Liquori, C.L., Ricker, K., Moseley, M.L., Jacobsen, J.F., Kress, W.,Naylor, S.L.,Day, J.W., and Ranum, L.P. (2001). Myotonic dystrophy type 2 caused by a CCTG expansion in intron 1 of ZNF9. Science 293, 864–867

Lopatin AN, Makhina EN, Nichols CG. (1994). Potassium channel block by cytoplasmic polyamines as the mechanism of intrinsic rectification. Nature 372(6504), 366-9

Lupa, M. T. & Caldwell, J. H. (1994). Sodium channels aggregate at former synaptic sites in innervated and denervated regenerating muscles. Journal of Cell Biology 124, 139-147

Mac Dermot V. (1961). The histology of neuromuscular junction in myotonic dystrophy. Brain 84, 75-84

MacKinnon R. (1991). Determination of the subunit stoichiometry of a voltage-activated potassium channel. Nature 350(6315), 232-5

Mankodi, A., Logigian, E., Callahan, L., McClain, C., White, R., Hen-derson, D., Krym, M., and Thornton, C.A. (2000). Myotonic dystrophy in transgenic mice expressing an expanded CUG repeat. Science 289, 1769–1773

Martin, K. J. (1991). The interactions of transcription factors and their adaptors, coactivators and accessory proteins. Bioessays 13(10), 499-503

Matsuda H. (1988). Open-state substructure of inwardly rectifying potassium channels revealed by magnesium block in guinea-pig heart cells. Journal of Physiology397, 237-58

McCrohon JA, Walters WA, Robinson JT, McCredie RJ, Turner L, Adams MR, Handelsman DJ, Celermajer DS. (1997). Arterial reactivity is enhanced in genetic males taking high dose estrogens. J Am Coll Cardiol. 29(7),1432-6

McManus OB, Helms LM, Pallanck L, Ganetzky B, Swanson R, Leonard RJ. (1995). Functional role of the beta subunit of high conductance calcium-activated potassium channels. Neuron 14(3), 645-50

Meech RW. (1972). Intracellular calcium injection causes increased potassium conductance in Aplysia nerve cells. Comparative Biochemical Physiology A 42(2), 493-9

Miller C. (2000). An overview of the potassium channel family.
Genome Biology 1(4), S0004

Mishina, M., Takai, T., Imoto, K., Noda, M., Takahashi, T., Numa, S., Methfessel, C. & Sakmann, B. (1986). Molecular distinction between fetal and adult forms of muscle acetylcholine receptor. Nature 321, 406-411

Mondelli M, Rossi A, Malandrini A, Della Porta P, Guzaai GC. (1993). Axonal motor and sensory neuropathy in myotonic dystrophy. Acta Neurology Scandinavica 88(2), 141-8

Mourre C, Schmid-Antomarchi H, Hugues M, Lazdunski M. (1984). Autoradiographic localization of apamin-sensitive Ca2+-dependent K+ channels in rat brain. European Journal of Pharmacology 100(1),135-6

Murphy ME, Brayden JE. (1995). Apamin-sensitive K+ channels mediate an endothelium-dependent hyperpolarization in rabbit mesenteric arteries. Journal of Physiology 489 (Pt 3), 723-34

Neelands TR, Herson PS, Jacobson D, Adelman JP, Maylie J. (2001). Small-conductance calcium-activated potassium currents in mouse hyperexcitable denervated skeletal muscle. Journal of Physiology 536(Pt 2), 397-407

Nimigean CM, Magleby KL. (2000). Functional coupling of the beta(1) subunit to the large conductance Ca(2+)-activated K(+) channel in the absence of Ca(2+). Increased Ca(2+) sensitivity from a Ca(2+)-independent mechanism. Journal of General Physiolology115(6), 719-36

Numan, M., and Sheehan, T. P. (1997) Annals of the New York Academy of Sciences 807, 101-25

Papazian DM, Schwarz TL, Tempel BL, Jan YN, Jan LY. (1987) Cloning of genomic and complementary DNA from Shaker, a putative potassium channel gene from Drosophila. Science 14;237(4816), 749-53

Park YB. (1994). Ion selectivity and gating of small conductance Ca(2+)-activated K+ channels in cultured rat adrenal chromaffin cells. Journal of Physiology 481(Pt 3), 555-70

Patel AJ, Maingret F, Magnone V, Fosset M, Lazdunski M, Honore E. (2002).
TWIK-2, an inactivating 2P domain K+ channel. Journal of Biological Chemistry
275, 28722–28730

Pennisi DJ, Rentschler S, Gourdie RG, Fishman GI, Mikawa T. (2002).
Induction and patterning of the cardiac conduction system. International Journal
of Developmental Biology 46(6), 765-75

Pfaffinger PJ, Furukawa Y, Zhao B, Dugan D, Kandel ER. (1991). Cloning and
expression of an Aplysia K+ channel and comparison with native Aplysia K+
currents. Journal of Neuroscience 11(4), 918-27

Philips, A.V., Timchenko, L.T., and Cooper, T.A. (1998). Disruption of splicing
regulated by a CUG-binding protein in myotonic dystrophy. Science 280,
737–741

Pinney DF, Pearson-White SH, Konieczny SF, Latham KE, Emerson C. (1988).
Myogenic lineage determination and differentiation: evidence for a regulatory
gene pathway. Cell 53, 781-793

Pountney DJ, Gulkarov I, Vega-Saenz de Miera E, Holmes D, Saganich M, Rudy B, Artman M, Coetzee and WA. (1999). Identification and cloning of TWIK-originated similarity sequence (TOSS): a novel human 2-pore K+ channel principal subunit. FEBS Letter 450, 191–196

Porter W, Saville B, Hoivik D, Safe S. (1997). Functional synergy between the transcription factor Sp1 and the estrogen receptor. Mol. Endocrinol. 11, 1569-1580

Pribnow D, Johnson-Pais T, Bond CT, Keen J, Johnson RA, Janowsky A, Silvia C, Thayer M, Maylie J, Adelman JP. (1999). Skeletal muscle and small-conductance calcium-activated potassium channels. Muscle and Nerve 22(6), 742-50

Qin C, Singh P, Safe S. (1999). Transcriptional activation of insulin-like growth factor-binding protein-4 by 17beta-estradiol in MCF-7 cells: role of estrogen receptor-Sp1 complexes. Endocrinology 140, 2501-2508

Rao J, Zhang F, Donnelly RJ, Spector NL, Studzinski GP. (1998). Truncation of Sp1 transcription factor by myeloblastin in undifferentiated HL60 cells. Journal Cell Physiology 175(2), 121-8

Rajan S, Wischmeyer E, Liu GX, Preisig-Muller R, Daut J, Karschin A, Derst C. (2000). TASK-3, a novel tandem pore-domain acid-sensitive K+ channel: an extracellular histidine as pH sensor. Journal of Biological Chemistry 275, 16650–16657

Ramanathan K, Michael TH, Jiang GJ, Hiel H, Fuchs PA. (1999). A molecular mechanism for electrical tuning of cochlear hair cells. Science 283(5399), 215-7

Renaud JF, Desnuelle C, Schmid-Antomarchi H, Hugues M, Serratrice G, Lazdunski M. (1986). Expression of apamin receptor in muscles of patients with myotonic muscular dystrophy. Nature 319, 678-680

Reyes R, Duprat F, Lesage F, Fink M, Farman N, Lazdunski M. (1998). Cloning and expression of a novel pH-sensitive two pore domain potassium channel from human kidney. Journal of Biological Chemistry 273, 30863–30869

Robbins N. (1977). Cation movements in normal and short-term denervated rat fast twitch muscle. Journal of Physiology 271, 605-624

Rogart, R. B. & Regan, L. J. (1985). Two subtypes of sodium channel with tetrodotoxin sensitivity and insensitivity detected in denervated mammalian skeletal muscle. Brain Research 329, 314-318

Roncarati R, Di Chio M, Sava A, Terstappen GC, Fumagalli G. (2001). Presynaptic localization of the small conductance calcium-activated potassium channel SK3 at the neuromuscular junction. Neuroscience 104(1), 253-62

Rousset B. (1996). Introduction to the structure and functions of junction communications or gap junctions. Annals of Endocrinology 57(6), 476-80

Rudy B. (1988). Diversity and ubiquity of K channels. Neuroscience 25(3), 729-49

Sah, P. (1996). Ca^{2+} - activated K^+ currents in neurones: types, physiological roles and modulation. Trends in Neuroscience 19, 150-154

Sah P, Bekkers JM. (1996) Apical dendritic location of slow afterhyperpolarization current in hippocampal pyramidal neurons: implications for the integration of long-term potentiation. Journal of Neuroscience 16(15), 4537-42

Sah P, Faber ES. (2002). Channels underlying neuronal calcium-activated potassium currents. Progressive Neurobiology 66(5), 345-53

Salkoff L, Wyman R. (1981). Outward currents in developing Drosophila flight muscle. Science 212(4493), 461-3

Samudio I, Vyhlidal C, Wang F, Stoner M, Chen I, Kladde M, Barhoumi R, Burghardt R, Safe S. (2001). Transcriptional activation of deoxyribonucleic acid polymerase alpha gene expression in MCF-7 cells by 17 beta-estradiol. Endocrinology 142,1000-1008

Savic N, Pedarzani P, Sciancalepore M. (2001). Medium afterhyperpolarization and firing pattern modulation in interneurons of stratum radiatum in the CA3 hippocampal region. Journal of Neurophysiology 85(5), 1986-97

Savkur, R.S., Philips, A.V., and Cooper, T.A. (2001). Aberrant regulation of insulin receptor alternative splicing is associated with insulin resistance in myotonic dystrophy. Nature Genetics 29, 40–47

Saville B, Wormke M, Wang F, Nguyen T, Enmark E, Kuiper G, Gustafsson JA, Safe S. (2000). Ligand-, cell-, and estrogen receptor subtype (alpha/beta)-dependent activation at GC-rich (Sp1) promoter elements. Journal Biol. Chem. 275, 5379-5387

Schaefer BC. (1995) Revolutions in rapid amplification of cDNA ends: new strategies for polymerase chain reaction cloning of full-length cDNA ends. Anal. Biochem. 227, 255-273

Schmid-Antomarchi H, Renaud JF, Romey G, Hugues M, Schmid A, Lazdunski M. (1985). The all-or-none role of innervation in expression of apamin receptor and of apamin-sensitive Ca^{2+}-activated K^+ channel in mammalian skeletal muscle. Proceedings of the National Academy of Sciences USA 82, 2188-2191

Schumacher MA, Rivard AF, Bachinger HP, Adelman JP. (2001). Structure of the gating domain of a Ca2+-activated K+ channel complexed with Ca2+/calmodulin. Nature 410(6832), 1120-4

Sellin LC, Thesleff S. (1980). Alterations in membrane electrical properties during long-term denervation of rat skeletal muscles. Acta Physiologica Scandinavica 108(3), 243-6

Shield MA, Haugen HS, Clegg CH, Hauschka SD. (1996) E-box sites and a proximal regulatory region of the muscle creatine kinase gene differentially regulate expression in diverse skeletal muscles and cardiac muscle of transgenic mice. Mol Cell Biol. 16(9), 5058-68

Silverman A J, Krey LC, and Zimmerman E A. (1979) Biology of

Reproduction 20(1), 98-110

Skynner MJ, Sim JA, Herbison AE. (1999) Detection of estrogen receptor alpha

and beta messenger ribonucleic acids in adult gonadotropin-releasing hormone

neurons. [erratum appears in Endocrinology 2001 Jan;142(1), 492-3.].

Endocrinology 140, 5195-201

Soh H, Park CS. (2002). Localization of divalent cation-binding site in the pore of

a small conductance Ca(2+)-activated K(+) channel and its role in determining

current-voltage relationship. Biophysical Journal 83(5), 2528-38

Stocker M, Krause M, Pedarzani P. (1999). An apamin-sensitive Ca2+-activated

K+ current in hippocampal pyramdial neurons. Proceedings of the National

Academy of Sciences USA 96, 4662-4667

Stocker M, Pedarzani P. (2000). Differential distribution of three Ca(2+)-activated

K(+) channel subunits, SK1, SK2, and SK3, in the adult rat central nervous

system. Molecular and Cellular Neuroscience 15(5), 476-93

Stoner M, Wang F, Wormke M, Nguyen T, Samudio I, Vyhlidal C, Marme D, Finkenzeller G, Safe S. (2000). Inhibition of vascular endothelial growth factor expression in HEC1A endometrial cancer cells through interactions of estrogen receptor alpha and Sp3 proteins. Journal Biological Chemistry 275(30), 22769-79

Sun G, Porter W, Safe S. (1998). Estrogen-induced retinoic acid receptor alpha 1 gene expression: role of estrogen receptor-Sp1 complex. Mol. Endocrinol. 12, 882-890

Suske, G. (1999). The Sp-family of transcription factors. Gene 238(2), 291-300

Suter KJ, Wuarin JP, Smith BN, Dudek FE, Moenter SM. (2000). Whole-cell recordings from preoptic/hypothalamic slices reveal burst firing in gonadotropin-releasing hormone neurons identified with green fluorescent protein in transgenic mice. Endocrinology 141(10), 3731-6

Szasz I, Sarkadi B, Gardos G. (1974) Erythrocyte parameters during induced CA-2+-dependent rapid K+-efflux: optimum conditions for kinetic analysis. Haematologia. 8(1-4), 143-51

Takekura H, Nishi M, Noda T, Takeshima H, Franzini-Armstrong C. (1995). Abnormal junctions between surface membrane and sarcoplasmic reticulum in skeletal muscle with a mutation targeted to the ryanodine receptor. Proceedings of the National Academy of Sciences USA 92(8), 3381-5

Tanouye MA, Ferrus A, Fujita SC. (1981). Abnormal Action potentials in associated with the Shaker locus of Drosophila. Proceedings of the National Academy of Sciences USA78, 6548-6552

Timpe LC, Schwarz TL, Tempel BL, Papazian DM, Jan YN, Jan LY. (1988). Expression of functional potassium channels from Shaker cDNA in Xenopus oocytes. Nature 331(6152), 143-5

Tower, S. S. (1939). The reaction of muscle to denervation. Physiological Research 19, 1-48

Trimmer JS, Cooperman SS, Agnew WS, Mandel G. (1990). Regulation of muscle sodium channel transcripts during development and in response to denervation. Developmental Biology. 142(2), 360-7

Tse A, Hille B. (1992) GnRH-induced Ca2+ oscillations and rhythmic hyperpolarizations of pituitary gonadotropes. Science 255, 462-4

Tse A, Tse F W, Almers W, Hille B. (1993) Rhythmic exocytosis stimulated by GnRH-induced calcium oscillations in rat gonadotropes. Science 260, 82-84

Tse A, Tse FW, Hille B. (1995) Modulation of Ca2+ oscillation and apamin-sensitive, Ca2+-activated K+ current in rat gonadotropes. Pflugers Arch. 430(5), 645-52

Venosa RA, Kotsias BA. (1985). Potassium movements in denervated frog sartorius muscle. Am erican Journal of Physiology 248(3 Pt 1), C219-27

Vergara, C., Ramirez, B. & Beherens, M. I. (1993). Colchicine alters apamin receptors, electrical activity, and skeletal muscle relaxation. Muscle and Nerve 16, 935-940

Vinals F, Fandos C, Santalucia T, Ferre J, Testar X, Palacin M, Zorzano A. (1997). Myogenesis and MyoD down-regulate Sp1. A mechanism for the repression of GLUT1 during muscle cell differentiation. Journal of Biological Chemistry 272(20), 12913-21

Vullhorst D, Klocke R, Bartsch JW, Jockusch H. (1998). Expression of the potassium channel KV3.4 in mouse skeletal muscle parallels fiber type maturation and depends on excitation pattern. FEBS Letter 421(3), 259-62

Wagner EJ, Ronnekleiv OK, Kelly MJ. (2001). The noradrenergic inhibition of an apamin-sensitive, small-conductance Ca2+-activated K+ channel in hypothalamic gamma-aminobutyric acid neurons: pharmacology, estrogen sensitivity, and relevance to the control of the reproductive axis. Journal of Pharmacology Experimental Therapeutics 299(1), 21-30

Wallner M, Meera P, Toro L. (1999). Molecular basis of fast inactivation in voltage and Ca2+-activated K+ channels: a transmembrane beta-subunit homolog Proceedings of the National Academy of Sciences 96(7), 4137-42

Wang F, Hoivik D, Pollenz R, Safe S. (1998). Functional and physical interactions between the estrogen receptor Sp1 and nuclear aryl hydrocarbon receptor complexes. Nucleic Acids Res. 26, 3044-3052

Wang W, Dong L, Saville B, Safe S. (1999). Transcriptional activation of E2F1 gene expression by 17beta-estradiol in MCF-7 cells is regulated by NF-Y-Sp1/estrogen receptor interactions. Mol. Endocrinol. 13,1373-1387

Wei A, Covarrubias M, Butler A, Baker K, Pak M, Salkoff L.   (1990). K+ current diversity is produced by an extended gene family conserved in Drosophila and mouse. Science 248(4955), 599-603

Wellman GC, Bonev AD, Nelson MT, Brayden JE. (1996). Gender differences in coronary artery diameter involve estrogen, nitric oxide, and Ca(2+)-dependent K+ channels. Circ.Res.79, 1024-1030

Wu CF, Ganetzky B, Haugland FN, Liu AX.   (1983). Potassium currents in Drosophila: different components affected by mutations of two genes. Science 220(4601),1076-8

Wu CF, Haugland FN. (1985). Voltage clamp analysis of membrane currents in larval muscle fibers of Drosophila: alteration of potassium currents in Shaker mutants. Journal of Neuroscience 5(10), 2626-40

Wu YC, Fettiplace R. (1996). A developmental model for generating frequency maps in the reptilian and avian cochleas. Biophysical Journal 70(6), 2557-70

Xia XM, Fakler B, Rivard A, Wayman G, Johnson-Pais T, Keen JE, Ishii T, Hirschberg B, Bond CT, Lutsenko S, Maylie J, Adelman JP. (1998). Mechanism of calcium gating in small-conductance calcium-activated potassium channels. Nature 395, 503-507

Xie W, Duan R, Chen I, Samudio I, Safe S. (2000). Transcriptional activation of thymidylate synthase by 17beta-estradiol in MCF-7 human breast cancer cells. Endocrinology 141, 2439-2449

Zhang L, McBain CJ. (1995). Potassium conductances underlying repolarization and after-hyperpolarization in rat CA1 hippocampal interneurones. Journal of Physiology 488 (Pt 3), 661-72

Zhu, Q. and K. Liao (2000). Differential expression of the adipocyte amino acid transporter is transactivated by SP1 and SP3 during the 3T3-L1 preadipocyte differentiation process. Biochemistry and Biophysical Research Communication 271(1), 100-6